

# Accepted Manuscript

The relevance of  $K_i$  calculation for bi-substrate enzymes illustrated by kinetic evaluation of a novel lysine (K) acetyltransferase 8 inhibitor

Hannah Wapenaar, Thea van den Bosch, Niek G.J. Leus, Petra E. van der Wouden, Nikolaos Eleftheriadis, Jos Hermans, Gebremedhin Solomon Hailu, Dante Rotili, Antonello Mai, Alexander Dömling, Rainer Bischoff, Hidde J. Haisma, Frank J. Dekker

PII: S0223-5234(17)30376-8

DOI: [10.1016/j.ejmech.2017.05.015](https://doi.org/10.1016/j.ejmech.2017.05.015)

Reference: EJMECH 9445

To appear in: *European Journal of Medicinal Chemistry*

Received Date: 17 February 2017

Revised Date: 11 April 2017

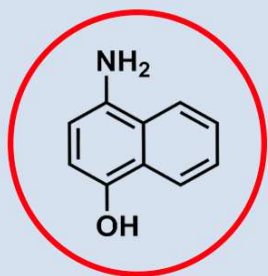
Accepted Date: 4 May 2017

Please cite this article as: H. Wapenaar, T. van den Bosch, N.G.J. Leus, P.E. van der Wouden, N. Eleftheriadis, J. Hermans, G.S. Hailu, D. Rotili, A. Mai, A. Dömling, R. Bischoff, H.J. Haisma, F.J. Dekker, The relevance of  $K_i$  calculation for bi-substrate enzymes illustrated by kinetic evaluation of a novel lysine (K) acetyltransferase 8 inhibitor, *European Journal of Medicinal Chemistry* (2017), doi: 10.1016/j.ejmech.2017.05.015.

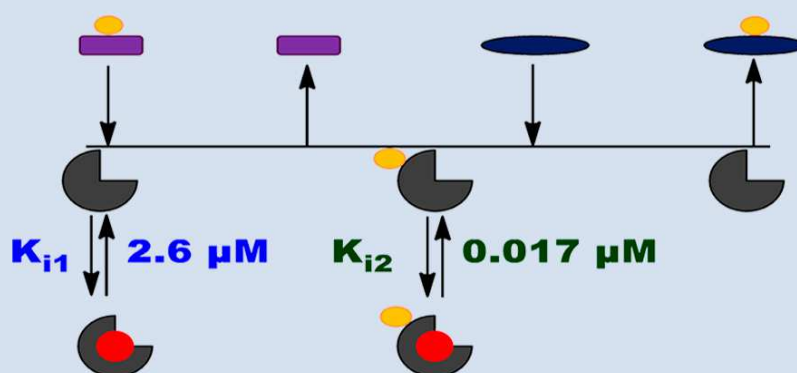
This is a PDF file of an unedited manuscript that has been accepted for publication. As a service to our customers we are providing this early version of the manuscript. The manuscript will undergo copyediting, typesetting, and review of the resulting proof before it is published in its final form. Please note that during the production process errors may be discovered which could affect the content, and all legal disclaimers that apply to the journal pertain.



## KAT8 inhibitor



## Mechanism of inhibition



# The relevance of $K_i$ calculation for bi-substrate enzymes illustrated by kinetic evaluation of a novel lysine (K) acetyltransferase 8 inhibitor

Hannah Wapenaar<sup>a1</sup>, Thea van den Bosch<sup>a1</sup>, Niek G. J. Leus<sup>a</sup>, Petra E. van der Wouden<sup>a</sup>, Nikolaos Eleftheriadis<sup>a</sup>, Jos Hermans<sup>b</sup>, Gebremedhin Solomon Hailu<sup>c</sup>, Dante Rotili<sup>c</sup>, Antonello Mai<sup>c</sup>, Alexander Dömling<sup>d</sup>, Rainer Bischoff<sup>b</sup>, Hidde J. Haisma<sup>a</sup>, Frank J. Dekker<sup>a\*</sup>

<sup>1</sup>These authors contributed equally to this work

\* Corresponding author

Frank J. Dekker, Department of Chemical and Pharmaceutical Biology, Groningen Research Institute of Pharmacy (GRIP), University of Groningen. Antonius Deusinglaan 1, 9713 AV Groningen, The Netherlands. Email f.j.dekker@rug.nl, tel. +31 503638030.

Author affiliations:

- a. Department of Chemical and Pharmaceutical Biology, Groningen Research Institute of Pharmacy (GRIP), University of Groningen, Antonius Deusinglaan 1, 9713 AV Groningen, The Netherlands.
- b. Department of Analytical Biochemistry, Groningen Research Institute of Pharmacy (GRIP), University of Groningen, Antonius Deusinglaan 1, 9713 AV Groningen, The Netherlands.
- c. Department of Drug Chemistry and Technologies, Sapienza University of Rome, P.le A. Moro 5, 00185 Rome, Italy
- d. Department of Drug Design, Groningen Research Institute of Pharmacy (GRIP), University of Groningen, Antonius Deusinglaan 1, 9713 AV Groningen, The Netherlands.

**Abstract**

Histone acetyltransferases (HATs) are important mediators of epigenetic post-translational modifications of histones that play important roles in health and disease. A disturbance of these modifications can result in disease states, such as cancer or inflammatory diseases. Inhibitors of HATs (HATi) such as lysine (K) acetyltransferase 8 (KAT8), could be used to study the epigenetic processes in diseases related to these enzymes or to investigate HATs as therapeutic targets. However, the development of HATi is challenged by the difficulties in kinetic characterization of HAT enzymes and their inhibitors to enable calculation of a reproducible inhibitory potency. In this study, a fragment screening approach was used, enabling identification of 4-amino-1-naphthol, which potently inhibited KAT8. The inhibitor was investigated for enzyme inhibition using kinetic and calorimetric binding studies. This allowed for calculation of the  $K_i$  values for both the free enzyme as well as the acetylated intermediate. Importantly, it revealed a striking difference in binding affinity between the acetylated enzyme and the free enzyme, which could not be revealed by the  $IC_{50}$  value. This shows that kinetic characterization of inhibitors and calculation of  $K_i$  values is crucial for determining the binding constants of HAT inhibitors. We anticipate that more comprehensive characterization of enzyme inhibition, as described here, is needed to advance the field of HAT inhibitors.

**Keywords**

Histone acetyltransferases, KAT8, fragment screening, histone acetylation, inhibitor, enzyme kinetics.

**Abbreviations**

HAT, histone acetyltransferase; HATi, histone acetyltransferase inhibitor; KAT8, Lysine (K) acetyltransferase 8; Ac-CoA, acetyl coenzyme A.

## Introduction

Epigenetics is a field of study in which novel therapeutic targets are found for various diseases, such as inflammatory diseases and cancer (1). It is defined as the structural adaptation of chromosomal regions so as to register, signal or perpetuate altered transcriptional activity (2). Epigenetic processes include post-translational modifications of histones such as lysine acetylations, which play an important role in the regulation of gene transcription by controlling the chromatin structure of DNA (3). Lysine acetylations are installed by histone acetyltransferases (HATs) and removed by histone deacetylases (HDACs). These enzymes balance lysine acetylation, resulting in a controlled expression of genes. A disturbance of this balance can result in disease states, such as cancer or inflammatory diseases (4). Therefore, restoring the balance between HAT and HDAC activity using small molecule HAT inhibitors (HATi) could be a therapeutic strategy for several diseases.

Development of HATi is an important challenge that has been addressed with limited success so far. Important drawbacks of current HATi include intrinsic chemical reactivity, instability, low potency, lack of selectivity as well as the limited kinetic characterization of the inhibitors (5). Kinetic characterization of inhibitors in an early stage of lead identification is essential. Since enzyme activity assays are often used for the discovery of novel inhibitors, the 50% inhibitory concentration ( $IC_{50}$ ) is a common measure for the potency of inhibitors. However, the  $IC_{50}$  depends on the conditions used in the assay, such as the concentration of the enzyme substrates and their respective  $K_m$  values. This value is therefore not reproducible unless exactly the same assay conditions are used. The inhibitory potency ( $K_i$ ) value is a potency value independent of the assay conditions and is therefore much more representative as potency of the inhibitor (6). Calculation of the  $K_i$  value from the  $IC_{50}$  is crucial for the comparison of the potency with known inhibitors or between different assays and for the determination of selectivity. In case of competitive inhibitors of enzymes converting only one substrate, the  $K_i$  can be calculated using methods like the Cheng-Prusoff equation, Dixon plot or using double reciprocal plots (7-9). However, since HATs use a

cofactor, acetyl coenzyme A (Ac-CoA), for the acetylation of the lysine, they are bisubstrate enzymes: they convert two substrates into two products. In this case, it is not possible to use standard methods for calculation of the  $K_i$  and more elaborate kinetic evaluations are necessary (10). It is therefore important to investigate the kinetic behavior of HAT inhibitors toward determination of reproducible inhibitory constants.

The HATs are a disparate group of enzymes from which most isoenzymes can be assigned to five main families based on primary structure homology. Three families that have been studied extensively are the GNAT (GCN5-related N-acetyltransferase) family, the p300/CBP (p300/CREB binding protein) family and the MYST (acronym for MOZ, Ybf2, Sas2, and Tip60) family (11). In this study, we focused on Lysine (K) acetyltransferase 8 (KAT8), a member of the MYST HAT family. KAT8 (also: males absent on the first, MOF, or MYST 1) is part of the male-specific-lethal (MSL) complex, which specifically acetylates histone H4 lysine 16 (12). KAT8 has additionally been shown to form different complexes containing WD repeat domain 5 (WDR5, MSL1v1 or NSL complex) and MLL, broadening the substrate specificity to histone H4 lysines 5 and 8 and non-histone targets, such as lysine 120 on the tumor-suppressor protein p53 (13-15). As part of these complexes, KAT8 has been shown to play a role in stem cell pluripotency, cell proliferation and DNA damage response (16). Using KAT8 conditional deletion and a small molecule inhibitor for MYST family HATs in cell lines and a mouse model, it was recently shown to be important for sustaining MLL-AF9-driven leukemia and was suggested as a potential therapeutic target for MLL-rearranged leukemia (17). Therefore, small molecule KAT8 inhibitors could facilitate investigation of its function in disease or may be used as potential therapeutic agents.

Currently, one class of HATi have been described to inhibit KAT8, which are anacardic acid and a number of its derivatives (18). These inhibitors were shown to inhibit KAT8 by interacting with an acetylated form of the enzyme, required the binding of Ac-CoA and competed with the lysine substrate. Calculation of the  $K_i$  values revealed that although the determined  $IC_{50}$  values were above 200  $\mu$ M, the  $K_i$  values were in the range of 37 - 64  $\mu$ M. This shows that the  $k_i$  value can differ significantly from tested  $IC_{50}$  values and that this is

dependent on the mechanism of inhibition of the inhibitors. Therefore, we aimed at discovering novel, structurally unrelated KAT8 inhibitors and determining their kinetic profile.

Using a fragment screening approach, 4-amino-1-naphthol (compound **13**) was identified as a potent KAT8 inhibitor. The mechanism of KAT8 inhibition and structure-activity relationship (SAR) were investigated. Enzyme kinetic measurements as well as calorimetric binding studies suggested a reversible inhibition mode and a direct interaction with KAT8 for compound **13**. Kinetic studies allowed calculation of the  $K_i$  value for both the free enzyme form of KAT8 ( $K_{i1} = 2.6 \mu\text{M}$ ), and the acetylated form ( $K_{i2} = 0.017 \mu\text{M}$ ), which indicated very high potency for the acetylated enzyme intermediate. Taken together, our approach to link fragment screening with enzyme kinetic analysis demonstrated large affinity differences for the different enzyme species involved in catalysis, which is not obvious from the  $\text{IC}_{50}$  values. We anticipate that unravelling the inhibitory potencies of inhibitors for individual enzyme species is key to inhibitor discovery for this type of enzymes.

## Results and Discussion

### Fragment screening

Towards discovery of a novel inhibitor of KAT8, an in-house library of fragments with a broad range of structures and low molecular weight ( $\text{MW} < 250 \text{ Da}$ ), was screened for inhibition of the KAT8 HAT. An assay based on fluorescence-detection of CoA was used to screen all fragments. Currently known KAT8 inhibitors showed an  $\text{IC}_{50}$  of higher than  $200 \mu\text{M}$  under the same assay conditions (18). Taking this potency as a reference, a concentration of  $200 \mu\text{M}$  was chosen for screening the fragments. A control was included for potential fluorescence quenching by the fragments to identify and rule out any hits directly interfering with the assay. Structures containing maleimide or thiol moieties were excluded due to reactivity with the assay product or fluorophore. The resulting hits (**1** and **10**) and a small number of similar fragments were tested for their 50% inhibitory concentration ( $\text{IC}_{50}$ ) (Table 1, figure S1).

4- fluoro phenyl hydrazine (**1**) showed an IC<sub>50</sub> of 310 μM. Several phenyl hydrazines similar to **1** were investigated. 4- methoxy phenyl hydrazine (**2**) lost activity compared to **1**. Other substitution patterns like hydrogen or chlorine were not active (**3-5**). To investigate the hydrazine moiety further, 4- fluoroaniline or benzylamine (**6, 7**) were tested. These were not active, and neither were two other aniline compounds (**8, 9**), showing that the inhibition was specific for the hydrazine moiety. Taken together, no phenyl hydrazine structures were found to be more potent inhibitors than **1**. Therefore, this structural entity was not further investigated.

The hit 1-aminonaphthalene (**10**), showed an IC<sub>50</sub> of 180 μM; the most potent hit from the screening. Testing similar structures showed that 1-nitro naphthalene (**11**) or a sulphonic acid substituted aminonaphthalene (**12**) were not active. The hydroxyl substituted fragment, 4-amino-1-naphthol (**13**), showed an excellent IC<sub>50</sub> of 9.7 ± 3.0 μM. Strikingly, **9**, which is very similar to **13**, was not active, showing that the naphthalene moiety is also important for KAT8 activity. Therefore, compound **13** was investigated in more detail.

### Structure-activity relationship

A SAR study was done around the structure of **13** to investigate the importance of the different parts of the scaffold. Derivatives of **13** were synthesized and tested for their inhibitory potency on KAT8 (Table 2, figure S2). The naphthalene ring was replaced by a isoquinoline (**14**). This moiety has a slightly different logP and is weakly basic, but it did not significantly influence the activity. To investigate the importance of the free amine on R<sup>1</sup> position, the amine was included in the ring (**16**) or a carbon or carboxyl spacer was introduced (**17, 18**). These compounds did not show inhibitory activity on KAT8. Additionally, the amine was replaced by a nitro (**19**). This compounds had a reduced potency compared to **13**, but still showed activity. This suggests that the position of the amine is important, but it can be slightly modified. To investigate an *ortho* substitution to the amine, a methoxy was inserted (**20**). This reduced activity compared to **13**, but was still reasonably active. Next, the hydroxyl group was investigated. Both replacing it with a nitrile (**15**) as well as introducing a

carbon spacer (**21**), completely abolished activity. When the hydroxyl moiety was substituted with a methyl (**22**), it retained reasonable activity, but the acetyl and benzyl (**23-24**) substituted compounds lost activity, suggesting that the free hydroxyl is important for activity and there is little space for substituents here. Subsequently, substitutions to the amine were investigated. The dimethylated amine (**25**) showed good potency, but the acetylated (**26**) and propionylated (**27**) amine lost activity. Strikingly, substituting with a long aliphatic tail (**28**) recovered activity again, which is probably due to lipophilic interactions. The preference of KAT8 for lipophilic substitutions has been previously observed with the anacardic acid derived inhibitors as well (18). A phenyl instead of a aliphatic tail (**29**) also showed better activity than the propionyl, suggesting that a lipophilic or aromatic interaction is gained close to the aminonaphthol scaffold. This was observed with two sulphonamide derivatives as well (**30, 31**). These derivatives showed good activity for KAT8 and the toluene sulphonyl derivative was approximately twice as active as the methyl sulphonyl, suggesting a gained lipophilic or aromatic interaction. However, none of the derivatives was significantly more active than compound **13**. Therefore, compound **13** was chosen for further investigation.

### **Inhibitor properties**

An often encountered problem with high-throughput screening is the discovery of hits that turn out to be pan assay-interfering compounds (PAINS) (19). Computational tools are available to easily test structural entities for PAIN properties (20), but recent criticism warns against blind use of these tools, since it was observed that the tools will not recognize all PAIN structures (21). It is therefore necessary to experimentally test the properties of the high throughput hit to test for PAINS behavior. Therefore, compound **13** was investigated for thiolreactivity, stability, reversibility, anti-oxidant properties and selectivity.

Compounds similar to compound **13** were discovered to be assay interfering compounds (PAINS), seeming to inhibit the HAT Rtt109 in an assay based on detection of the product CoA, but instead reacting with the thiol group of the product, which prevented detection of CoA (22). The proposed mechanism was a Michael addition-elimination reaction

in which the thiol, glutathion, replaced a thiol or halogen substituent on position 2 from the hydroxyl moiety. Therefore, the thiolreactivity of compound **13** was investigated in an assay containing all elements of the  $IC_{50}$  assay, but where Ac-CoA was replaced with CoA (Figure S3). No reduction in fluorescence was found in this assay, suggesting that compound **13** does not react with thiols under these conditions. Additionally, the stability of compound **13** was investigated using HPLC and no degradation of the compound was observed for at least 4 hours of incubation with the assay buffer (Figure S4). Longer incubation times were not tested.

To investigate whether **13** shows irreversible inhibition, a pre-incubation assay was performed (Figure 1A). Three different concentrations (0.75, 2 and 10 x the  $IC_{50}$ ) of compound **13** were pre-incubated with KAT8 for 2, 5 or 10 minutes before adding the enzyme substrates and measuring enzyme activity. An irreversible inhibitor will show time-dependent inhibition and therefore give more inhibition when pre-incubated with the enzyme for a longer time. However, no difference was observed between 2, 5 or 10 minutes pre-incubation with any of the concentrations, indicating that **13** is a reversible inhibitor of KAT8. This was confirmed using a dilution experiment (Figure 1A) in which KAT8 was pre-incubated with **13** at a concentration of > 5 times the  $IC_{50}$  value and subsequently diluted 100 times in a solution containing the substrates. The enzyme activity was measured over time and was shown to recover linearly, indicating a fully reversible inhibitor (23). These data are consistent with a model where **13** is a reversible inhibitor of KAT8.

Due to their phenolic structure, **13** and several other derivatives from the SAR have anti-oxidant activity. Although KAT8 does not depend on redox cycling mechanisms in its enzymatic reaction, it may interfere with the assay, which could lead to observation of inhibition, where no true inhibition of KAT8 takes place. Therefore, the anti-oxidant activity of **13** and all derivatives was determined in a DPPH (2,2-diphenyl-1-picrylhydrazyl) assay, a widely used assay for determination of anti-oxidant activity of single molecules (24). The concentration that gave 50% reduction in DPPH absorbance ( $EC_{50}$ ) was determined for all compounds (Figure S5A). As expected, many derivatives containing the phenolic structure

were anti-oxidants, showing very similar  $EC_{50}$ 's between 7 and 26  $\mu$ M. However, their anti-oxidant activity did not show a relationship with their inhibitory activity on KAT8. For example, many compounds showing anti-oxidant activity, did not show KAT8 inhibition (**9**, **23**, **26**, **27**). Compound **19** showed no anti-oxidant activity due to the strong deactivating properties of the nitro substituent, but did show inhibitory activity on KAT8. Additionally, the  $IC_{50}$  of compound **13** was determined in the presence of non-thiol containing redox active substances (tris(2-carboxyethyl)phosphine (TCEP, 1  $\mu$ M),  $NAD^+$  (nicotinamide adeninedinucleotide, 100  $\mu$ M) and  $NADH$  (100  $\mu$ M)) (Figure S5B). The presence of these redox active substances in the assay did not significantly influence the  $IC_{50}$  of **13**. Taken together, these data indicate that the anti-oxidant activity of compound **13** does not influence the inhibition of KAT8.

The selectivity of **13** and the active derivatives was investigated using KAT3B and KAT2B, representing two main other HAT families; p300/CBP and GNAT. An assay similar to that of KAT8 based on fluorescence detection of CoA was set up for KAT2B and KAT3B and the  $IC_{50}$  values of **13** and all derivatives showing activity on KAT8, were determined for KAT2B and KAT3B (Table 2, Figure S6 and S7). Compound **13** showed inhibitory activity for both KAT2B ( $IC_{50} = 3.6 \pm 1.1$ ) and KAT3B ( $IC_{50} = 1.4 \pm 0.1$ ). Although the derivatives showed in general no selectivity over KAT2B and KAT3B, based on  $IC_{50}$  values, some differences were observed. For example, compound **22** shows activity for KAT8 and KAT3B, but seems inactive on KAT2B, suggesting that substitutions on the hydroxyl group are even more constrained for this enzyme. Additionally, compound **19** shows moderate activity on KAT8 and is preferred above for example **20** and **28**, but on KAT2B and KAT3B, it is less active compared to these others. This suggests that the nitro group is not preferred on KAT2B and KAT3B as on KAT8. Therefore, although **13** and derivatives are generally non-selective between KAT8, KAT2B and KAT3B based on  $IC_{50}$  values, the different enzymes were inhibited to different extents by the derivatives.

However, due to differences in catalytic mechanisms, substrates and substrate affinities of the different HATs, which all influence the  $IC_{50}$  values, for accurate comparison of the potency for different enzymes, the  $K_i$  values should be calculated. For the calculation of

the  $K_i$  values it is essential to determine the  $K_m$  values of the substrates for KAT2B and KAT3B. Therefore, both KAT2B and KAT3B were kinetically investigated for their catalytic mechanisms as initially done for KAT8 (Figure S8A/B). KAT2B showed sigmoidal kinetics, suggesting a catalytic process with multiple steps of different velocities, for example cooperative subunits or two preferred catalytic mechanisms which depend on the concentration of Ac-CoA present (10) (Figure S8A). This deviation from Michaelis-Menten kinetics is clearly observed when transforming the data to a Lineweaver-Burke plot. The normally linear regression of the double reciprocal is not linear, but curves upward (Figure S8A). In case of KAT3B, it was not possible to fully reach saturation of the velocity (Figure S8B). The histone 3 peptide substrate (H3 substrate), for which p300 has affinity as well, showed the same behavior. Unfortunately, since the determination of  $K_m$  values is based on model enzymes that follow Michaelis-Menten kinetics, in both of these cases it is not currently described how to determine  $K_m$  values of the substrates. Therefore, calculation of the  $K_m$  values, and an accurate determination of the selectivity of the inhibitors, could not be done and remains to be investigated.

Additionally, the selectivity of compound **13** was investigated towards two unrelated enzymes, human arginase 1 and histone deacetylase 3 (HDAC3) (Figure S9). Compound **13** was tested for activity on HDAC3 in a biochemical enzyme activity assay and on human arginase 1 in a binding assay based on differential scanning fluorimetry (DSF). Compound **13** showed inhibition of HDAC3 at higher concentrations (estimated  $IC_{50} \approx 80 - 90 \mu M$ ). In the DSF assay, compound **13** showed no change in the melting temperature ( $T_m$ ) of human arginase 1, suggesting that compound **13** did not bind this enzyme.

Taken together, considering the lack of selectivity for other HATs and HDAC3 and its anti-oxidant properties, which could cause effects unrelated to KAT8 inhibition in more advanced systems such as cells, we would not suggest using compound **13** for development of a selective drug targeting KAT8. However, control experiments suggest compound **13** does not interfere in the KAT8 assay due to thiolreactivity or its anti-oxidant properties. Since the aim of this study was to investigate the kinetic behavior of an inhibitor structurally

unrelated to the current inhibitors on KAT8, compound **13** was considered suitable for further investigation of the mechanism of inhibition.

## Mechanism of inhibition

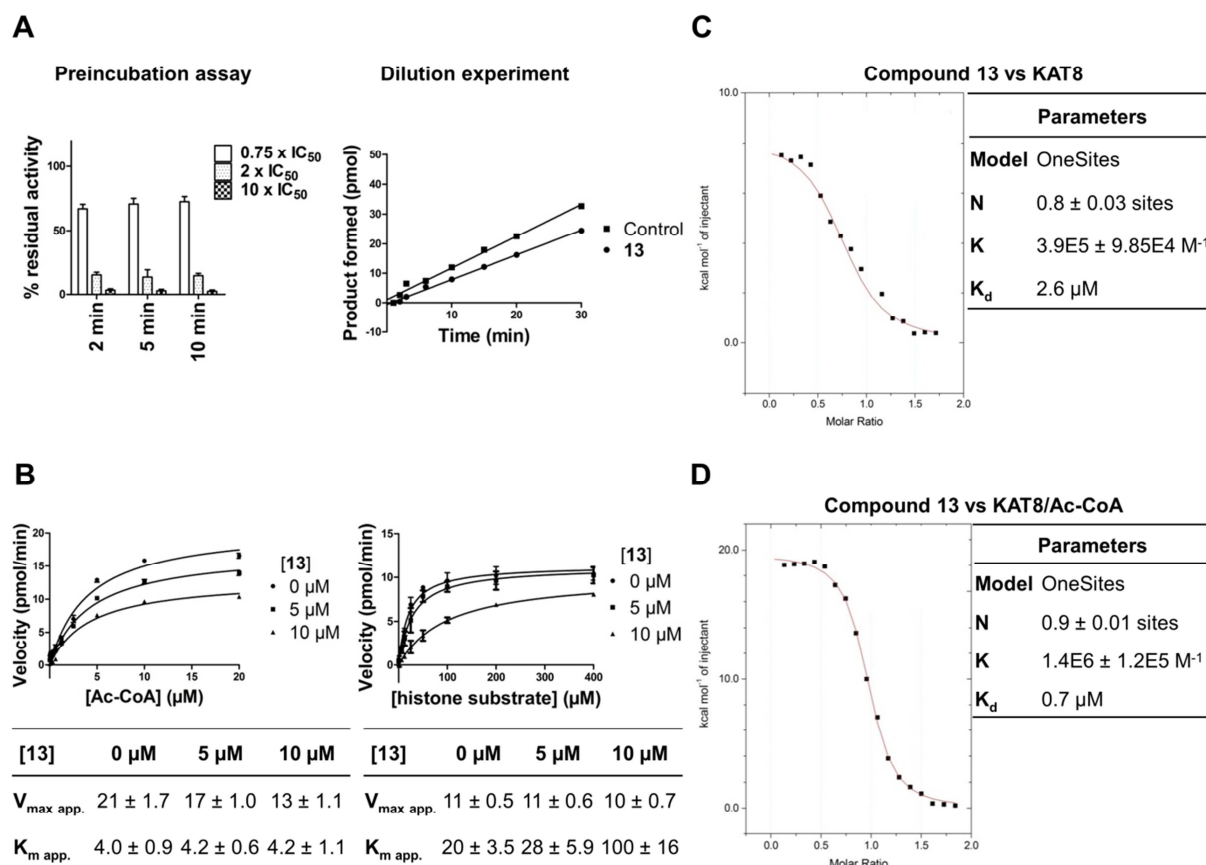


**Figure 1.** A) A preincubation assay was performed to investigate whether **13** is an irreversible inhibitor. Compound **13** ( $0.75$ ,  $2$  and  $10 \times \text{IC}_{50}$ ) was preincubated for  $2$ ,  $5$  or  $10$  minutes with KAT8. Subsequently, the substrates were added and the enzyme reaction was performed. No difference in percentage inhibition was observed between  $2$ ,  $5$  or  $10$  minutes preincubation with any of the concentrations. This indicates that **13** is a reversible inhibitor. A dilution experiment was done to further confirm that **13** is a reversible inhibitor. KAT8 was preincubated with **13** at a concentration of  $50 \mu\text{M}$  ( $> 5$  times the  $\text{IC}_{50}$ ) and subsequently diluted  $100$  times in a solution containing the substrates. The enzyme activity was recovered linearly over time, indicating fully reversible inhibition. B) The velocity of the substrate conversion of KAT8 was measured at increasing concentrations of Ac-CoA in the presence of different concentrations of **13**. An increase in **13** concentration resulted in a decrease in  $V_{\max}$ , but no change in the  $K_m$  of Ac-CoA. This indicates non-competitive behavior with Ac-CoA. The velocity of the substrate conversion of KAT8 was measured at increasing concentrations of histone substrate in the

presence of different concentrations of **13**. An increase in **13** concentration did not influence the  $V_{max}$ , but resulted in an increase in  $K_m$  of the histone substrate. This indicates competitive behavior with the histone substrate. C) The equilibrium dissociation constant ( $K_d$ ) of **13** to KAT8 was determined using isothermal titration calorimetry (ITC). Compound **13** showed a  $K_d$  of 2.6  $\mu$ M for KAT8. N = stoichiometry, K = association constant ( $1/K_d$ ),  $K_d$  = equilibrium dissociation constant ( $1/K$ ). D) The equilibrium dissociation constant ( $K_d$ ) of **13** to KAT8 in the presence of Ac-CoA was determined using isothermal titration calorimetry (ITC). Compound **13** showed a  $K_d$  of 0.7  $\mu$ M. N = stoichiometry, K = association constant ( $1/K_d$ ),  $K_d$  = equilibrium dissociation constant ( $1/K$ ).

To investigate the mechanism of inhibition by **13**, kinetic studies were done using Michaelis-Menten enzyme kinetics. The velocity of substrate conversion by KAT8 was measured at increasing concentrations of Ac-CoA or histone substrate in the presence of different concentrations of **13**. The apparent maximal velocity ( $V_{max\ app.}$ ) and Michaelis constants ( $K_{m\ app.}$ ) of Ac-CoA and the histone substrate were determined. In case of Ac-CoA, an increase in **13** concentration resulted in a decrease in  $V_{max\ app.}$ , but no change in the  $K_{m\ app.}$  of Ac-CoA (Figure 1B). This indicates non-competitive behavior with Ac-CoA, where binding of **13** does not influence binding of Ac-CoA. In case of the histone substrate, an increase in **13** concentration did not influence the  $V_{max\ app.}$ , but resulted in an increase in  $K_{m\ app.}$  of the histone substrate. This indicates competitive behavior with the histone substrate. KAT8 has been shown to operate via a ping-pong mechanism (18) in which Ac-CoA has to bind first to KAT8, followed by an acetylation of the enzyme, which creates a second intermediate form of the enzyme. Subsequently the histone substrate binds and is acetylated, generating the acetylated lysine and returning KAT8 back to its free form. Competitive behavior of **13** with the histone substrate therefore suggests that **13** binds not only to the free KAT8 enzyme, but also to the acetylated intermediate.

To further investigate this, binding studies of **13** to KAT8 were done using isothermal titration calorimetry (ITC). Compound **13** was titrated to KAT8 in the absence of Ac-CoA (the free enzyme) and the equilibrium dissociation constant ( $K_d$ ) of **13** was determined ( $2.6 \pm 0.7$   $\mu$ M, Figure 1C, Figure S10A). The stoichiometry of the interaction was close to one, suggesting that one molecule of **13** binds to one molecule of KAT8. Compound **13** thus

directly interacts with KAT8. Additionally, **13** was titrated to KAT8 in the presence of Ac-CoA to generate a certain amount of the acetylated/Ac-CoA bound enzyme form. The binding data showed a  $K_d$  of  $0.7 \pm 0.06 \mu\text{M}$  (Figure 1D, Figure S10B). The  $K_d$  for Ac-CoA bound KAT8 is lower than for free KAT8, indicating that **13** binds with a higher affinity to the acetylated intermediate than to the free enzyme. These data suggest that compound **13** inhibits KAT8 by interacting both with the free enzyme form as well as with the Ac-CoA bound form, but has higher affinity for the acetylated intermediate.

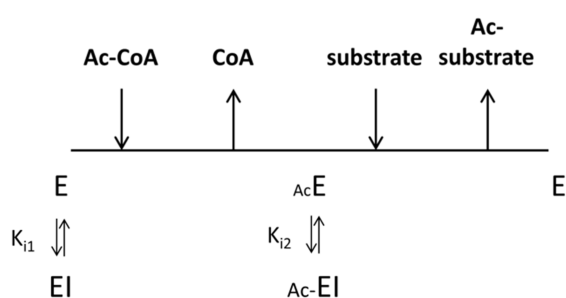


**Figure 2.** KAT8 uses a ping-pong mechanism in which the cofactor, acetyl coenzyme A (Ac-CoA), binds first to the free enzyme form (E) and acetylates a residue on the enzyme (AcE). Coenzyme A (CoA) leaves the enzyme as product. Subsequently, the histone substrate can bind and is acetylated by the enzyme. The enzyme returns to its free form (E). Compound **13** (I) can interact with the free enzyme (E), with an inhibitory potency ( $K_{i1}$ ). It can also interact with the acetylated enzyme form (AcE) with an inhibitory potency ( $K_{i2}$ ).

### Determination of the $K_i$ values

The  $IC_{50}$  value determined in an enzyme inhibition assay is dependent on the conditions used in the assay, such as the concentration of the enzyme substrates and their respective  $K_m$  values. This value is therefore not reproducible unless exactly the same assay conditions are used. The  $K_i$  value is a potency value independent of the substrate concentration and  $K_m$  values and is therefore much more representative as potency of the inhibitor (6). Calculation of the  $K_i$  value from the  $IC_{50}$  is crucial for the comparison of the potency with known inhibitors or between different assays and for the determination of selectivity. KAT8 is a bi-substrate enzyme that converts two substrates (Ac-CoA and the histone substrate) to two products (CoA and the acetylated histone substrate). Therefore, knowledge on the catalytic mechanism of the enzyme, as well as the mechanism of inhibition

by the inhibitor is needed to calculate the  $K_i$  value (9). It was previously reported by us that KAT8 follows a ping-pong mechanism in which Ac-CoA binds first and acetylates a residue on the enzyme. Subsequently the histone substrate binds and is acetylated (18). Combining the knowledge that KAT8 follows a ping-pong mechanism and that **13** inhibits KAT8 by interacting both with the free enzyme form as with the Ac-CoA bound form as determined from the kinetic experiments, equation 1 can be used to calculate the  $K_i$  values (9). It must be noticed that this equation yields two  $K_i$  values, one for the free KAT8 enzyme ( $K_{i1}$ ) and one for the acetylated intermediate ( $K_{i2}$ ). Figure 2 schematically shows the ping-pong mechanism of KAT8 and the inhibition of **13** of the free enzyme (E) and the acetylated enzyme form (AcE) and its respective  $K_i$  values. The  $K_m$  values of Ac-CoA and the histone substrate were derived from a kinetic assay with both substrates as described by Segel (10) and were consistent with previously reported values (Figure S10C/D) (18). We assumed that the  $K_{i1}$  was equal to the  $K_d$  of **13** to KAT8 as determined by ITC, since for the process of inhibiting the free enzyme (E), only binding of **13** is of influence. The  $K_{i1}$  of **13** was therefore assumed to be 2.6  $\mu\text{M}$  and the  $K_{i2}$  was 0.017  $\mu\text{M}$  as derived from the equation (see SI for calculation). This suggests that the inhibitory potency was much better for the acetylated intermediate than for the free enzyme. This stronger interaction was also observed in the  $K_d$  value of **13** for KAT8 in presence Ac-CoA as determined by ITC, which was lower than the  $K_d$  for KAT8 in absence of Ac-CoA. Additionally, the kinetic behavior of **13** is different from the behavior of the previously reported anacardic acid derivatives, which did not interact with the free enzyme (18). This kinetic behavior has a large influence on the calculation of the resulting  $K_i$  values, suggesting that kinetic evaluations of inhibitors for this enzyme are crucial for determining inhibitory potency. Taken together, this suggests that the inhibition of compound **13** is mostly due to inhibition of the acetylated enzyme intermediate by competition with the histone substrate and that these kinetic evaluations are crucial for determining the inhibitory potency of KAT8 inhibitors.

$$K_b A + K_a B + AB = \left( \frac{K_b}{B} \frac{1}{K_{i2}} + \frac{K_a}{A} \frac{1}{K_{i1}} \right) IC_{50}$$

Eq.1

IC<sub>50</sub> = the IC<sub>50</sub> determined in the enzyme inhibition assay

K<sub>a</sub> = K<sub>m</sub> of Ac-CoA

K<sub>b</sub> = K<sub>m</sub> of the histone substrate

A = the concentration of Ac-CoA used in the IC<sub>50</sub> assay

B = the concentration of the histone substrate used in the IC<sub>50</sub> assay

K<sub>i1</sub> = the K<sub>i</sub> of **13** for the free enzyme

K<sub>i2</sub> = the K<sub>i</sub> of **13** for the acetylated intermediate

## Conclusion

In conclusion, this study describes the discovery of a potent fragment inhibitor of KAT8, compound **13**, via a fragment screening approach. A SAR study was done, which showed that **13** could be modified, although no derivatives were found that were significantly more potent. Investigation of the compound properties suggested that compound **13** was not selective for other HATs or HDAC3 and had anti-oxidant properties. However, experiments with CoA and redox active substances suggest compound **13** was a reversible inhibitor that did not interfere in the KAT8 assay due to thiolreactivity or its anti-oxidant properties. Therefore it was used for investigation of its mechanism of inhibition of KAT8. The results of kinetic studies and ITC are consistent with a model where the fragment interacts with both the free enzyme and the acetylated intermediate form. This enabled the calculation of the assay-independent K<sub>i</sub> values of **13** for both the free enzyme form of KAT8 (K<sub>i1</sub> = 2.6 μM), and the acetylated form (K<sub>i2</sub> = 0.017 μM), which suggested that its inhibition is mostly due to interaction with the acetylated form of the enzyme. Taken together, in this study a fragment screening is presented that provides a fragment inhibitor of KAT8 that is further characterized by enzyme kinetics and biophysics. This combination reveals a striking difference in binding affinity between the acetylated enzyme and the free enzyme that is not revealed by the IC<sub>50</sub> determinations. This shows that kinetic characterization of inhibitors and calculation of K<sub>i</sub>

values is crucial for determining the binding constants of HAT inhibitors. We anticipate that more comprehensive characterization of enzyme inhibition, as described here, is needed to advance the field of HAT inhibitors.

### **Experimental Procedures**

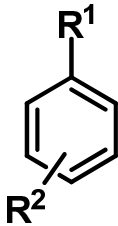
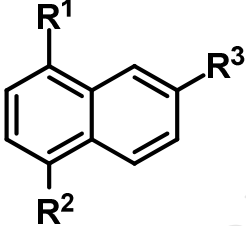
Detailed description of the experimental procedures can be found in the supplementary material.

### **Acknowledgements**

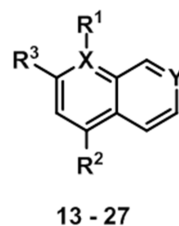
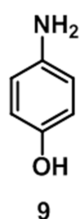
We acknowledge the European Research Council for providing an ERC starting grant (309782) and the NWO for providing a VIDI grant (723.012.005) to F. J. Dekker. This work was supported by PRIN 2012 (prot. 2012CTAYSY) to D. Rotili and PRIN 2016 (prot. 20152TE5PK) to A. Mai.

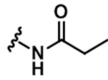
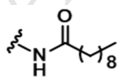
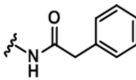
## Tables

**Table 1:** IC<sub>50</sub> values of the fragment screening hits and a small number of related structures.

Compound	R <sup>1</sup>	R <sup>2</sup>	R <sup>3</sup>	IC <sub>50</sub> (μM)
<b>1-9</b>				
<b>10-13</b>				
<b>1</b>	-NHNH <sub>3</sub> <sup>+</sup> Cl <sup>-</sup>	4 - F	-	310
<b>2</b>	-NHNH <sub>3</sub> <sup>+</sup> Cl <sup>-</sup>	4 - OCH <sub>3</sub>	-	680
<b>3</b>	-NHNH <sub>2</sub>	H	-	>1000
<b>4</b>	-NHNH <sub>3</sub> <sup>+</sup> Cl <sup>-</sup>	H	-	>1000
<b>5</b>	-NHNH <sub>3</sub> <sup>+</sup> Cl <sup>-</sup>	2, 4 - Cl	-	>1000
<b>6</b>	-NH <sub>2</sub>	4- F	-	>1000
<b>7</b>	-CH <sub>2</sub> NH <sub>2</sub>	4-F	-	>1000
<b>8</b>	-NH <sub>2</sub>	4- Cl	-	>1000
<b>9</b>	-NH <sub>2</sub>	4- OH	-	>1000
<b>10</b>	-NH <sub>2</sub>	H	H	181
<b>11</b>	-NO <sub>2</sub>	H	H	>1000
<b>12</b>	-NH <sub>2</sub>	H	SO <sub>3</sub> <sup>-</sup>	940
<b>13</b>	-NH <sub>2</sub>	OH	H	9.7 ± 3.0

**Table 2:** IC<sub>50</sub> values of compound **13** derivatives and the selectivity of compounds **13**, **9** and the derivatives showing activity on KAT8. Data presented are IC<sub>50</sub> values. Me = methyl, Ac = acetyl, Bn = benzyl, n.d = not determined



Compound	R <sup>1</sup>	R <sup>2</sup>	R <sup>3</sup>	X	Y	IC <sub>50</sub> KAT8 (μM)	IC <sub>50</sub> KAT2B (μM)	IC <sub>50</sub> KAT3B (μM)
<b>13</b>	NH <sub>2</sub>	OH	H	C	C	9.7 ± 3.0	3.6 ± 1.1	1.4 ± 0.1
<b>9</b>						> 500	> 500	> 500
<b>14</b>	NH <sub>2</sub>	OH	H	C	N	7.6 ± 0.8	7.1 ± 0.8	1.1 ± 0.3
<b>15</b>	NH <sub>2</sub>	CN	H	C	C	> 500	n.d.	n.d.
<b>16</b>	-	OH	H	N	C	> 500	n.d.	n.d.
<b>17</b>	CH <sub>2</sub> NH <sub>2</sub>	OH	H	C	C	> 500	n.d.	n.d.
<b>18</b>	CONH <sub>2</sub>	OH	H	C	C	> 500	n.d.	n.d.
<b>19</b>	NO <sub>2</sub>	OH	H	C	C	141 ± 43	221 ± 115	106 ± 22
<b>20</b>	NH <sub>2</sub>	OH	OMe	C	C	177 ± 22	200 ± 28	52 ± 28
<b>21</b>	NH <sub>2</sub>	CH <sub>2</sub> O H	H	C	C	> 500	n.d.	n.d.
<b>22</b>	NH <sub>2</sub>	OMe	H	C	C	89 ± 11	> 500	95 ± 60
<b>23</b>	NH <sub>2</sub>	OAc	H	C	C	> 500	n.d.	n.d.
<b>24</b>	NH <sub>2</sub>	OBn	H	C	C	> 500	n.d.	n.d.
<b>25</b>	NMe <sub>2</sub>	OH	H	C	C	23 ± 4	4.2 ± 1.9	3.7 ± 2.1
<b>26</b>	NHAc	OH	H	C	C	> 500	n.d.	n.d.
<b>27</b>		OH	H	C	C	> 500	n.d.	n.d.
<b>28</b>		OH	H	C	C	250 ± 96	160 ± 25	60 ± 22
<b>29</b>		OH	H	C	C	365 ± 110	> 500	250 ± 137
<b>30</b>	NHSO <sub>2</sub> Me	OH	H	C	C	66 ± 12	3.8 ± 2.8	3.0 ± 1.9
<b>31</b>	NHSO <sub>2</sub> <sup>t</sup> oluene	OH	H	C	C	37 ± 5.3	12 ± 1.4	2.6 ± 1.4

Me = methyl, Ac = acetyl, Bn = benzyl, n.d = not determined

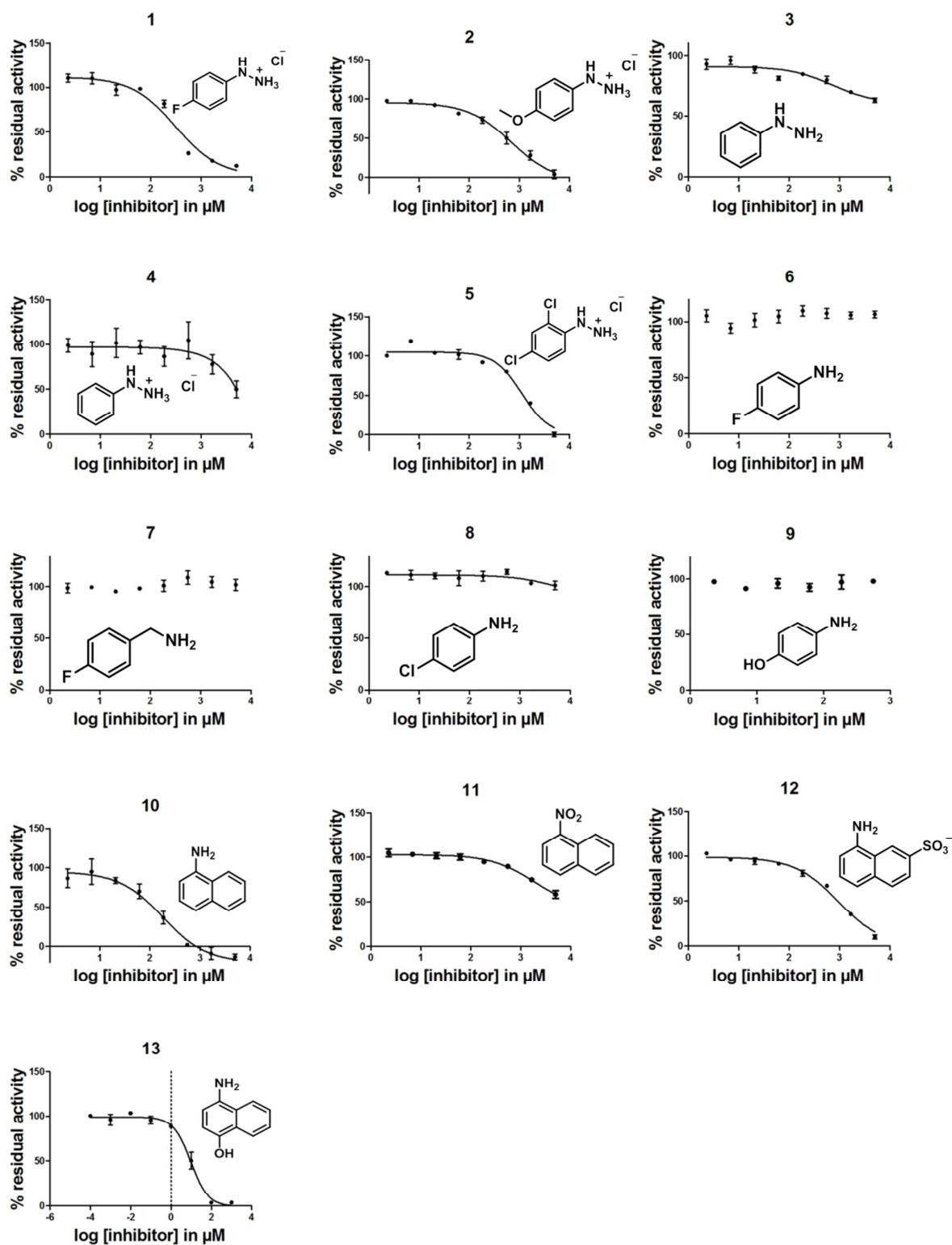
**References**

- (1) Ganesan A. Multitarget Drugs: an Epigenetic Epiphany. *ChemMedChem* 2016 Jun 20;11(12):1227-1241.
- (2) Bird A. Perceptions of epigenetics. *Nature* 2007;447(7143):396-398.
- (3) Strahl BD, Allis CD. The language of covalent histone modifications. *Nature* 2000;403(6765):41-45.
- (4) Kaypee S, Sudarshan D, Shanmugam MK, Mukherjee D, Sethi G, Kundu TK. Aberrant lysine acetylation in tumorigenesis: Implications in the development of therapeutics. *Pharmacol Ther* 2016 Jun;162:98-119.
- (5) Simon RP, Robaa D, Alhalabi Z, Sippl W, Jung M. KATching-Up on Small Molecule Modulators of Lysine Acetyltransferases. *J Med Chem* 2016 Feb 25;59(4):1249-1270.
- (6) Wapenaar H, Dekker FJ. Histone acetyltransferases: challenges in targeting bi-substrate enzymes. *Clin Epigenetics* 2016 May 26;8:59-016-0225-2.
- (7) Lineweaver H, Burk D. The Determination of Enzyme Dissociation Constants. *J Am Chem Soc* 1934 03/01;56(3):658-666.
- (8) Dixon M. The determination of enzyme inhibitor constants. *Biochem J* 1953 Aug;55(1):170-171.
- (9) Cheng Y, Prusoff WH. Relationship between the inhibition constant (K<sub>1</sub>) and the concentration of inhibitor which causes 50 per cent inhibition (I<sub>50</sub>) of an enzymatic reaction. *Biochem Pharmacol* 1973 Dec 1;22(23):3099-3108.
- (10) Segel I, H. *Enzyme Kinetics: Behavior and Analysis of Rapid Equilibrium and Steady-State Enzyme Systems.* : Wiley Classics Library; 1993.
- (11) Marmorstein R. Structure and function of histone acetyltransferases. *Cell Mol Life Sci* 2001 May;58(5-6):693-703.
- (12) Smith ER, Cayrou C, Huang R, Lane WS, Cote J, Lucchesi JC. A human protein complex homologous to the Drosophila MSL complex is responsible for the majority of histone H4 acetylation at lysine 16. *Mol Cell Biol* 2005 Nov;25(21):9175-9188.
- (13) Dou Y, Milne TA, Tackett AJ, Smith ER, Fukuda A, Wysocka J, et al. Physical association and coordinate function of the H3 K4 methyltransferase MLL1 and the H4 K16 acetyltransferase MOF. *Cell* 2005 Jun 17;121(6):873-885.
- (14) Li X, Wu L, Corsa CA, Kunkel S, Dou Y. Two mammalian MOF complexes regulate transcription activation by distinct mechanisms. *Mol Cell* 2009 Oct 23;36(2):290-301.
- (15) Cai Y, Jin J, Swanson SK, Cole MD, Choi SH, Florens L, et al. Subunit composition and substrate specificity of a MOF-containing histone acetyltransferase distinct from the male-specific lethal (MSL) complex. *J Biol Chem* 2010 Feb 12;285(7):4268-4272.

- (16) Rea S, Xouri G, Akhtar A. Males absent on the first (MOF): from flies to humans. *Oncogene* 2007 Aug 13;26(37):5385-5394.
- (17) Valerio DG, Xu H, Chen CW, Hoshii T, Eisold ME, Delaney C, et al. Histone Acetyltransferase Activity of MOF Is Required for MLL-AF9 Leukemogenesis. *Cancer Res* 2017 Apr 1;77(7):1753-1762.
- (18) Wapenaar H, van der Wouden PE, Groves MR, Rotili D, Mai A, Dekker FJ. Enzyme kinetics and inhibition of histone acetyltransferase KAT8. *Eur J Med Chem* 2015 Nov 13;105:289-296.
- (19) Baell JB. Observations on screening-based research and some concerning trends in the literature. *Future Med Chem* 2010 Oct;2(10):1529-1546.
- (20) Aldrich C, Bertozzi C, Georg GI, Kiessling L, Lindsley C, Liotta D, et al. The Ecstasy and Agony of Assay Interference Compounds. *ACS Chem Biol* 2017 Mar 17;12(3):575-578.
- (21) Capuzzi SJ, Muratov EN, Tropsha A. Phantom PAINS: Problems with the Utility of Alerts for Pan-Assay INterference CompoundS. *J Chem Inf Model* 2017 Mar 27;57(3):417-427.
- (22) Dahlin JL, Nissink JW, Strasser JM, Francis S, Higgins L, Zhou H, et al. PAINS in the assay: chemical mechanisms of assay interference and promiscuous enzymatic inhibition observed during a sulfhydryl-scavenging HTS. *J Med Chem* 2015 Mar 12;58(5):2091-2113.
- (23) Copeland R. Evaluation of Enzyme Inhibitors in Drug Discovery: A Guide for Medicinal Chemists and Pharmacologists. 2nd ed.: Wiley; 2013.
- (24) Kedare SB, Singh RP. Genesis and development of DPPH method of antioxidant assay. *J Food Sci Technol* 2011 Aug;48(4):412-422.

## Supplementary material

## Fragment screening

Figure S1. IC<sub>50</sub> curves of compound 1 - 13 from the fragment screening

## Structure activity relationship

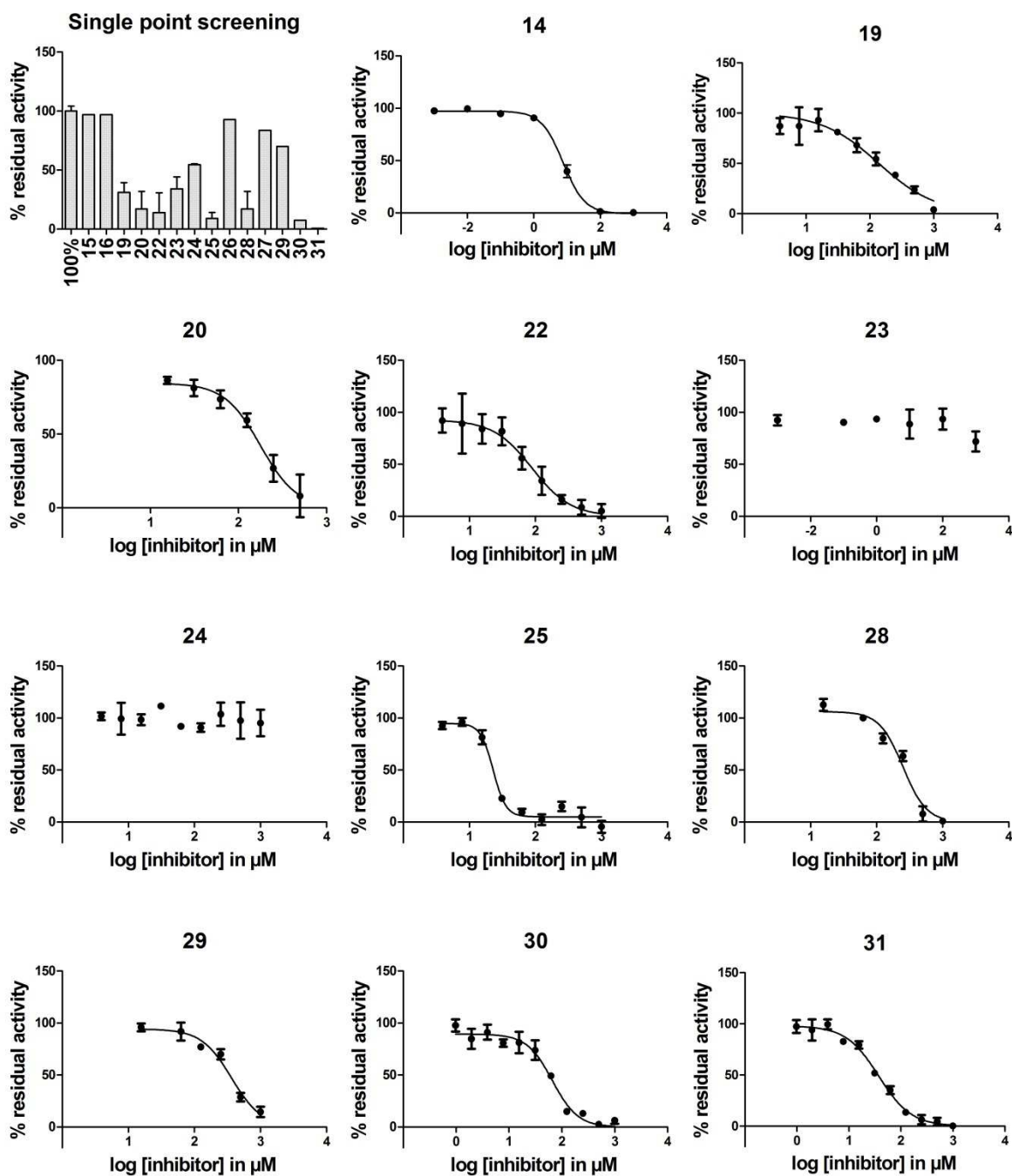


**Figure S2.** The derivatives of 13 were tested for inhibition of KAT8. A single point screening was done at a concentration of 250  $\mu\text{M}$ . Derivatives showing inhibition, were tested for their  $\text{IC}_{50}$  values.

## Inhibitor properties

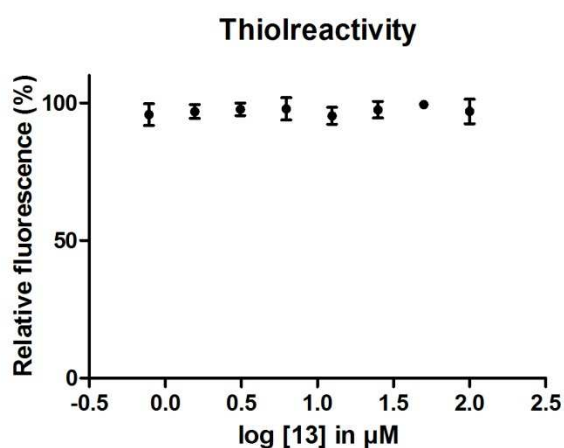


**Figure S3.** The thiolreactivity of compound **13** was investigated. The fluorescence intensity was measured in the presence of CoA (4  $\mu\text{M}$ ), histone substrate (60  $\mu\text{M}$ ), KAT8 (250 nM) and the compound **13** (0 – 100  $\mu\text{M}$  in 2% DMSO). No decrease in fluorescence was observed.

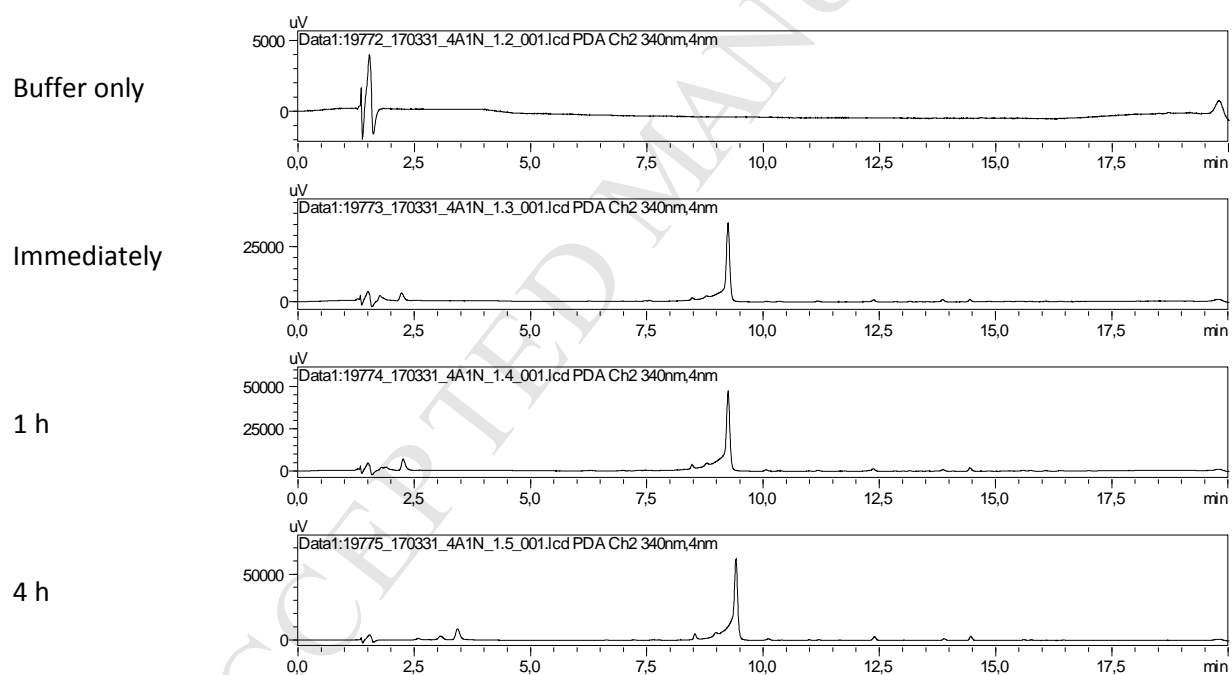
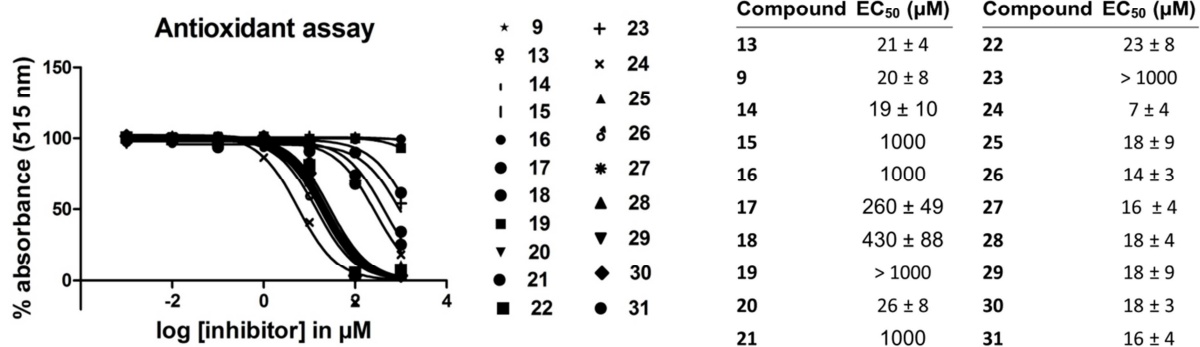


**Figure S4.** Stability of compound **13** in assay buffer. HPLC of compound **13** in assay buffer after 0, 1 and 4 hours of incubation.

A



B

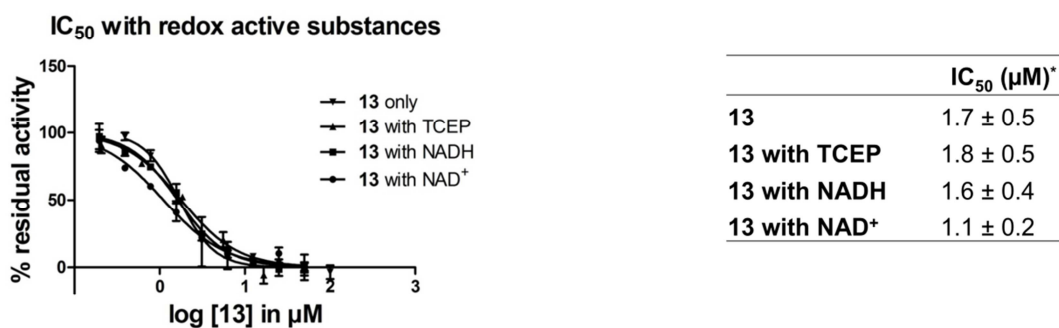


**Figure S5.** A) The antioxidant activity (EC<sub>50</sub>) of **9**, **13** and all derivatives was measured in a DPPH assay. B) The IC<sub>50</sub> of **13** was measured in the presence of TCEP (1 μM), NAD<sup>+</sup> (100 μM) and NADH (100 μM). \* Different conditions were used for this assay: Ac-CoA (1 μM), histone substrate (60 μM) and KAT8 (14.5 nM).

## Selectivity

## KAT2B

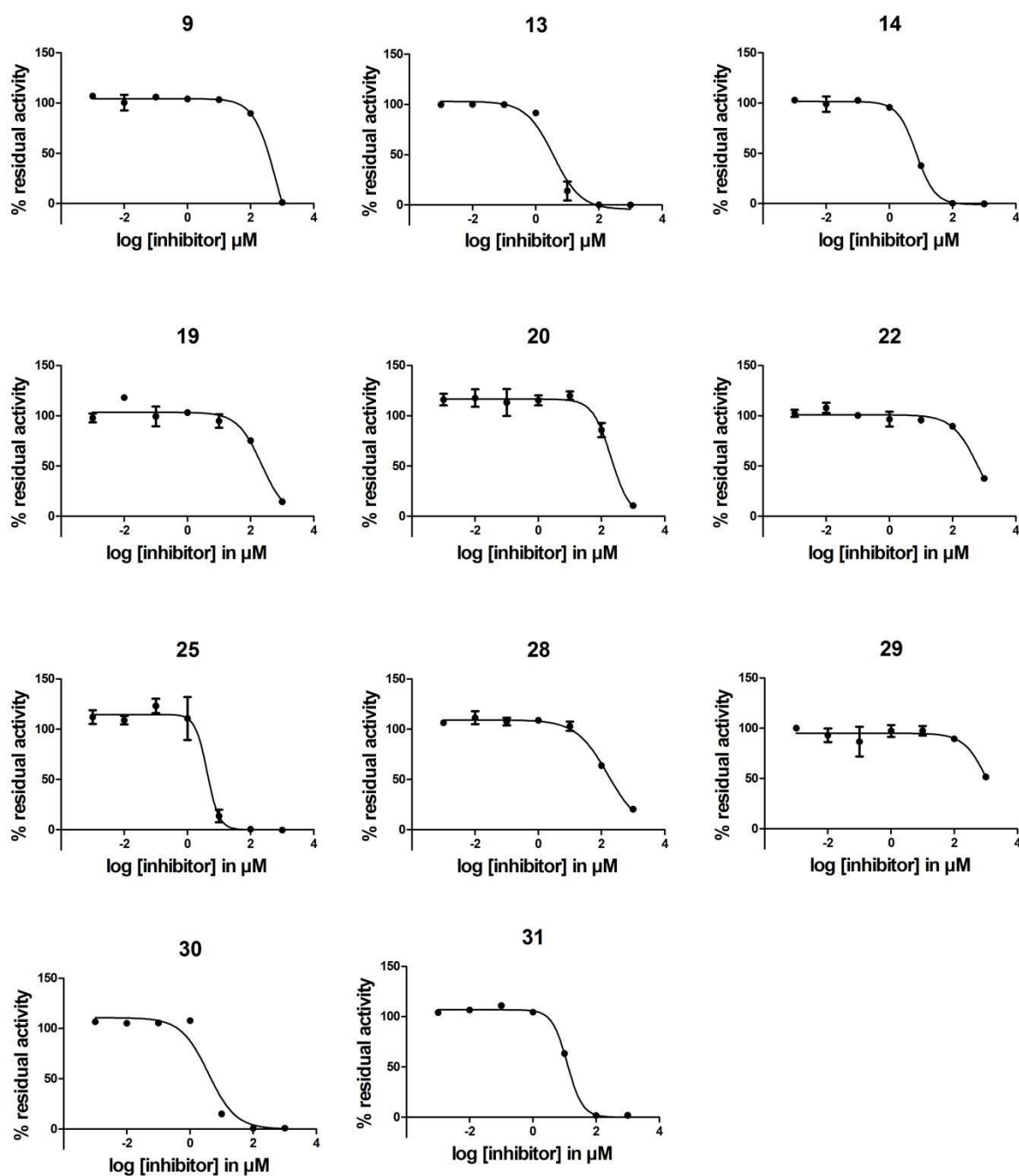


**Figure S6.** Compounds **9**, **13** and all derivatives active on KAT8, were tested for activity on KAT2B. IC<sub>50</sub> curves of these compounds on KAT2B under the following conditions: 25  $\mu\text{M}$  histone H3 substrate, 10  $\mu\text{M}$  Ac-CoA and 100 nM KAT2B.

## KAT3B

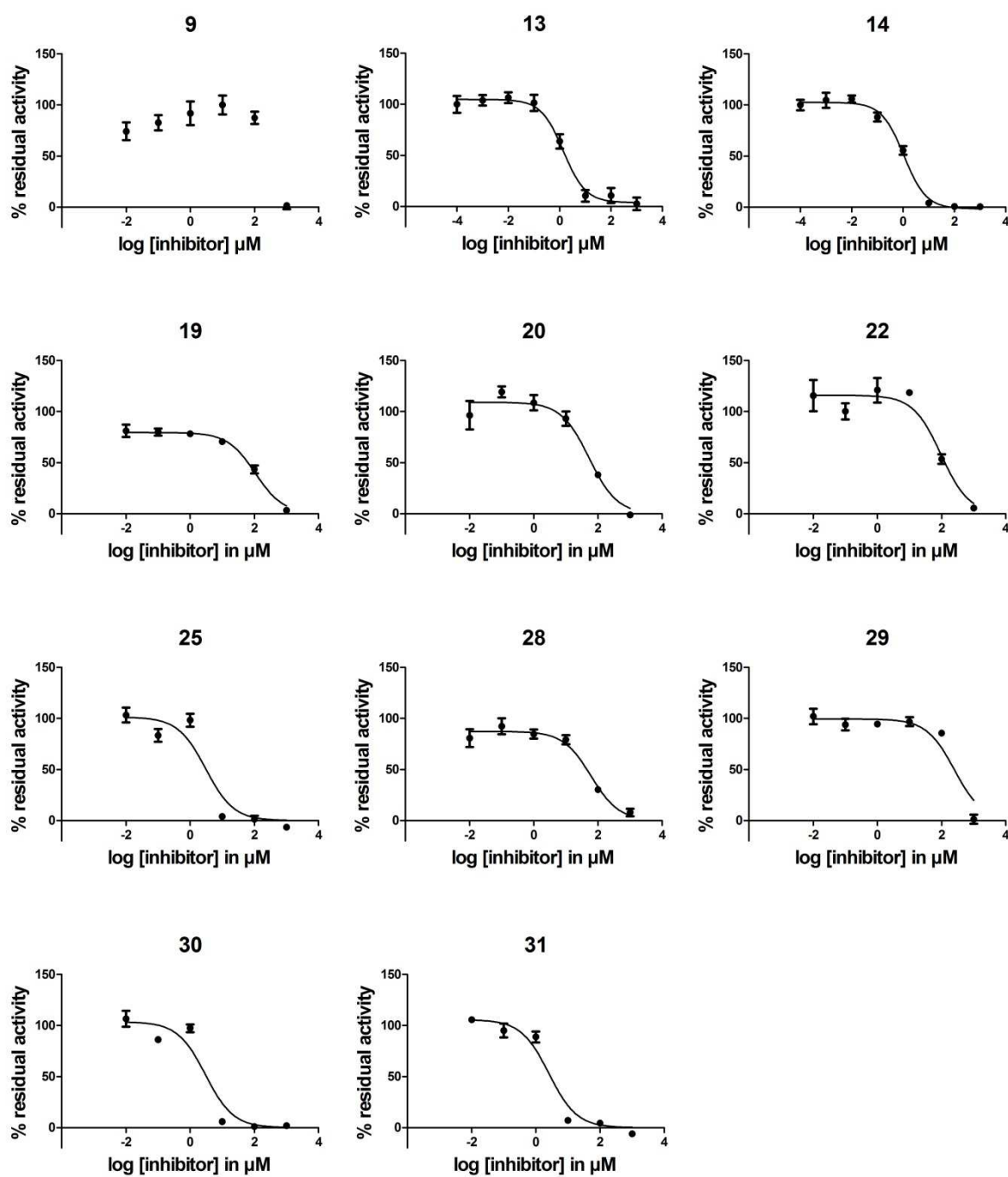


**Figure S7.** Compounds **9**, **13** and all derivatives active on KAT8, were tested for activity on KAT3B. IC<sub>50</sub> curves of these compounds on KAT2B under the following conditions: 100 μM histone H4 substrate, 50 μM Ac-CoA and 100 nM KAT3B.

## Kinetic evaluation of KAT2B and KAT3B

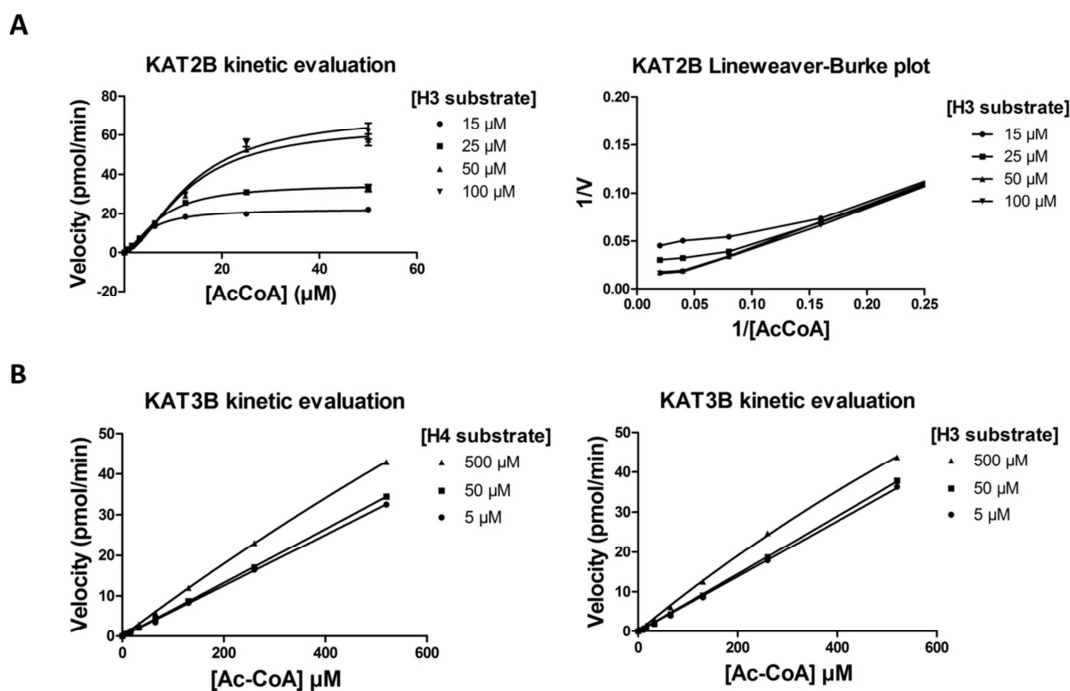


**Figure S8.** The catalytic mechanism of KAT2B and KAT3B was investigated with the aim of determining the  $K_m$  values of their substrates. A) The velocity of KAT2B was measured at increasing concentrations of Ac-CoA (0-20  $\mu\text{M}$ ) in the presence of different concentrations of the histone H3 substrate (15, 25, 50 and 100  $\mu\text{M}$ ). The enzyme showed sigmoidal kinetics. The Lineweaver-Burke plot was created by transforming the data to the double reciprocal and was shown to be not linear. B) The velocity of KAT3B was measured at increasing concentrations of Ac-CoA (0-500  $\mu\text{M}$ ) in the presence of different concentrations of histone H3 substrate or histone H4 substrate (5, 50 and 500  $\mu\text{M}$ ). Saturation could not be reached under these conditions.

## HDAC3 and arginase 1

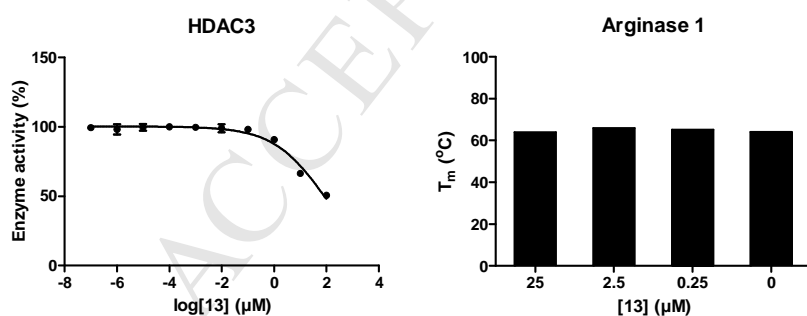


**Figure S9.** The selectivity of compound 13 was tested for HDAC3 in a biochemical enzyme inhibition assay and for arginase 1 in a differential scanning fluorimetry based assay.

## Mechanism of inhibition

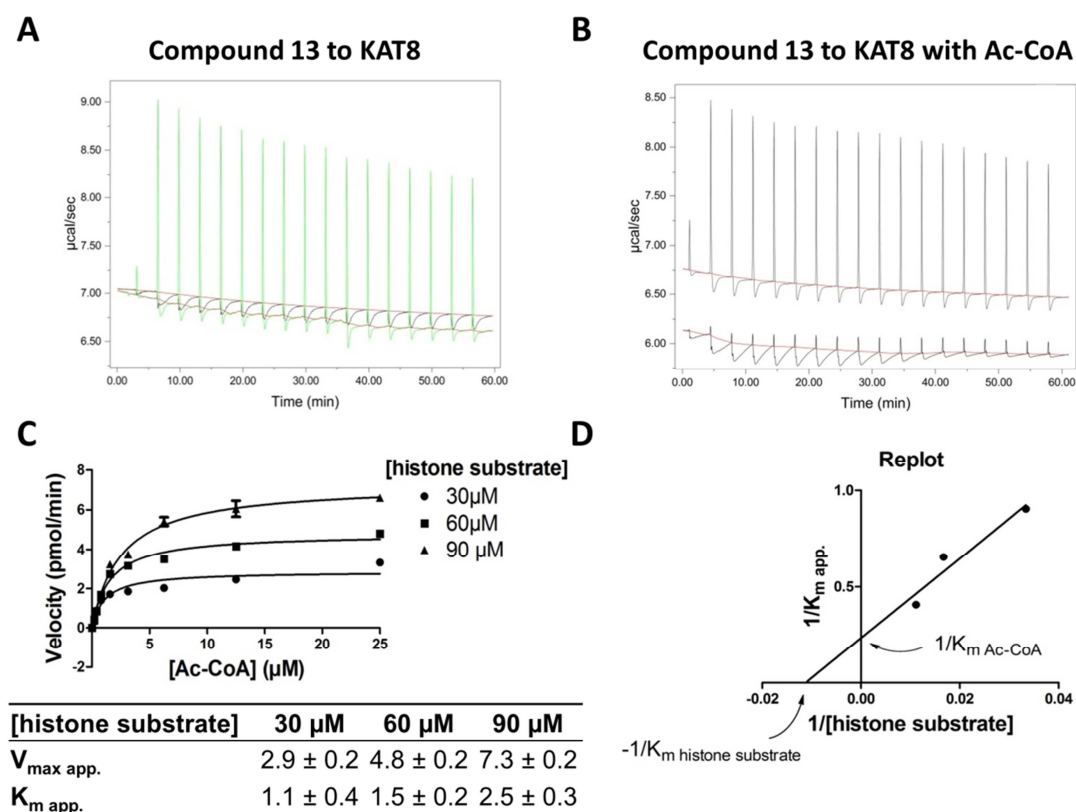


**Figure S10.** A) Compound **13** (400  $\mu\text{M}$ ) was titrated to KAT8 (top), raw data. A baseline was generated by titrating **13** to buffer using the same settings (bottom). B) Compound **13** (400  $\mu\text{M}$ ) was titrated to KAT8 (40  $\mu\text{M}$ ) in the presence of Ac-CoA (80  $\mu\text{M}$ ) (top), raw data. A baseline was generated by titrating **13** to buffer with Ac-CoA (80  $\mu\text{M}$ ) using the same settings (bottom). C) Determination of  $K_{\text{m app.}}$  values of Ac-CoA for KAT8. The velocity was measured at increasing concentrations of Ac-CoA (0-25  $\mu\text{M}$ ) in the presence of different concentrations of the histone substrate (30, 60 and 90  $\mu\text{M}$ ). Representative graph (triplicate) of two individual experiments. This yielded three apparent  $K_{\text{m}}$  values for Ac-CoA, which are dependent on the concentration of histone substrate. D) Determination of the real  $K_{\text{m}}$  values of Ac-CoA and the histone substrate for KAT8. Replot of the reciprocal of the  $K_{\text{m app.}}$  values of Ac-CoA against the reciprocal of the histone substrate concentration used in the kinetic assay. A linear regression of these data points gave the  $K_{\text{m}}$  of Ac-CoA as reciprocal of the intercept of the X axis (4.3  $\mu\text{M}$ ) and the  $K_{\text{m}}$  of the histone substrate as negative reciprocal of the intercept with the X axis (89  $\mu\text{M}$ ).

**Calculation  $K_{i2}$  value of **13****

The  $K_i$  values of **13** can be calculated as described by Cheng and Prusoff (3). Based on the results of the kinetic assays showing that KAT8 uses a ping pong mechanism and that **13** interacts with both the free enzyme as well as the acetylated intermediate, the two  $K_i$  values for this inhibition can be calculated using equation 1.  $K_{i1}$  was assumed to be equal to the  $K_d$  of **13** to KAT8.  $K_{i2}$  could be calculated by solving the equation as follows:

$$K_b A + K_a B + AB = \left( \frac{K_b}{B} \frac{1}{K_{i2}} + \frac{K_a}{A} \frac{1}{K_{i1}} \right) IC_{50}$$

$$89 * 4 + 4.3 * 60 + 4 * 60 = \left( \frac{89}{60} \frac{1}{K_{i2}} + \frac{4.3}{4} \frac{1}{2.6} \right) 9.7$$

$$854 = \left( 1.48 \frac{1}{K_{i2}} + 0.413 \right) 9.7$$

$$88 = \left( 1.48 \frac{1}{K_{i2}} + 0.413 \right)$$

$$88 = \left( \frac{1.18}{K_{i2}} \right)$$

$$K_{i2} = 0.017 \mu\text{M}$$

## Experimental Procedures

### General Reagents and Materials

All chemicals and reagents were purchased from Sigma Aldrich (St. Louis, Missouri, USA) or Acros Organics (Geel, Belgium) unless otherwise stated.

### Expression and purification of KAT8-His<sub>6</sub>

The KAT8 catalytic domain (125-458), carrying an *N*-terminal His<sub>6</sub>-tag, was produced in *E. Coli* BL21(DE3) as previously described (4) using a pET15b expression plasmid (50 µg/mL ampicillin). Expression of the KAT8-His<sub>6</sub> gene was induced by adding isopropyl β-D-1-thiogalactopyranoside (IPTG, 300 µM). The cells were lysed in lysis buffer (10 mM Tris pH 7.4, 750 mM NaCl, 1% glycerol, 1 mM 2-mercaptoethanol and Pierce EDTA-free protease inhibitor cocktail tablet) by sonication for 2 times 30 seconds at 50% amplitude on a Branson digital sonifier W-250D and spun down 1 hour at 15000 x g. The supernatant was purified using Ni-sepharose resin and size-exclusion chromatography on a HiLoad 16/60 Superdex 200 pg (GE Healthcare) connected to a NGC Medium-Pressure Chromatography System (Bio-Rad) and eluted with elution buffer (10 mM MES, 750 mM NaCl, 10 mM MgCitrate, 1 mM 2-Mercaptoethanol, 1 % glycerol pH 6.5). Purity was analyzed by SDS-PAGE, protein concentration was measured by UV<sub>280</sub> and Pierce Coomassie Protein Assay (Thermo Scientific). Pure KAT8 was immediately aliquoted, flash-frozen in liquid nitrogen and stored at -80 °C. The protein was stable for at least 6 months.

### HAT activity assays - general procedures

The activity of KAT8 was measured using fluorescent chemical detection of coenzyme A (CoA). As substrate, a peptide of amino acids 1-21 of the *N*-terminal histone H4 tail was used: SGRGKGGKGLGKGGAKRHRK-NH<sub>2</sub> (Pepscan, The Netherlands), referred to as “the histone substrate”. Acetyl coenzyme A sodium salt (Sigma-aldrich, USA) (Ac-CoA) was used as cofactor. Stock concentrations of Ac-CoA in water were determined using the extinction coefficient ( $\epsilon_{260\text{nm}} = 16400 \text{ M}^{-1}\text{cm}^{-1}$ ) and stored in aliquots at -80°C. 7-diethylamino-3-(4'-maleimidylphenyl)-4-methylcoumarin (CPM, Sigma-aldrich) was used to detect CoA produced in the enzymatic reaction (5). The fluorescence intensity was measured using a BioTek Synergy H1 hybrid plate reader at an excitation wavelength of 392 nm and emission wavelength of 470 nm, the gain was set to 50. All experiments were done in duplicate or triplicate and repeated at least two times unless otherwise indicated.

### Fragment screening

A collection of approximately 700 fragment-like compounds with a low molecular weight (MW < 250), mainly aromatic rings, containing nitrogen or sulphur, with different substitution patterns (hydrogen bond donors < 5, hydrogen bond acceptors < 4) were screened for inhibition of KAT8 in a single point assay. All dilutions were made in assay buffer containing 50 mM HEPES pH7.4, 0.1 mM EDTA and 0.01% TritonX100. Ac-CoA (4 µM), histone substrate (60 µM) and the compounds (200 µM, 10% DMSO) were added to a black 96-well plate. KAT8 (250 nM) was added to start the reaction and the mixture was incubated 15 minutes at room temperature. The reaction volume was 50 µL. The positive control contained the same conditions without compounds, but with DMSO. A negative control was made using the same conditions as the positive control, but using heat inactivated KAT8 (incubated 5 minutes at 100 °C). The enzymatic reaction was stopped by adding 2-propanol (50 µL) and CPM (12.5 µM) was added. The final volume was 200 µL. The mixture was incubated for 15 minutes at room temperature and the fluorescence was measured. The data were analyzed by subtracting the negative control and normalizing to the positive control as 100%. All compounds showing more than 50% inhibition were considered as hits, but structures containing maleimide or thiol moieties were excluded due to reactivity with the assay product or fluorophore. The resulting compounds were tested for their 50 % inhibitory concentration (IC<sub>50</sub>). The newly synthesized derivatives were screened similarly at a concentration of 250 µM.

### IC<sub>50</sub> measurements

The 50 % inhibitory concentration (IC<sub>50</sub>) was measured of the hits, several similar, commercially available compounds and the newly synthesized derivatives. All dilutions were made in assay buffer containing 50 mM HEPES pH7.4, 0.1 mM EDTA and 0.01% TritonX100. Ac-CoA (4 µM), histone substrate (60 µM) and the compound (0 - 5mM for the fragments or 0 – 1 mM for the derivatives, 2 or 10 x dilution series, 2- 10% DMSO)

were added to a black 96-well plate. KAT8 (250 nM) was added to start the reaction. The reaction time was 15 minutes at room temperature and the reaction volume was 50  $\mu$ L. A negative control was made using the same conditions including all dilutions of the compound, but using heat inactivated KAT8 (incubated 5 minutes at 100  $^{\circ}$ C). The enzymatic reaction was stopped by adding 2-propanol (50  $\mu$ L) and subsequently CPM (12.5  $\mu$ M) was added. The final volume was 200  $\mu$ L. The mixture was incubated for 15 minutes at room temperature and the fluorescence was measured. The data were analyzed by subtracting the negative control and normalizing to the positive control (no compound) as 100%. The x axis was converted to log scale giving the characteristic sigmoidal curve. The  $IC_{50}$  was determined as the concentration of compound giving 50% inhibition of KAT8 activity.

### Thiolreactivity

All dilutions were made in assay buffer containing 50 mM HEPES pH7.4, 0.1 mM EDTA and 0.01% TritonX100. CoA (4  $\mu$ M), histone substrate (60  $\mu$ M), KAT8 (250 nM) and the compound **13** (0 – 100  $\mu$ M in 2% DMSO) were added to a black 96-well plate. A negative control was made using the same conditions including all dilutions of the compound, but without CoA. The reaction time was 15 minutes at room temperature and the reaction volume was 50  $\mu$ L. 2-propanol (50  $\mu$ L) was added and subsequently CPM (12.5  $\mu$ M) was added. The final volume was 200  $\mu$ L. The mixture was incubated for 15 minutes at room temperature and the fluorescence was measured. The data were analyzed by subtracting the negative control and normalizing to the positive control (no compound) as 100%. The x axis was converted to log scale.

### HPLC

To a solution of compound **13** (20 mM in methanol, 200  $\mu$ L) assay buffer was added (50 mM HEPES pH7.4, 0.1 mM EDTA and 0.01% TritonX100, 200  $\mu$ L). Then 800  $\mu$ L methanol was added and the solution was injected on a Shimadzu LC-10A HPLC (5  $\mu$ L injection, EVO C18 100  $\text{Å}$  column, gradient 5-90% acetonitrile in water with 0.1% TFA). Samples were taken immediately, after 1 hour and 4 hours incubation. For the buffer control, the same sample preparation was followed, but without compound **13**.

### Preincubation experiment

To test whether **13** is an irreversible inhibitor, a preincubation experiment was done. Compound **13** (0.75, 2 and 10 x  $IC_{50}$  value) was preincubated with KAT8 (250 nM) for 2, 5 and 10 minutes. Subsequently Ac-CoA (4  $\mu$ M) and the histone substrate (60  $\mu$ M) were added. The reaction time was 15 minutes at room temperature and the reaction volume was 50  $\mu$ L. The reaction was stopped with 2-propanol (50  $\mu$ L) and CPM (12.5  $\mu$ M) was added. The final volume was 200  $\mu$ L. The mixture was incubated for 15 minutes at room temperature and the fluorescence was measured. The data were analyzed by subtracting the negative control and normalizing to the positive control (no **13**) as 100%.

### Dilution experiment

To confirm reversible inhibition of **13**, a dilution experiment was done. **13** (50  $\mu$ M, 0.5% DMSO) was preincubated with KAT8 (1450 nM) for 5 minutes. Subsequently, this mix was diluted 100 times in buffer containing Ac-CoA (4  $\mu$ M) and histone substrate (60  $\mu$ M) to start the enzyme reaction. The enzyme reaction (50  $\mu$ L) was stopped at different time points (0 - 30 minutes) by adding 2-propanol (50  $\mu$ L). and CPM (12.5  $\mu$ M) was added. The final volume was 200  $\mu$ L. The mixture was incubated for 15 minutes at room temperature and the fluorescence was measured. The positive control followed the same procedure, but without **13**. The data were analyzed by subtracting the negative control and normalizing to the positive control (no **13**) as 100%.

### Antioxidant activity

To test the antioxidant potency of **13** and the control compound **9**, a 2,2-diphenyl-1-picrylhydrazyl (DPPH) assay was used. The inhibitors (0 – 1 mM, 10 x dilution series) in methanol were added to a 96 well UV plate (greiner Bio-one). DPPH (0.1 mM) was added and incubated for 15 minutes at room temperature protected from light. As a control, a compound dilution series in methanol was used. The absorbance was measured at 515 nm using a BioTek Synergy H1 hybrid plate reader. The control was subtracted and the data were normalized to the absorbance without inhibitor. The x axis was converted to log scale yielding a sigmoidal curve. The concentration that gave 50% reduction in absorbance ( $EC_{50}$ ) was determined by dose response inhibition non-linear fit.

**IC<sub>50</sub> of 13 in presence of redox active substances**

The IC<sub>50</sub> of **13** was measured in the same assay as described in de IC<sub>50</sub> measurements. To the assay, tris(2-carboxyethyl)phosphine (TCEP, 1 μM), NAD<sup>+</sup> (nicotinamide adeninedinucleotide, 100 μM) or NADH (100 μM) were added. A higher concentration of TCEP could not be used due to a strong background fluorescence (data not shown). Note: A concentration of 1 μM instead of 4 μM Ac-CoA and 14.5 nM instead of 250 nM was used. The IC<sub>50</sub> of **13** under these conditions without redox active substance was 1.7 ± 0.5 μM (the calculated K<sub>i2</sub> value using the adapted concentration of Ac-CoA and resulting IC<sub>50</sub> was 0.011 μM).

**Selectivity**

To evaluate the selectivity of **13**, **9** and the active derivatives from the SAR study for other HATs, the inhibitory potency was tested on KAT3B (p300), as representative of the p300/CBP family, and on KAT2B (PCAF), as representative of the GNAT family. KAT3B (aa 1284-1673) and KAT2B (aa 492-658) catalytic domains were purchased from Enzo Lifesciences as human recombinant pure enzymes. The same fluorescence-based assay was employed as for KAT8 as described below.

In case of KAT2B, a 20 amino acid peptide resembling the N-terminal histone H3 tail was used: H-ARTKQTARKSTGGKAPRKQL-OH (Pepscan, The Netherlands). All dilutions were made in buffer (50 mM Tris pH 8.0, 0.1 mM EDTA). The histone H3 substrate (25 μM), Ac-CoA (10 μM) and **13**, **9** or active derivatives from the SAR study (0 – 1 mM, 10 x dilution series, 2% DMSO final) were added to a black 96-well plate. KAT3B (100 nM) was added and incubated 15 minutes at room temperature. The reaction volume was 50 μL. The negative control contained the same conditions including all dilutions of the compound, but using heat-inactivated KAT2B (incubated 5 minutes at 100 °C). The enzymatic reaction was stopped by adding 2-propanol (50 μL) and CPM (12.5 μM) was added. The final volume was 200 μL. The mixture was incubated for 15 minutes at room temperature and the fluorescence was measured. The data were analyzed by subtracting the negative control and normalizing to the positive control (no compound) as 100%. The x axis was converted to log scale giving the characteristic sigmoidal curve. The IC<sub>50</sub> was determined as the concentration of compound giving 50% inhibition of KAT2B activity. Experiments done in duplicate.

In case of KAT3B the same histone H4 substrate was used as for KAT8, Ac-CoA was used as cofactor. All dilutions were made in buffer (50 mM Tris pH 8.0, 0.1 mM EDTA). The histone substrate (100 μM), Ac-CoA (50 μM) and **13**, **9** or active derivatives from the SAR study (0 – 1 mM, 10 x dilution series, 2% DMSO final) were added to a black 96-well plate. KAT3B (100 nM) was added and incubated 20 minutes at 37 °C. The reaction volume was 50 μL. The negative control contained the same conditions including all dilutions of the compound, but using heat-inactivated KAT3B (incubated 5 minutes at 100 °C). The enzymatic reaction was stopped by adding 2-propanol (50 μL) and subsequently CPM (12.5 μM) was added. The final volume was 200 μL. The mixture was incubated for 15 minutes at room temperature and the fluorescence was measured. The data were analyzed by subtracting the negative control and normalizing to the positive control (no compound) as 100%. The x axis was converted to log scale giving the characteristic sigmoidal curve. The IC<sub>50</sub> was determined as the concentration of compound giving 50% inhibition of KAT3B activity. Experiments were done in duplicate.

**Kinetic evaluation KAT2B and KAT3B**

The catalytic mechanism of KAT2B and KAT3B was investigated with the aim of determining the K<sub>m</sub> values of their substrates.

In case of KAT2B, the velocity of the enzyme was measured at increasing concentrations of Ac-CoA (0-20 μM) in the presence of different concentrations of the histone H3 substrate (15, 25, 50 and 100 μM). The fluorescence intensity was converted to velocity using the standard curve. The blank was (0 μM Ac-CoA) was subtracted and the curve was plotted following sigmoidal kinetics non-linear regression. The Lineweaver-Burke plot was created by transforming the data to the double reciprocal.

In case of KAT3B, the velocity was measured at increasing concentrations of Ac-CoA (0-500 μM) in the presence of different concentrations of histone H3 substrate or histone H4 substrate (5, 50 and 500 μM). The

fluorescence intensity was converted to velocity using the standard curve. The blank was (0  $\mu\text{M}$  Ac-CoA) was subtracted and the curve was plotted following Michaelis-menten non-linear regression.

### HDAC3 inhibition

Human recombinant C-terminal His-tag HDAC3/NcoR2 (BPS Bioscience, Catalog #: 50003) was diluted in incubation buffer (25 mM Tris-HCl, pH 8.0, 137 mM NaCl, 2.7 mM KCl, 1 mM MgCl<sub>2</sub>, 0.01% Triton-X and 1 mg/mL BSA). 40  $\mu\text{L}$  of this dilution was incubated with 10  $\mu\text{L}$  of different concentrations of compound **13** in 10% DMSO/incubation buffer and 50  $\mu\text{L}$  of the fluorogenic Boc-Lys( $\epsilon$ -Ac)-AMC (20  $\mu\text{M}$ , Bachem, Germany) at 37  $^{\circ}\text{C}$  in a black 96-well plate. After 90 min incubation time, 50  $\mu\text{L}$  of the stop solution (25 mM Tris-HCl (pH 8), 137 mM NaCl, 2.7 mM KCl, 1 mM MgCl<sub>2</sub>, 0.01% Triton-X, 6.0 mg/mL trypsin from porcine pancreas Type IX-S, lyophilized powder, 13,000-20,000 BAEE units/mg protein (Sigma Aldrich) and 200  $\mu\text{M}$  vorinostat) was added. After a following incubation at 37  $^{\circ}\text{C}$  for 30 min, the fluorescence was measured on a Synergy H1 Hybrid Multi-Mode Microplate Reader (BioTek, USA) with a gain of 70 and an excitation wavelength of 390 nm and an emission wavelength of 460 nm.

### Arginase 1

All dilutions were made in buffer (50 mM HEPES pH7.4). 1.25 x SYPRO orange (ThermoFisher Scientific) was added to human recombinant arginase 1 (2.5  $\mu\text{M}$ ) and compound **13** (0, 0.25, 2.5 and 25  $\mu\text{M}$  in 5% DMSO) in PCR tubes and spun 1 minute at 700 rpm. The differential scanning fluorimetry was done on a C100 Thermal cycler (Biorad, CFX96 real time system) using 0.5 degree per cycle starting from 20 degrees and fluorescence was measured. The melting temperature ( $T_m$ ) was determined as the midpoint of the curve of transition from folded to unfolded protein.

### Isothermal titration calorimetry (ITC)

ITC experiments were done using KAT8 (40  $\mu\text{M}$ ) in buffer (10 mM MES, 750 mM NaCl, 10 mM MgCitrate, 1 mM 2-Mercaptoethanol, 1% glycerol, 0.5% DMSO) (Figure S2). The MicroCal iTC200 (Malvern) was equilibrated at 20  $^{\circ}\text{C}$ . **13** (400  $\mu\text{M}$ ) was titrated to KAT8 with 2  $\mu\text{L}$  per injection, 20 injections in total, 200 seconds spacing and 0.7  $\mu\text{L}$  pre-injection. A baseline was generated by titrating **13** to buffer using the same settings (Figure S2A). The data ( $N = 1$ ) were analyzed using MicroCal ITC-ORIGIN Analysis Software by calculating the area under the peak (AUP) and subtracting the baseline.

**13** (400  $\mu\text{M}$ ) was titrated to KAT8 (40  $\mu\text{M}$ ) in the presence of Ac-CoA (80  $\mu\text{M}$ ) with 2  $\mu\text{L}$  per injection, 20 injections in total, 200 seconds spacing and 0.7  $\mu\text{L}$  pre-injection. A baseline was generated by titrating **13** to buffer with Ac-CoA (80  $\mu\text{M}$ ) using the same settings (Figure S2B). The data ( $N = 1$ ) were analyzed using MicroCal ITC-ORIGIN Analysis Software by calculating the area under the peak (AUP) and subtracting the baseline.

### Kinetic assays

#### *Kinetic evaluation of 13*

To investigate the mechanism of inhibition, kinetic studies were done with **13**. All dilutions were made in assay buffer containing 50 mM HEPES pH7.4, 0.1 mM EDTA and 0.01% TritonX100. The velocity of the substrate conversion of KAT8 was measured at increasing concentrations of Ac-CoA in the presence of different concentrations of **13**. Histone substrate (60  $\mu\text{M}$ ), Ac-CoA (0 – 20  $\mu\text{M}$ ) and **13** (0, 5 and 10  $\mu\text{M}$ ) were added to a black 96-well plate. KAT8 (250 nM) was added to start the reaction and the mixture was incubated 15 minutes at room temperature. The reaction volume was 50  $\mu\text{L}$ . The enzymatic reaction was stopped by adding 2-propanol (50  $\mu\text{L}$ ) and CPM (12.5  $\mu\text{M}$ ) was added. The final volume was 200  $\mu\text{L}$ . The mixture was incubated for 15 minutes at room temperature and the fluorescence was measured.

The velocity of the substrate conversion of KAT8 was measured at increasing concentrations of histone substrate in the presence of different concentrations of **13**. Ac-CoA (4  $\mu\text{M}$ ), histone substrate (0-400  $\mu\text{M}$ ) and **13** (0, 5 and 10  $\mu\text{M}$ ) were added to a black 96-well plate. KAT8 (250 nM) was added to start the reaction and the mixture was incubated 15 minutes at room temperature. The reaction volume was 50  $\mu\text{L}$ . The enzymatic reaction was stopped

by adding 2-propanol (50  $\mu\text{L}$ ) and CPM (12.5  $\mu\text{M}$ ) was added. The final volume was 200  $\mu\text{L}$ . The mixture was incubated for 15 minutes at room temperature and the fluorescence was measured.

The raw data were analyzed by converting the fluorescence intensity to velocity using the standard curve described previously (4). The background (0  $\mu\text{M}$  Ac-CoA/histone substrate) was subtracted and the curve was fitted using non-linear regression – “Michaelis-Menten”.

#### *Calculation $K_m$ values of Ac-CoA and the histone substrate*

To calculate the  $K_m$  values of Ac-CoA and the histone substrate, a kinetic assay was done and the data were analyzed as described by Segel (6). The velocity was measured at increasing concentrations of Ac-CoA (0-25  $\mu\text{M}$ ) in the presence of different concentrations of the histone substrate (30, 60 and 90  $\mu\text{M}$ ). The fluorescence intensity was converted to velocity using the standard curve described previously (4). The blank (0  $\mu\text{M}$  Ac-CoA) was subtracted and the curve was plotted following Michaelis-Menten non-linear regression. This yielded three apparent  $K_m$  values for Ac-CoA and three apparent  $V_{\max}$  values, which are dependent on the concentration of histone substrate (Figure S3A). The actual or non-dependent  $K_m$  values of both Ac-CoA and the histone substrate could be derived by plotting the reciprocal of the apparent  $K_m$  values against the reciprocal of the histone substrate concentration used in the kinetic assay (Figure S3B). A linear regression of these data points gave the  $K_m$  of Ac-CoA as reciprocal of the intercept of the X axis (4.3  $\mu\text{M}$ ) and the  $K_m$  of the histone substrate as negative reciprocal of the intercept with the X axis (89  $\mu\text{M}$ ). These values are consistent with previously reported values (4).

#### **References**

- (1) Kessler J, Hahnel A, Wichmann H, Rot S, Kappler M, Bache M, et al. HIF-1 $\alpha$  inhibition by siRNA or chetomin in human malignant glioma cells: effects on hypoxic radioresistance and monitoring via CA9 expression. *BMC Cancer* 2010 Nov 4;10:605-2407-10-605.
- (2) Hemshekhar M, Sebastin Santhosh M, Kemparaju K, Girish KS. Emerging roles of anacardic acid and its derivatives: a pharmacological overview. *Basic Clin Pharmacol Toxicol* 2012 Feb;110(2):122-132.
- (3) Cheng Y, Prusoff WH. Relationship between the inhibition constant (KI) and the concentration of inhibitor which causes 50 per cent inhibition (I50) of an enzymatic reaction. *Biochem Pharmacol* 1973 12/1;22(23):3099-3108.
- (4) Wapenaar H, van der Wouden PE, Groves MR, Rotili D, Mai A, Dekker FJ. Enzyme kinetics and inhibition of histone acetyltransferase KAT8. *Eur J Med Chem* 2015 Nov 13;105:289-296.
- (5) Gao T, Yang C, Zheng YG. Comparative studies of thiol-sensitive fluorogenic probes for HAT assays. *Anal Bioanal Chem* 2013 Feb;405(4):1361-1371.
- (6) Segel I, H. *Enzyme Kinetics: Behavior and Analysis of Rapid Equilibrium and Steady-State Enzyme Systems*. : Wiley Classics Library; 1993.

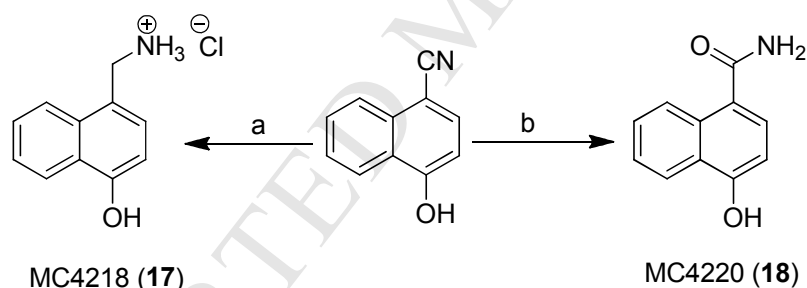
## Chemistry

Compounds **14-16**, **20** and **21** are commercially available, while compounds **13**, **17-19** and **22-31** have been prepared according to literature procedures.<sup>1-9</sup>

Melting points were determined on a Buchi 530 melting point apparatus and are uncorrected. The <sup>1</sup>H and <sup>13</sup>C-NMR spectra were recorded at 400 MHz and 100 MHz, respectively, on a Bruker AC 400 spectrometer, reporting chemical shifts in  $\delta$  (ppm) units relative to the internal reference tetramethylsilane (Me<sub>4</sub>Si). HR-MS spectra were recorded on an Exactive Orbitrap, source: ESI (+), (Thermo Fisher Scientific Inc.). Elemental analyses were performed by a PE 2400 (Perkin-Elmer) analyzer and have been used to determine purity of the compounds **13**, **17-19** and **22-25**, which is > 95%. HPLC was used to determine purity of **26-31** on a TharSFC, Waters (Milford, USA) with eluent 3-50% methanol in supercritical carbon dioxide, pyridine column, which is > 95%. Analytical results are within  $\pm 0.40\%$  of the theoretical values.

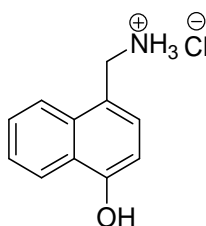
All compounds were routinely checked by TLC and <sup>1</sup>H-NMR. TLC was performed on aluminum-backed silica gel plates (Merck DC, Alufolien Kieselgel 60 F254) with spots visualized by UV light. All solvents were reagent grade and, when necessary, were purified and dried by standard methods. Concentration of solutions after reactions and extractions involved the use of a rotary evaporator operating at a reduced pressure of *ca.* 20 Torr. Organic solutions were dried over anhydrous sodium sulfate or magnesium sulfate. All chemicals were purchased from Aldrich Chimica, Milan (Italy), or from TCI Europe NV, Zwijndrecht (Belgium), Sigma Aldrich (USA) or Acros Organics (Geel, Belgium) and were of the highest purity. As a rule, samples prepared for physical and biological studies were dried in high vacuum over P<sub>2</sub>O<sub>5</sub> for 20 h at temperature ranging from 25 to 40 °C, depending on the sample melting point.

### Preparation of compounds 17-18



<sup>a</sup> Regents and conditions: (a) (1) LiAlH<sub>4</sub>, dry THF, rt → reflux, 3 h, (2) HCl 4N in dioxane, dry Et<sub>2</sub>O; (b) NaBH<sub>4</sub>, H<sub>2</sub>O, EtOH, 80 °C, 8 h.

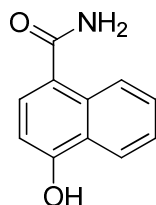
### Preparation of 4-hydroxynaphthalen-1-yl-methanaminium chloride (MC4218, 17).



The commercially available 4-hydroxy-1-naphthonitrile (0.305 g, 1.76 mmol) was dissolved into 20 mL of anhydrous THF. The resulting solution was then added dropwise to a stirred suspension of LiAlH<sub>4</sub> (2 mmol) in dry THF (10 mL) under nitrogen atmosphere. Then the suspension was slowly heated to reflux. After 3 h the suspension was cooled with an ice bath and then the excess of hydride was decomposed by adding first dropwise

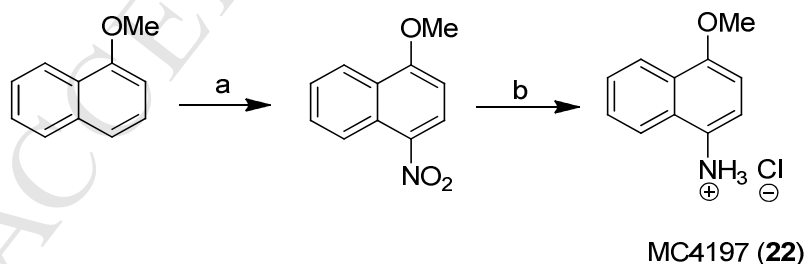
ethyl acetate and then water until the total volume reached was 50 mL. The solution was extracted with ethyl acetate (10 mL x 3). The organic layers were collected, dried on sodium sulfate and the solvent was removed under vacuum. After purification by flash chromatography (AcOEt/MeOH 7/3), the resulting 4-(aminomethyl)naphthalen-1-ol was dissolved in dry diethyl ether and treated with a solution of 4 N HCl (4.4 mL) in dioxane to produce the corresponding amine salt **17**. Yield: 65%. mp > 290 °C. <sup>1</sup>H-NMR (400 MHz, DMSO) δ 4.38 (s, 2H, CH<sub>2</sub>), 6.91-6.93 (d, 1H, C<sub>3</sub>-H naphthyl ring), 7.44-7.46 (d, 1H, C<sub>2</sub>-H naphthyl ring), 7.51-7.55 (t, 1H, C<sub>7</sub>-H naphthyl ring), 7.60-7.64 (t, 1H, C<sub>6</sub>-H naphthyl ring), 8.04-8.06 (d, 1H, C<sub>8</sub>-H naphthyl ring), 8.21-8.24 (d, 4H, C<sub>5</sub>-H naphthyl ring and NH<sub>2</sub>·HCl), 10.33-10.55 (sb, 1H, OH). <sup>13</sup>C-NMR (100 MHz, DMSO) δ 42.38, 112.80, 122.52, 124.99, 125.45, 125.97, 126.34, 127.10, 129.07, 133.71, 152.27. HR-MS (ESI) calcd for C<sub>11</sub>H<sub>12</sub>NO [M+H]<sup>+</sup> 174.0913, found 174.0915. Anal. (C<sub>11</sub>H<sub>12</sub>ClNO) Calcd. (%): C, 63.01; H, 5.77; Cl, 16.91; N, 6.68; O, 7.63. Found (%): C, 63.06; H, 5.78; Cl, 16.88; N, 6.66; O, 7.62.

#### Preparation of 4-hydroxy-1-naphthalencarboxamide (MC4220, **18**).



To a mixture of commercial 4-hydroxy-1-naphthonitrile (0.34 g, 2 mmol) and EtOH-H<sub>2</sub>O (1:1, 10 mL), sodium borohydride (56.7 mg, 1.50 mmol) was added. The resulting solution was stirred at 80 °C, and the progress of the reaction was monitored by thin-layer chromatography. After 8 hours, the reaction mixture was diluted with MeOH to dissolve all the precipitate. The entire mixture was transferred into a 50-mL round-bottom flask, evaporated under vacuum, and concentrated. The residue was purified by column chromatography on silica gel (hexane-ethyl acetate) to give **18**. Yield: 88%. mp 187-189 °C. <sup>1</sup>H-NMR (400 MHz, DMSO) δ 6.76-6.78 (d, 1H, C<sub>3</sub>-H naphthyl ring), 7.22 (sb, 1H, NH<sub>2</sub>), 7.40-7.50 (m, 3H, C<sub>2,6,7</sub>-H naphthyl ring), 7.69 (sb, 1H, NH<sub>2</sub>), 8.10-8.12 (d, 1H, C<sub>5</sub>-H naphthyl ring), 8.37-8.39 (d, 1H, C<sub>8</sub>-H naphthyl ring), 10.50 (s, 1H, OH). <sup>13</sup>C-NMR (100 MHz, DMSO) δ 108.59, 122.86, 124.68, 124.77, 128.15, 129.92, 131.63, 131.78, 132.57, 151.92, 170.67. HR-MS (ESI) calcd for C<sub>11</sub>H<sub>10</sub>NO<sub>2</sub> [M+H]<sup>+</sup> 188.0712, found 188.0710. Anal. (C<sub>11</sub>H<sub>9</sub>NO<sub>2</sub>) Calcd. (%): C, 70.58; H, 4.85; N, 7.48; O, 17.09. Found (%): C, 70.64; H, 4.86; N, 7.46; O, 17.04.

#### Preparation of 4-methoxynaphthalen-1-aminium chloride (MC4197, **22**).



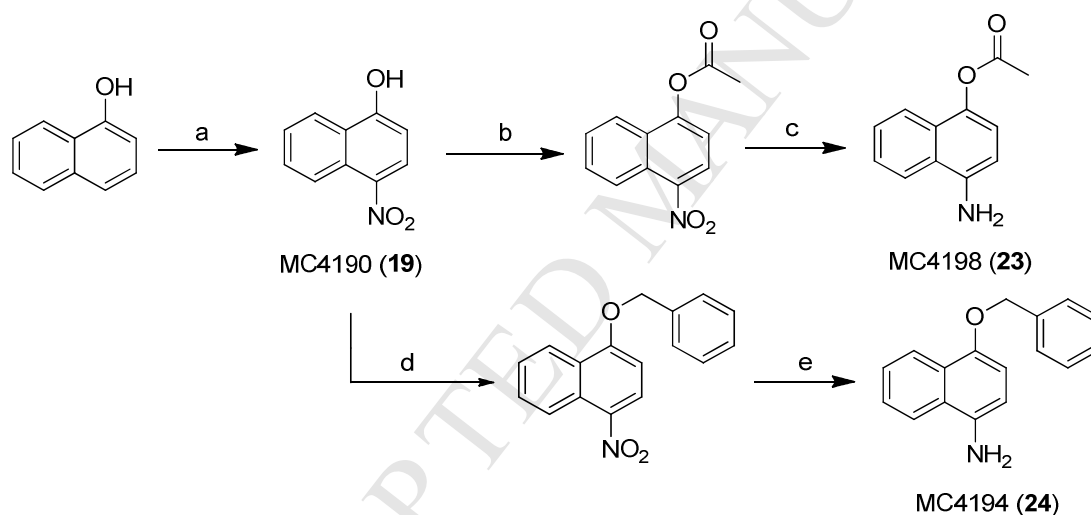
Reagents and conditions: (a) (1) LiAlH<sub>4</sub>, dry THF, rt → reflux, 3 h, (2) HCl 4N in dioxane, dryEt<sub>2</sub>O; (b) NaBH<sub>4</sub>, H<sub>2</sub>O, EtOH, 80 °C, 8 h.

To a mixture of commercially available 1-methoxynaphthalene (1.58 g, 10 mmol) and NaNO<sub>3</sub> (1.02 g, 12 mmol) in acetonitrile (50 mL), benzyltriphenylphosphonium peroxodisulfate (8.99 g, 10 mmol) was added, and the resulting mixture was stirred under reflux conditions for 5 h. After completion of the reaction, the mixture was filtered, and the filtrate was separated and diluted with n-hexane (50 mL). The resulting solution was transferred to a separatory funnel and washed with aqueous solution of Na<sub>2</sub>S<sub>2</sub>O<sub>3</sub> (0.1M, 100 mL) and then H<sub>2</sub>O (100 mL).

The organic layer was separated and dried over anhydrous  $\text{Na}_2\text{SO}_4$ . Evaporation of the solvent under reduced pressure gave the product which was used in the next step without further purification. Yield: 87%. m.p. 79-81 °C.  $^1\text{H-NMR}$  (400 MHz,  $\text{CDCl}_3$ )  $\delta$  3.95 (s, 3H), 6.61-6.65 (d, 1H,  $\text{C}_3\text{-H}$  naphthyl ring), 7.42-7.46 (m, 2H,  $\text{C}_{6,7}\text{-H}$  naphthyl ring), 7.60-7.64 (m, 1H,  $\text{C}_5\text{-H}$  naphthyl ring), 8.19-8.24 (m, 1H,  $\text{C}_2\text{-H}$  naphthyl ring), 8.66-8.71 (d, 1H,  $\text{C}_8\text{-H}$  naphthyl ring).

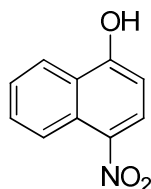
1-Methoxy-4-nitronaphthalene (1 g, 4.9 mmol) was dissolved in 10 mL of methanol followed by addition of 80% hydrazine hydrate (1 mL). Raney nickel (0.3 mg) was carefully added before the mixture was refluxed. After completion of the reduction (2 hours), the catalyst was filtered out and methanol was removed under reduced pressure. The obtained crude 4-methoxynaphthalen-1-amine was converted to the corresponding hydrochloric salt (**22**) via treatment of the amine in dry diethyl ether with 4 N HCl in dioxane (12.5 mL). Yield: 90%. mp 249-250 °C.  $^1\text{H-NMR}$  (400 MHz, DMSO)  $\delta$  4.0 (s, 3H,  $\text{OCH}_3$ ), 6.94-6.96 (d, 1H,  $\text{C}_3\text{-H}$  naphthyl ring), 7.47-7.50 (d, 1H,  $\text{C}_2\text{-H}$  naphthyl ring), 7.55-7.60 (m, 1H,  $\text{C}_7\text{-H}$  naphthyl ring), 7.63-7.67 (m, 1H,  $\text{C}_6\text{-H}$  naphthyl ring), 7.91-7.93 (d, 1H,  $\text{C}_8\text{-H}$  naphthyl ring), 8.16-8.18 (d, 1H,  $\text{C}_5\text{-H}$  naphthyl ring), 10.18 (sb, 3H,  $\text{NH}_2\cdot\text{HCl}$ ).  $^{13}\text{C-NMR}$  (100 MHz, DMSO)  $\delta$  55.74, 110.71, 117.93, 122.97, 123.59, 123.97, 126.94, 128.57, 129.72, 140.75, 151.37. HR-MS (ESI) calcd for  $\text{C}_{11}\text{H}_{12}\text{NO}$   $[\text{M}+\text{H}]^+$  174.0913, found 174.0915. Anal. ( $\text{C}_{11}\text{H}_{12}\text{ClNO}$ ) Calcd. (%): C, 63.01; H, 5.77; Cl, 16.91; N, 6.68; O, 7.63. Found (%): C, 63.08; H, 5.78; Cl, 16.87; N, 6.66; O, 7.61.

### Preparation of compounds 19, 23, 24



Reagents and conditions: (a) benzyltriphenylphosphonium peroxodisulfate,  $\text{NaNO}_3$ , MeCN, reflux, 2 h; (b)  $(\text{CH}_3\text{CO})_2\text{O}$ , dry pyridine, 10h; (c) Pd/charcoal,  $\text{H}_2$  (3 atm), EtOAc, rt, 4 h; (d) benzyl bromide, NaH, dry THF, dry DMF,  $\text{N}_2$ , 0 °C  $\rightarrow$  rt, 3 h; (e) Fe, AcOH, 70 °C, 1.5 h.

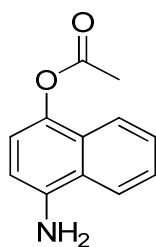
### Preparation of 4-nitronaphthalen-1-ol (MC4190, 19).



To a mixture of commercial 1-naphthol (1.44 g, 10 mmol) and  $\text{NaNO}_3$  (1.02 g, 12 mmol) in acetonitrile (50 mL), benzyltriphenylphosphonium peroxodisulfate (8.99 g, 10 mmol) was added, and the resulting mixture was stirred under reflux conditions for 2 h. After completion of the reaction, the mixture was filtered, and the filtrate was separated and diluted with *n*-hexane (50 mL). The resulting solution was transferred to a separatory funnel and washed with aqueous solution of  $\text{Na}_2\text{S}_2\text{O}_3$  (0.1M, 100 mL) and then  $\text{H}_2\text{O}$  (100 mL). The organic layer was separated and dried over anhydrous  $\text{Na}_2\text{SO}_4$ . The solvent was removed under reduced pressure and was purified

by flash column chromatography (hexane/AcOEt 3:2) on silica gel to afford **19**. Yield: 88%. mp 166-168 °C. <sup>1</sup>H-NMR (400 MHz, DMSO) δ 6.96-6.98 (d, 1H, C<sub>2</sub>-H naphthyl ring), 7.62-7.66 (t, 1H, C<sub>6</sub>-H naphthyl ring), 7.81-7.83 (t, 1H, C<sub>7</sub>-H naphthyl ring), 8.32-8.34 (d, 1H, C<sub>3</sub>-H naphthyl ring), 8.43 (d, 1H, C<sub>5</sub>-H naphthyl ring), 8.67-8.70 (d, 1H, C<sub>8</sub>-H naphthyl ring), 11.66-12.20 (sb, 1H, OH). <sup>13</sup>C-NMR (100 MHz, DMSO) δ 112.73, 123.07, 123.66, 123.81, 125.12, 126.62, 129.88, 130.52, 136.71, 154.77. HR-MS (ESI) calcd. for C<sub>10</sub>H<sub>8</sub>NO<sub>3</sub> [M+H]<sup>+</sup> 190.0504, found 190.0501. Anal. (C<sub>10</sub>H<sub>7</sub>NO<sub>3</sub>) Calcd. (%): C, 63.49; H, 3.73; N, 7.40; O, 25.37. Found (%): C, 63.56; H, 3.74; N, 7.37; O, 25.32.

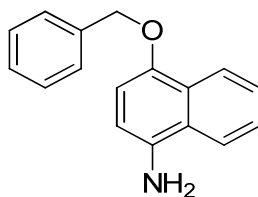
#### Preparation of 4-aminonaphthalen-1-yl acetate (MC4198, **23**).



4-Nitronaphthalen-1-ol **19** (0.45 g, 1.95 mmol) was treated with acetic anhydride (49.6 mmol, 5 mL) and dry pyridine (31 mmol, 2.5 mL) at room temperature for 10 h. After the completion of the reaction, the mixture was concentrated in vacuo, and the crude residue was purified by HPLC to obtain the intermediate 4-acetoxy-1-nitro-naphthalene. Yield: 55%. <sup>1</sup>H-NMR (400 MHz, DMSO) δ 2.52 (s, 3H, CH<sub>3</sub>), 7.39 (d, 1H, C<sub>3</sub>-H naphthyl ring), 7.68 (t, 1H, C<sub>6</sub>-H naphthyl ring), 7.78 (t, 1H, C<sub>7</sub>-H naphthyl ring), 8.06 (d, 1H, C<sub>5</sub>-H naphthyl ring), 8.31 (d, 1H, C<sub>2</sub>-H naphthyl ring), 8.66 (d, 1H, C<sub>8</sub>-H naphthyl ring).

A solution of 4-acetoxy-1-nitro-naphthalene (0.742 g, 3.21 mmol) in ethyl acetate (5 mL) in the presence of 5% palladium on charcoal (5 mg) was treated with hydrogen gas at 3 atm under stirring for 4 h at room temperature. After the completion of the reaction, the mixture was filtered off, evaporated and subjected to flash chromatography eluting with different mixtures of hexanes-AcOEt (hexanes-AcOEt, 80:20, 50:50, then 0:100) to produce pure 4-aminonaphthalen-1-yl acetate **23**. Yield: 64%. mp 100-102 °C. <sup>1</sup>H-NMR (400 MHz, DMSO) δ 2.21 (s, 3H, CH<sub>3</sub>), 5.72 (s, 2H, NH<sub>2</sub>), 6.61-6.63 (d, 1H, C<sub>2</sub>-H naphthyl ring), 6.96-6.98 (d, 1H, C<sub>3</sub>-H naphthyl ring), 7.41-7.50 (m, 2H, C<sub>6,7</sub>-H naphthyl ring), 7.67-7.70 (d, 1H, C<sub>5</sub>-H naphthyl ring), 8.09-8.11 (d, 1H, C<sub>8</sub>-H naphthyl ring). <sup>13</sup>C-NMR (100 MHz, DMSO) δ 20.92, 115.01, 115.25, 123.56 (x2), 124.73, 126.73, 128.86, 129.32, 143.51, 144.95, 169.28. HR-MS (ESI) calcd. for C<sub>12</sub>H<sub>12</sub>NO<sub>2</sub> [M+H]<sup>+</sup> 202.0863, found 202.0866. Anal. (C<sub>12</sub>H<sub>11</sub>NO<sub>2</sub>) Calcd. (%): C, 71.63; H, 5.51; N, 6.96; O, 15.90. Found (%): C, 71.68; H, 5.52; N, 6.93; O, 15.87.

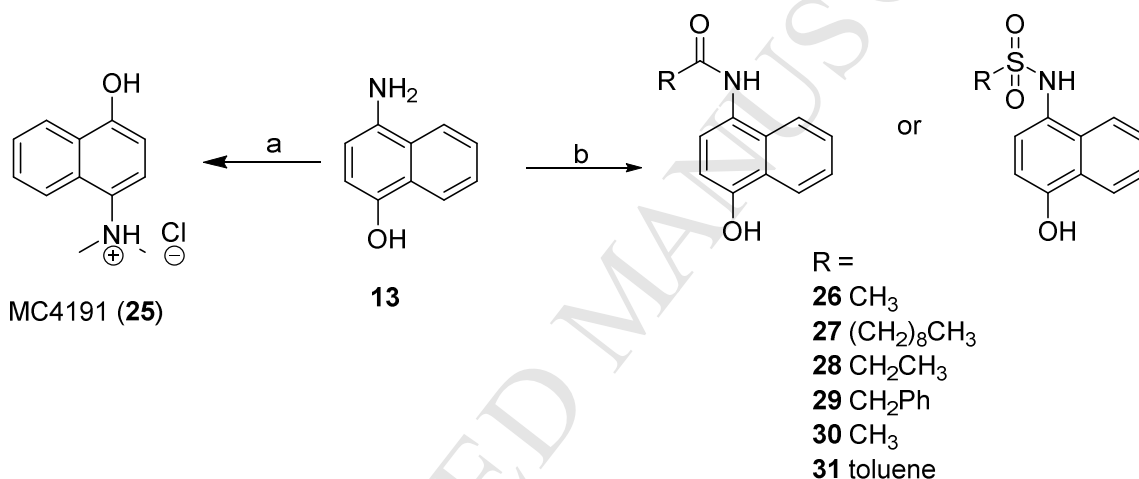
#### Preparation of 4-(benzyloxy)naphthalen-1-amine (MC4194, **24**).



To a stirred solution of 4-nitronaphthalen-1-ol **19** (505 mg, 2.7 mmol) in dry DMF (3 mL) was added NaH (60 wt% dispersion in oil, 193 mg, 4.8 mmol) suspended in dry DMF (3 mL) at 0 °C. Benzyl bromide (0.46 mL, 3.9 mmol) in dry THF (3 mL) was then added at 0 °C. The mixture was warmed up to room temperature and stirred under nitrogen atmosphere for 3 h. After the completion of the reaction, the mixture was diluted with AcOEt (10 mL), washed with H<sub>2</sub>O (10 mL x 4) and brine (10 mL). The organic phase was dried over MgSO<sub>4</sub>, filtered, concentrated and purified by column chromatography on silica gel to obtain the desired 1-(benzyloxy)-4-nitronaphthalene as a light brown solid. Yield: 54%. <sup>1</sup>H-NMR (400 MHz, CDCl<sub>3</sub>) δ 5.34 (s, 2H, PhCH<sub>2</sub>O), 6.88 (d, 1H, C<sub>2</sub>-H naphthyl ring), 7.46-7.35 (m, 3H, C<sub>3,4,5</sub>-H phenyl ring), 7.53-7.47 (m, 2H, C<sub>2,6</sub>-H phenyl ring), 7.58 (t, 1H, C<sub>7</sub>-H naphthyl ring), 7.73 (t, 1H, C<sub>6</sub>-H naphthyl ring), 8.36 (d, 1H, C<sub>5</sub>-H naphthyl ring), 8.43 (d, 1H, C<sub>2</sub>-H naphthyl ring), 8.77 (d, 1H, C<sub>8</sub>-H naphthyl ring).

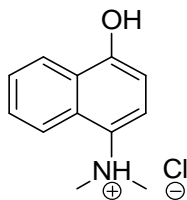
To a suspension of iron powder (601 mg, 10.7 mmol) in glacial acetic acid (6 mL) was added 1-(benzyloxy)-4-nitronaphthalene (301 mg, 1.08 mmol). The mixture was stirred at 70 °C under nitrogen atmosphere for 1.5 h when the mixture turned milky. The mixture was then diluted with AcOEt (10 mL) and washed with a saturated aqueous solution of NaHCO<sub>3</sub> (15 mL x 2) and brine (15 mL). The organic phase was dried over MgSO<sub>4</sub>, filtered and the solvent was removed under reduced pressure to give the crude product as a purple oil. The crude was finally purified by flash chromatography on silica gel by eluting with AcOEt / hexane (1:2) and then AcOEt / hexane (2:1) mixtures to obtain **24**. Yield: 69%. mp 53-55 °C. <sup>1</sup>H-NMR (400 MHz, DMSO) δ 4.98 (s, 2H, ArCH<sub>2</sub>O), 5.20 (s, 2H, NH<sub>2</sub>), 6.59-6.61 (d, 1H, C<sub>2</sub>-H naphthyl ring), 6.85-6.87 (d, 1H, C<sub>7</sub>-H naphthyl ring), 7.32-7.36 (m, 1H, C<sub>4</sub>-H phenyl ring), 7.40-7.47 (m, 4H, C<sub>2,3,5,6</sub>-H phenyl ring), 7.52-7.54 (m, 2H, C<sub>3,6</sub>-H naphthyl ring), 8.01-8.03 (d, 1H, C<sub>8</sub>-H naphthyl ring), 8.11-8.13 (d, 1H, C<sub>5</sub>-H naphthyl ring). <sup>13</sup>C-NMR (100 MHz, DMSO) δ 70.59, 111.20, 115.55, 123.33, 123.59, 124.57, 126.82, 127.66 (x2), 127.98, 128.32 (x2), 128.66, 129.27, 137.04, 144.01, 151.2. HR-MS (ESI) calcd for C<sub>17</sub>H<sub>16</sub>NO [M+H]<sup>+</sup> 250.1226, found 250.1229. Anal. (C<sub>17</sub>H<sub>15</sub>NO) Calcd. (%): C, 81.90; H, 6.06; N, 5.62; O, 6.42. Found (%): C, 81.94; H, 6.07; N, 5.60; O, 6.39.

### Preparation of compounds 25 -31



<sup>a</sup> Regents and conditions: (a) (1) CH<sub>2</sub>O, NaBH<sub>4</sub>, MeOH, 0 °C → rt, (2) HCl 4N in dioxane, dry Et<sub>2</sub>O; (b) acid chloride or sulphonyl chloride, pyridine, dry DMF, 0 °C → rt.

### Preparation of 4-hydroxy-*N,N*-dimethylnaphthalen-1-aminium chloride (MC4191, 25).

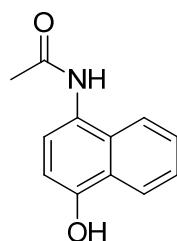


To a solution of **13** (0.44 g, 2.76 mmol) in 10 mL MeOH was added formaldehyde (27.6 mmol). The reaction mixture was cooled to 0 °C and stirred for 5 min. Then NaBH<sub>4</sub> (1.04 g, 27.6 mmol) was slowly added to the reaction mixture, that was stirred in turn at 0 °C for 1 h. After the completion of the reaction, H<sub>2</sub>O (10 mL) was added and the pH value was adjusted to 7 by using NaHSO<sub>4</sub> 0.1N solution. The product was extracted into AcOEt (3 x 10 mL). The organic layers were combined and the solvent was removed in vacuo. Flash chromatography (5 to 40% AcOEt: hexane) afforded 4-(dimethylamino)naphthalen-1-ol. The obtained 4-(dimethylamino)naphthalen-1-ol was dissolved in dry diethyl ether and treated with a solution of hydrochloric acid 4 N in dioxane. The formed precipitate was filtered and washed with dry diethyl ether to give the desired compound **25**. Yield: 61%. mp 224-226 °C. <sup>1</sup>H-NMR (400 MHz, DMSO) δ 3.21 (s, 6H, N(CH<sub>3</sub>)), 6.94-6.96 (d, 1H, C<sub>3</sub>-H naphthyl ring), 7.58-7.62 (d, 1H, C<sub>2</sub>-H naphthyl ring), 7.69-7.71 (t, 1H, C<sub>7</sub>-H naphthyl ring), 7.68-7.73

(t, 1H, C<sub>6</sub>-H naphthyl ring), 8.25-8.27 (d, 1H, C<sub>8</sub>-H naphthyl ring), 8.40-8.42 (d, 1H, C<sub>5</sub>-H naphthyl ring), 10.84 (sb, 1H, -NH), 12.02-12.36 (sb, 1H, OH). <sup>13</sup>C-NMR (100 MHz, DMSO) δ 43.25 (x2), 113.43, 118.26, 122.77, 124.20, 124.34, 129.05, 129.20, 129.57, 143.02, 151.04. HR-MS (ESI) calcd. for C<sub>12</sub>H<sub>14</sub>NO [M+H]<sup>+</sup> 188.1070, found 188.1068. Anal. (C<sub>12</sub>H<sub>14</sub>ClNO) Calcd. (%): C, 64.43; H, 6.31; Cl, 15.85; N, 6.26; O, 7.15. Found (%): C, 64.49; H, 6.32; Cl, 15.82; N, 6.24; O, 7.13.

### General procedure for compounds 26-31

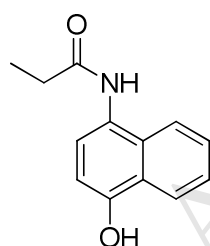
Pyridine (122 μL, 1.5 mmol) was added to 4-amino-1-naphthol (200 mg, 1 mmol) in DMF (10 mL) at 0°C under nitrogen atmosphere and stirred for 2 minutes. The corresponding acid chloride or sulphonyl chloride (1 mmol) was added dropwise. The reaction mixture was allowed to warm to room temperature and stirred for 3-16 hours. The mixture was concentrated under reduced pressure and redissolved in ethyl acetate. The product was extracted with ethyl acetate (3 x 20 mL) and washed with 1N HCl (2 x 10 mL) and water (3 x 20 mL). The combined organic layers were dried over MgSO<sub>4</sub>, filtered and concentrated under reduced pressure. The resulting mixture was dissolved in ethyl acetate and precipitated with petroleum ether. The solid was filtered, washed with DCM if necessary and concentrated under reduced pressure to give the product.



#### 26 N-(4-hydroxynaphthalen-1-yl)acetamide

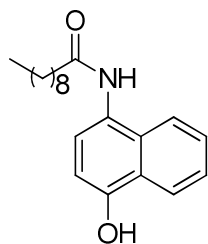
Pink crystal (56 mg, 0.28 mmol, 28 %), R<sub>f</sub> = 0.33 (1:1 ethyl acetate: petroleum ether), melting point 183 °C. <sup>1</sup>H NMR (500 MHz, (CD<sub>3</sub>)<sub>2</sub>SO/CDCl<sub>3</sub>) δ 9.10 (s, 1H), 8.80 (s, 1H), 7.50 (d, J = 8.2 Hz, 1H), 7.20 (d, J = 8.2 Hz, 1H), 6.78-6.72 (m, 2H), 6.62 (d, J = 8.0 Hz, 1H), 6.15 (d, J = 8.0 Hz, 1H), 1.51 (s, 3H). <sup>13</sup>C NMR (126 MHz, (CD<sub>3</sub>)<sub>2</sub>SO/CDCl<sub>3</sub>) δ 168.23, 150.28, 128.73, 124.61, 123.71, 123.52, 123.10, 122.50, 121.38, 121.21, 106.06, 21.98.

HRMS (FTMS-ESI): m/z [M-H], calculated 202.0863 for [C<sub>12</sub>H<sub>12</sub>O<sub>2</sub>N], found 202.0863 [M+H]<sup>+</sup>.



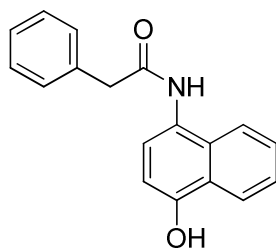
#### 27 N-(4-hydroxynaphthalen-1-yl)propionamide

Light pink solid (27 mg, 0.13 mmol, 13%), R<sub>f</sub> = 0.15 (1:1 ethyl acetate: petroleum ether). <sup>1</sup>H NMR (500 MHz, CD<sub>3</sub>OD) δ 9.73 (s, 1H), 9.34 (s, 1H), 8.21 (d, J = 8.2 Hz, 1H), 7.88 (d, J = 8.2 Hz, 1H), 7.51 – 7.36 (m, 2H), 7.32 (d, J = 8.0 Hz, 1H), 6.84 (d, J = 8.0 Hz, 1H), 2.49 (d, J = 7.5 Hz, 2H), 1.26 (t, J = 7.5 Hz, 3H). <sup>13</sup>C NMR (126 MHz, (CD<sub>3</sub>)<sub>2</sub>SO/CDCl<sub>3</sub>) δ 172.38, 150.49, 129.05, 124.84, 123.97, 123.69, 123.31, 122.79, 121.52, 121.45, 106.32, 28.35, 9.12. HRMS (FTMS-ESI): m/z calculated 216.1019 for [C<sub>13</sub>H<sub>14</sub>O<sub>2</sub>N], found 216.1019 [M+H]<sup>+</sup>.



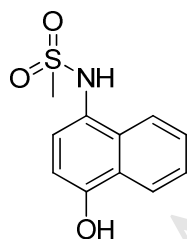
**28** N-(4-hydroxynaphthalen-1-yl)decanamide

Purple solid (143 mg, 0.43 mmol, 43%),  $R_f = 0.65$  (1:1 ethyl acetate: petroleum ether).  $^1\text{H}$  NMR (500 MHz,  $\text{CD}_3\text{OD}$ )  $\delta$  9.72 (s, 1H), 9.35 (s, 1H), 8.19 (d,  $J = 8.2$  Hz, 1H), 7.86 (d,  $J = 8.2$  Hz, 1H), 7.43 (m, 2H), 7.30 (d,  $J = 8.0$  Hz, 1H), 6.83 (d,  $J = 8.0$  Hz, 1H), 2.44 (t,  $J = 7.5$  Hz, 2H), 1.77 – 1.67 (m, 2H), 1.42–1.29 (m, 12H), 0.88 (t,  $J = 6.7$  Hz, 3H).  $^{13}\text{C}$  NMR (126 MHz,  $(\text{CD}_3)_2\text{SO}/\text{CDCl}_3$ )  $\delta$  171.58, 150.38, 128.96, 124.71, 123.87, 123.64, 123.20, 122.73, 121.46, 121.34, 106.22, 35.18, 30.45, 28.12, 28.04, 28.01, 27.87, 24.69, 21.25, 12.90. HRMS (FTMS-ESI):  $m/z$  calculated 314.2115 for  $[\text{C}_{20}\text{H}_{28}\text{O}_2\text{N}]$ , found 314.2113  $[\text{M}+\text{H}]^+$ .



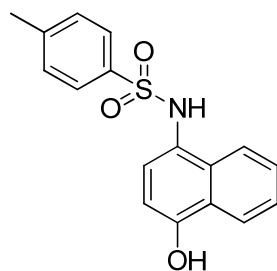
**29** N-(4-hydroxynaphthalen-1-yl)-2-phenylacetamide

Purple solid (45 mg, 0.16 mmol, 16%),  $R_f = 0.56$  (1:1 ethyl acetate: petroleum ether).  $^1\text{H}$  NMR (500 MHz,  $\text{CDCl}_3$ )  $\delta$  9.76 (s, 1H), 9.61 (s, 1H), 8.19 (d,  $J = 8.1$  Hz, 1H), 7.81 (d,  $J = 8.1$  Hz, 1H), 7.45 – 7.25 (m, 8H), 6.82 (d,  $J = 8.0$  Hz, 1H), 3.77 (s, 2H).  $^{13}\text{C}$  NMR (126 MHz,  $(\text{CD}_3)_2\text{SO}/\text{CDCl}_3$ )  $\delta$  169.04, 150.40, 135.06, 128.69, 127.88 (2x), 127.11, 125.29, 124.75, 123.79, 123.31, 123.19, 122.46, 122.37, 121.33, 121.17, 106.11, 42.08. HRMS (FTMS-ESI):  $m/z$  calculated 278.1176 for  $[\text{C}_{18}\text{H}_{16}\text{O}_2\text{N}]$ , found 278.1175  $[\text{M}+\text{H}]^+$ .



**30** N-(4-hydroxynaphthalen-1-yl)methanesulfonamide

Brown solid (39 mg, 0.16 mmol, 16%).  $R_f = 0.33$  (1:1 ethyl acetate/petroleum ether).  $^1\text{H}$  NMR (500 MHz,  $\text{CDCl}_3$ )  $\delta$  9.33 (s, 1H), 8.59 (s, 1H), 7.63 (d,  $J = 8.2$  Hz, 1H), 7.60 (d,  $J = 8.2$  Hz, 1H), 6.94–6.92 (m, 2H), 6.72 (d,  $J = 8.0$  Hz, 1H), 6.27 (d,  $J = 8.0$  Hz, 1H), 2.33 (s, 3H).  $^{13}\text{C}$  NMR (126 MHz,  $(\text{CD}_3)_2\text{SO}/\text{CDCl}_3$ )  $\delta$  151.85, 130.65, 125.41, 124.76, 124.26, 123.62, 122.36, 122.09, 121.46, 106.35, 38.23. HRMS (FTMS-ESI):  $m/z$  calculated 238.0532 for  $[\text{C}_{11}\text{H}_{12}\text{O}_3\text{NS}]$ , found 238.0532  $[\text{M}-\text{H}]^+$ .

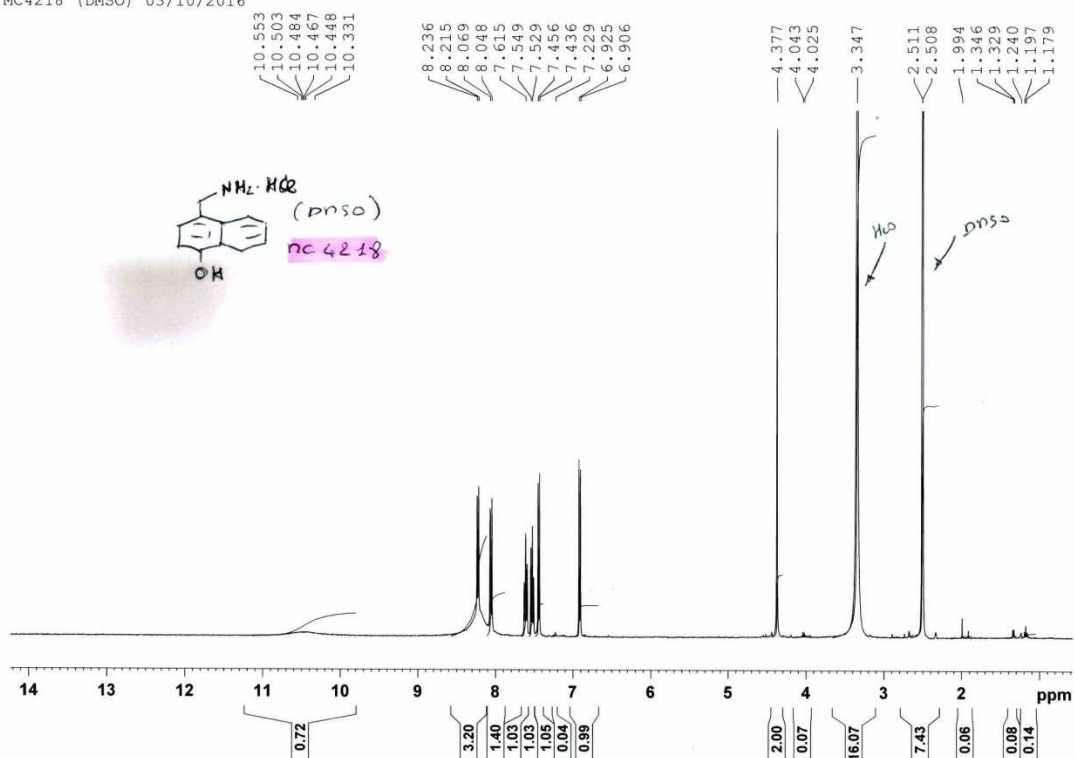
**31** N-(4-hydroxynaphthalen-1-yl)-4-methylbenzenesulfonamide

Purple solid (53 mg, 0.17 mmol, 17%).  $R_f = 0.55$  (1:1 ethyl acetate/petroleum ether).  $^1\text{H}$  NMR (500 MHz,  $\text{CD}_3\text{OD}$ )  $\delta$  9.89 (s, 1H), 9.45 (s, 1H), 8.06 (d,  $J = 8.5$  Hz, 1H), 7.89 (d,  $J = 8.5$  Hz, 1H), 7.49 (d,  $J = 7.7$  Hz, 2H), 7.31 (m, 2H), 7.16 (d,  $J = 6.9$  Hz, 2H), 6.77 (d,  $J = 8.0$  Hz, 1H), 6.62 (d,  $J = 8.0$  Hz, 1H), 2.32 (s, 3H).  $^{13}\text{C}$  NMR (126 MHz,  $(\text{CD}_3)_2\text{SO}/\text{CDCl}_3$ )  $\delta$  151.23, 141.12, 136.20, 130.49, 127.75 (2x), 125.57 (2x), 124.58, 124.15, 123.68, 123.10, 121.96, 121.82, 120.79, 105.77, 19.84. HRMS (FTMS-ESI):  $m/z$  calculated 314.0845 for  $[\text{C}_{17}\text{H}_{16}\text{O}_3\text{NS}]$ , found 314.0845  $[\text{M}+\text{H}]^+$ .

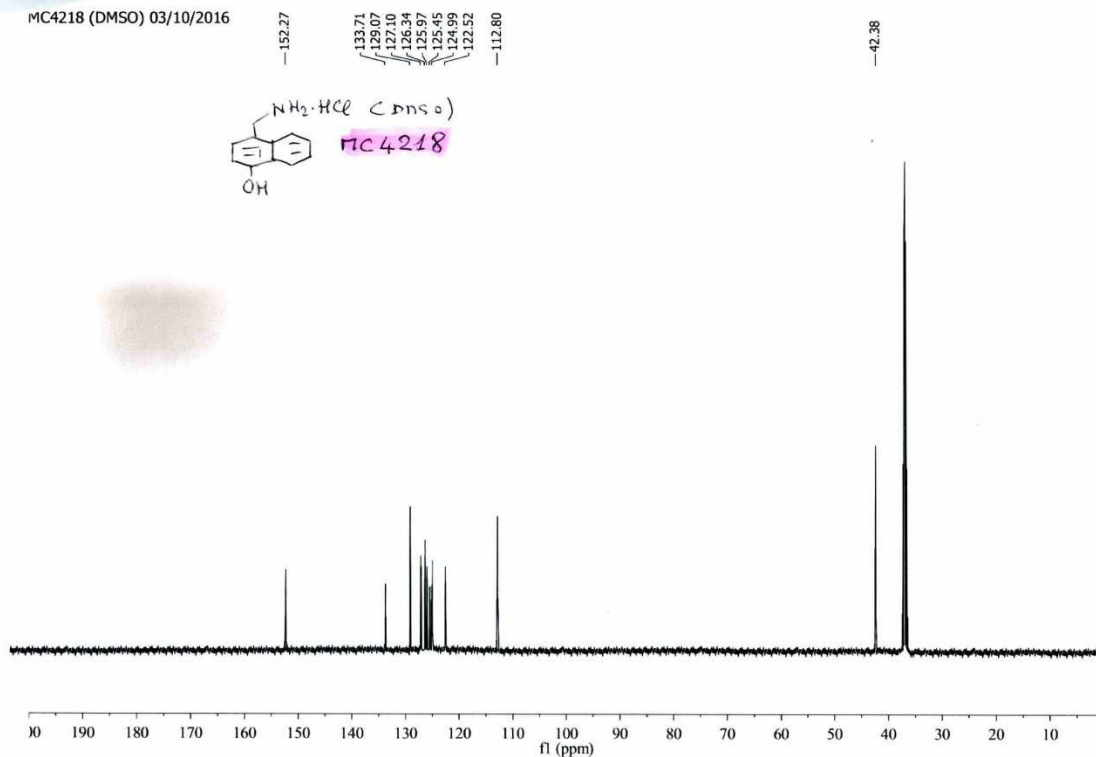
## References

1. Di Antonio, M. Doria, F., Richter, S. N., et al. Quinone methides tethered to naphthalene diimides as selective G-quadruplex alkylating agents. *J. Am. Chem. Soc.*, 2009, 131, 13132–13141.
2. Verma, P. M., Kumar, N., Sharma, U., Bala, M., Kumar, V. and Singh, B. Transition metal-free sodium borohydride promoted controlled hydration of nitriles to amides. *Synthetic Communications*, 2013, 43: 2867-2875.
3. Tajik, H., Zolfigol, M. A., Albadi, J. and Eslami, R. Nitration of some aromatic compounds by sodium nitrate in the presence of benzyltriphenylphosphonium peroxodisulfate. *Synthetic Communication*, 2007, 37, 2771-2776.
4. Röhrig, U. F., Awad, L., Grosdidier, A., Larrieu, P., Stroobant, V., Colau, D., Cerundolo, V., Simpson, A. J. G., Vogel, P., Van den Eynde, B. J., Zoete, V. and Michielin, O. Rational design of indoleamine 2,3-dioxygenase inhibitors. *J. Med. Chem.* 2010, 53, 1172-1189.
5. Fukuhara, K., Hara, Y., Nakanishi, I., Miyata, N. Hydroxylation of nitrated naphthalenes with KO<sub>2</sub>/Crown ether. *Chem. Pharm. Bull.*, 2000, 48, 1532-1535.
6. Elhalem, E., Bailey, B. N., Docampo, R., Ujváry, I., Szajnman, S. H. and Rodriguez, J. B. Design, synthesis, and biological evaluation of aryloxyethyl thiocyanate derivatives against *Trypanosoma cruzi*. *J. Med. Chem.* 2002, 45, 3984-3999.
7. Abulwerdi, F. A., Liao, C., Ahmed S. Mady, A. S., Gavin, J., Shen, C., Cierpicki, T., Stuckey, J. A., Showalter, H. D. H. and Nikolovska-Coleska, Z. 3-Substituted-N-(4-hydroxynaphthalen-1-yl)arylsulfonamides as a novel class of selective Mcl-1 inhibitors: structure-based design, synthesis, SAR, and biological evaluation. *J. Med. Chem.* 2014, 57, 4111-4133.
8. Haftchenary, S., Luchman, H. A., Jouk, A. O., Veloso, A. J., Page, B. D. G., Cheng, X. R., Dawson, S. S., Grinshtein, N., Shahani, V. M., Kerman, K., Kaplan, D. R., Griffin, C., Aman, A. M., Al-awar, R., Weiss, S. and Gunning, P. T. Potent targeting of the STAT3 protein in brain cancer stem cells: a promising route for treating glioblastoma. *ACS Med. Chem. Lett.* 2013, 4, 1102-1107.
9. Seim, K. L., Obermeyer, A. C. and Francis, M. B. Oxidative modification of native protein residues using cerium(IV) ammonium nitrate. *J. Am. Chem. Soc.* 2011, 133, 16970-16976.

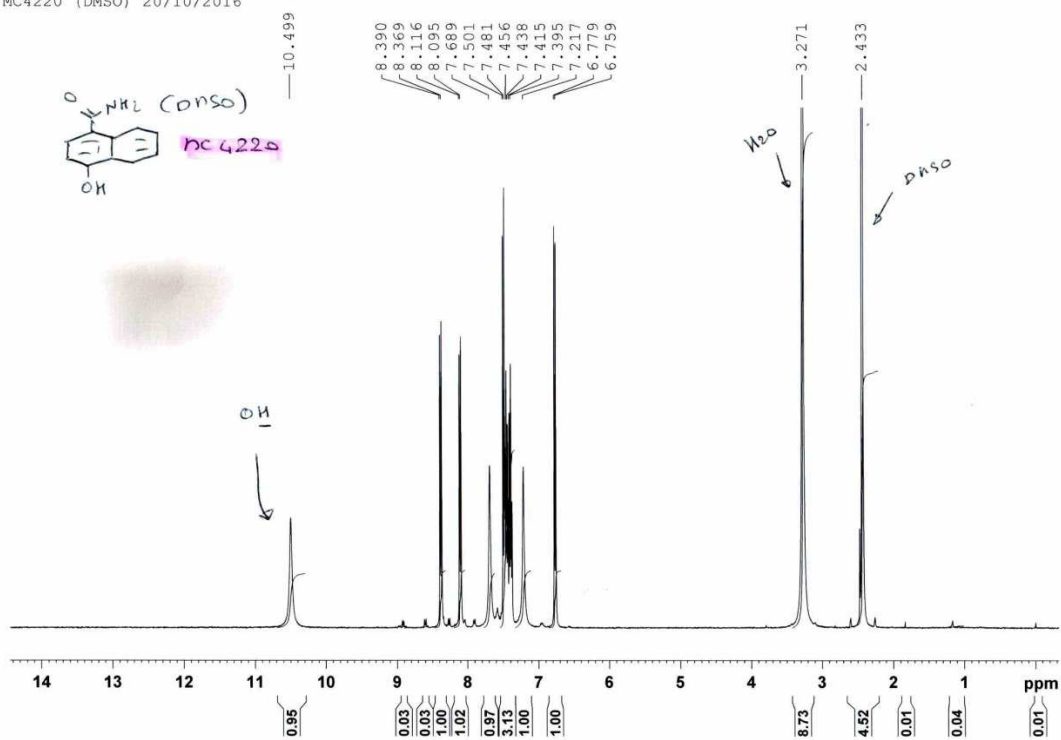
MC4218 (DMSO) 03/10/2016



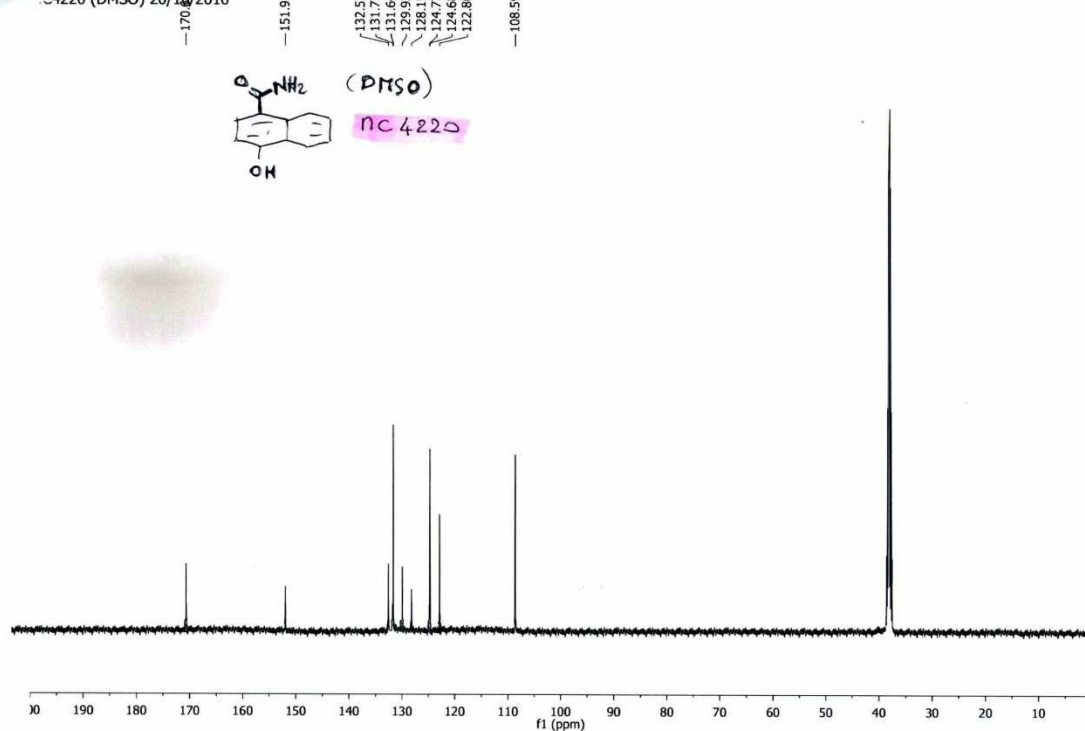
MC4218 (DMSO) 03/10/2016

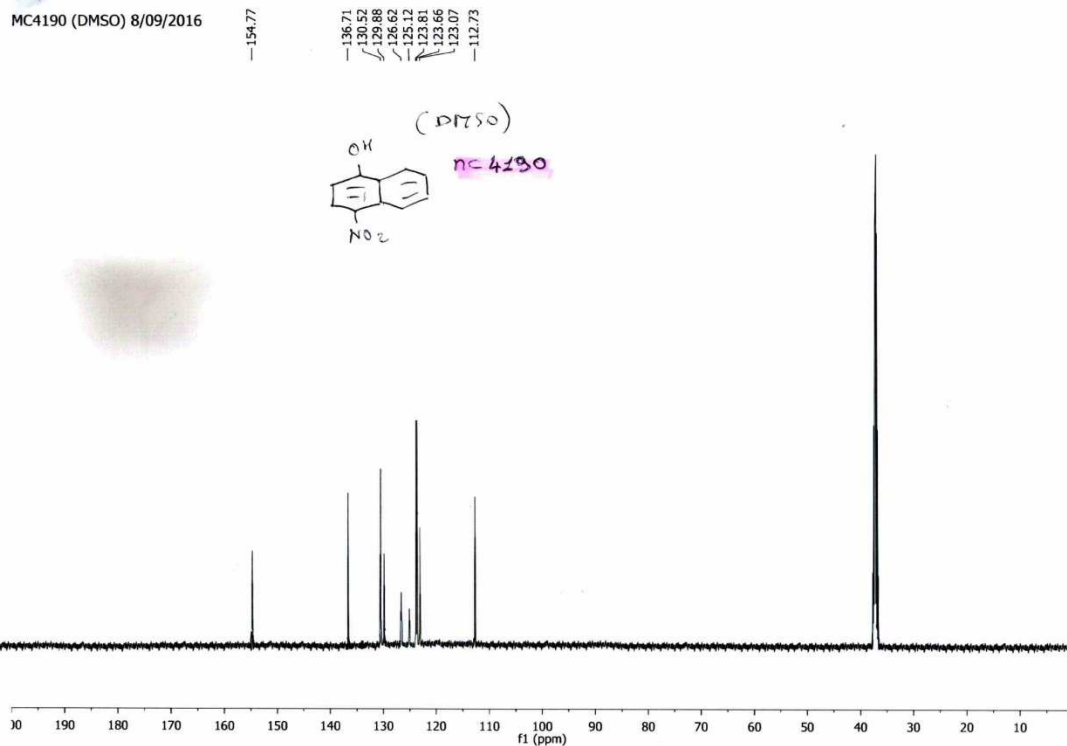
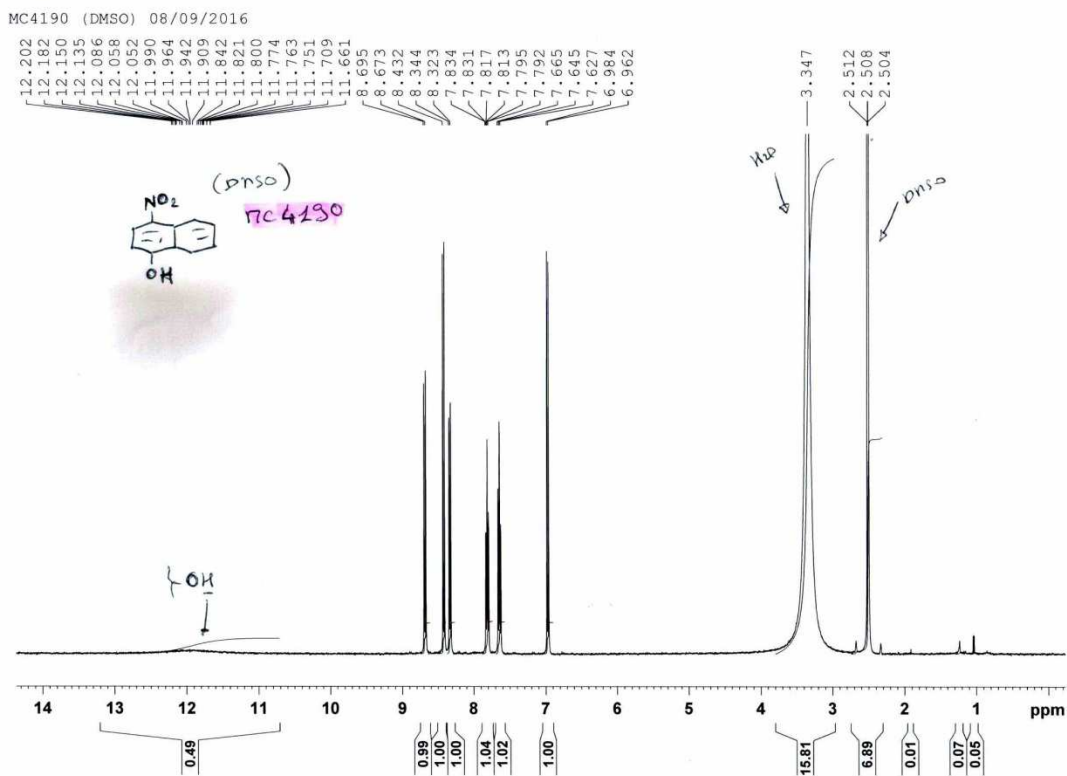


MC4220 (DMSO) 20/10/2016

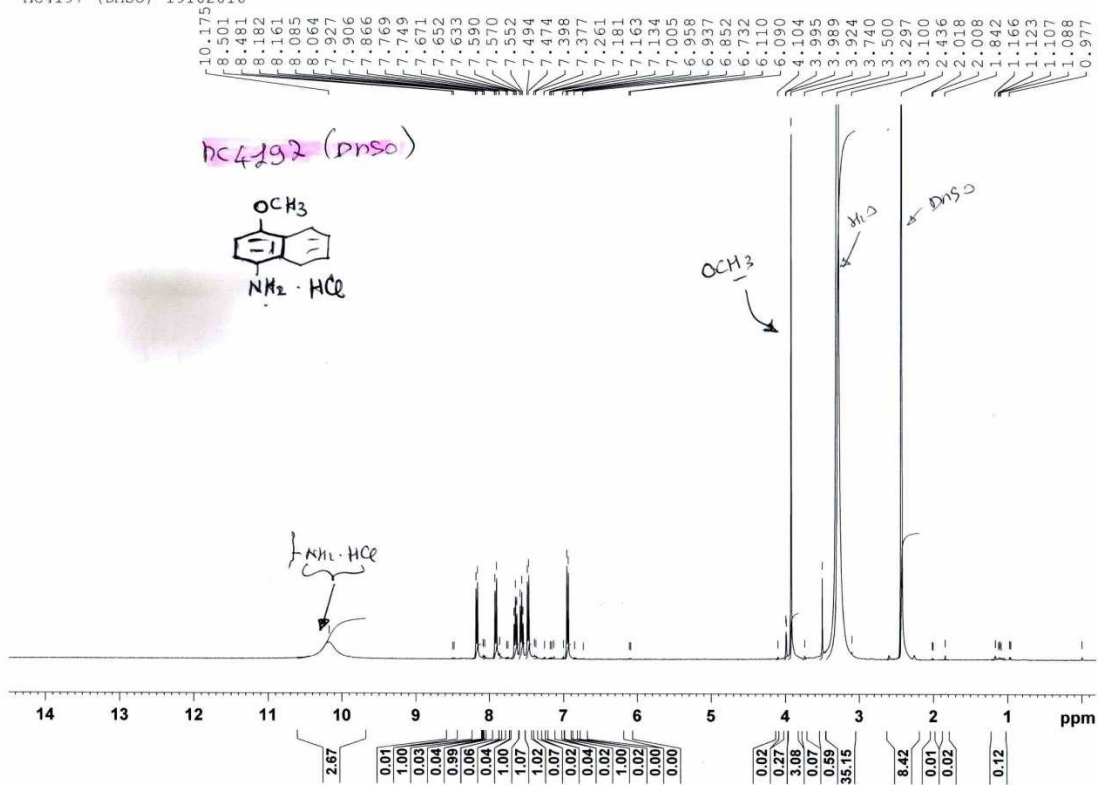


MC4220 (DMSO) 20/10/2016

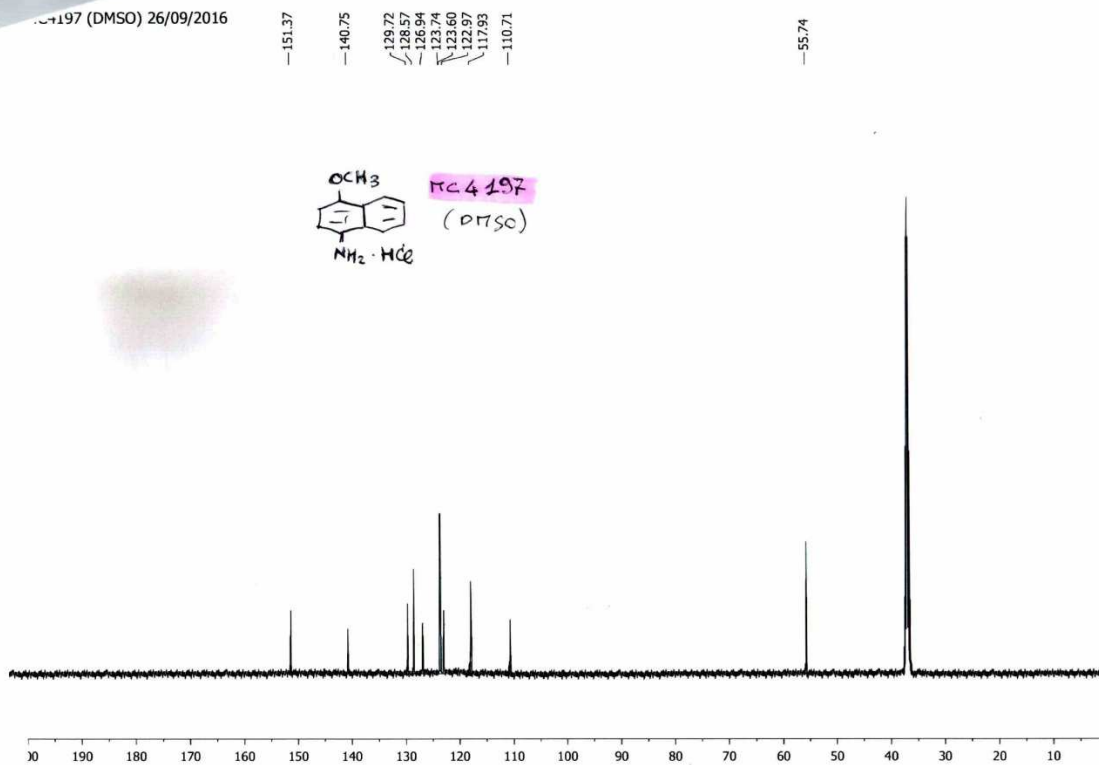


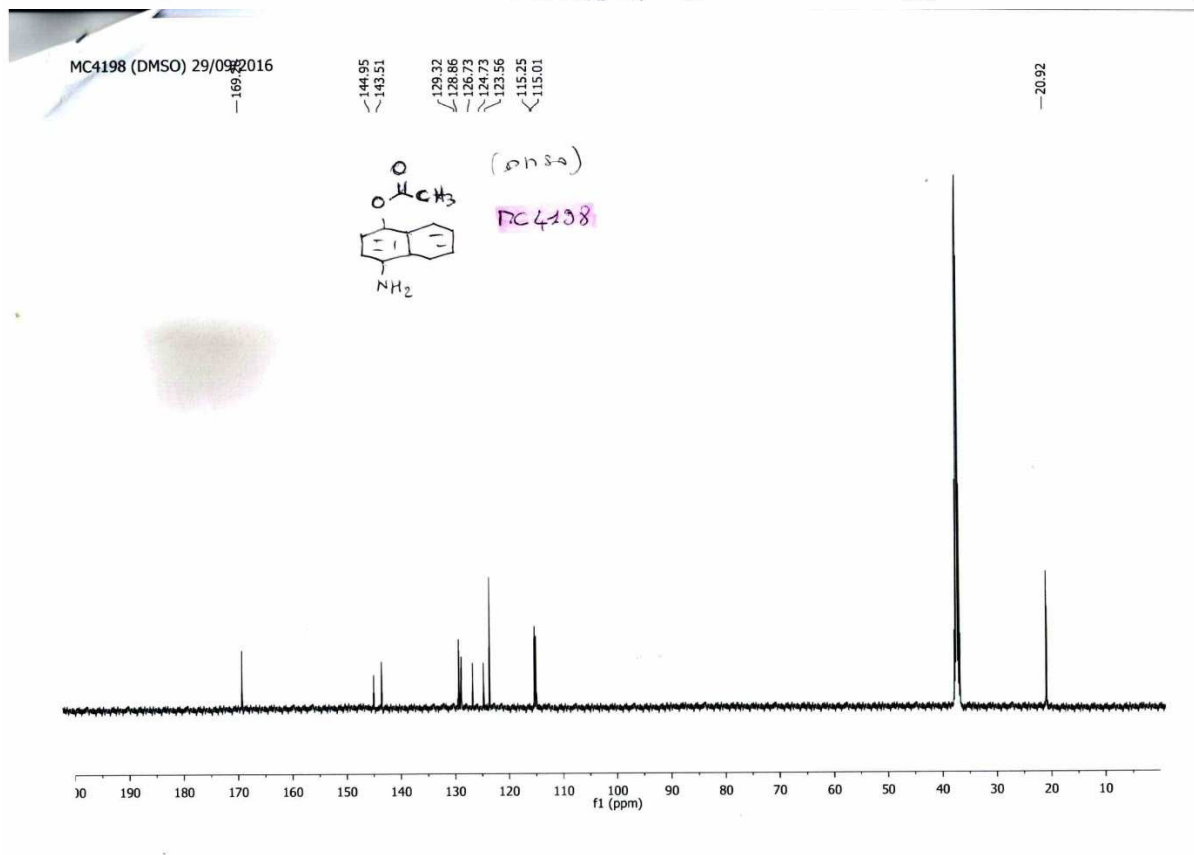
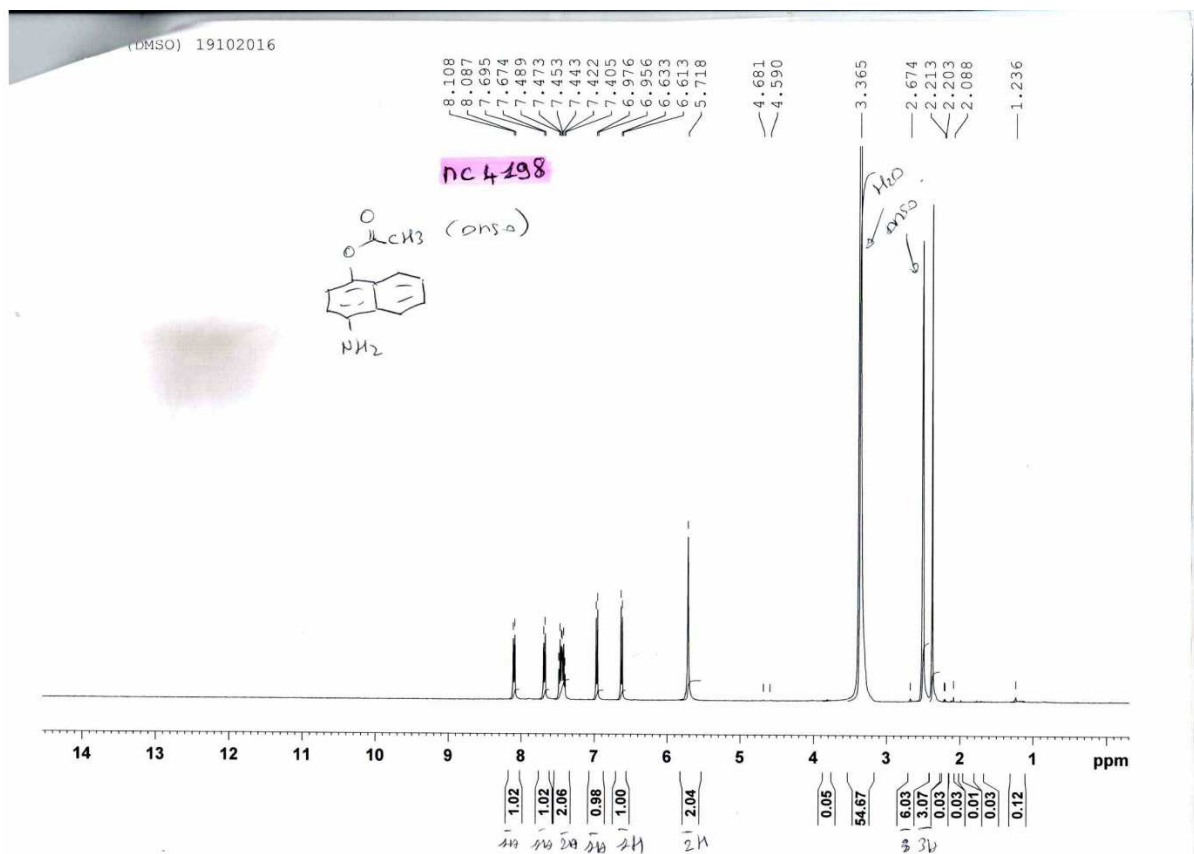


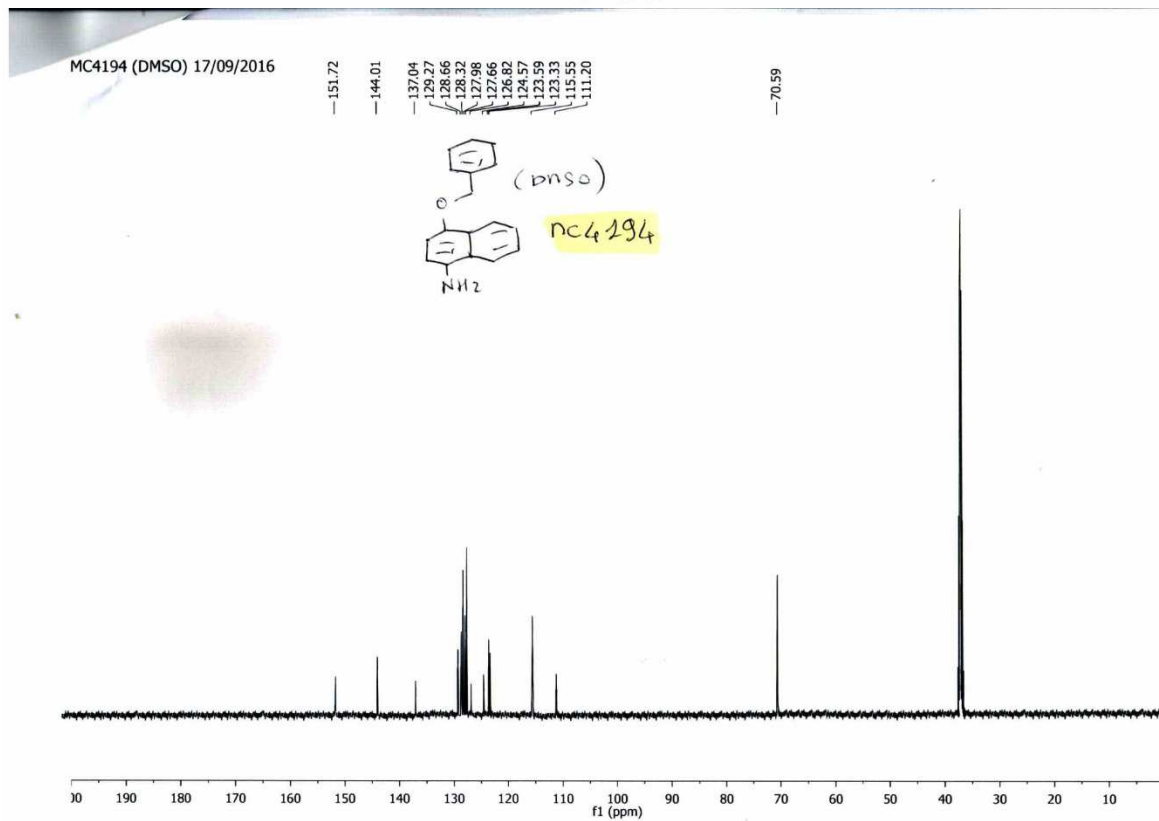
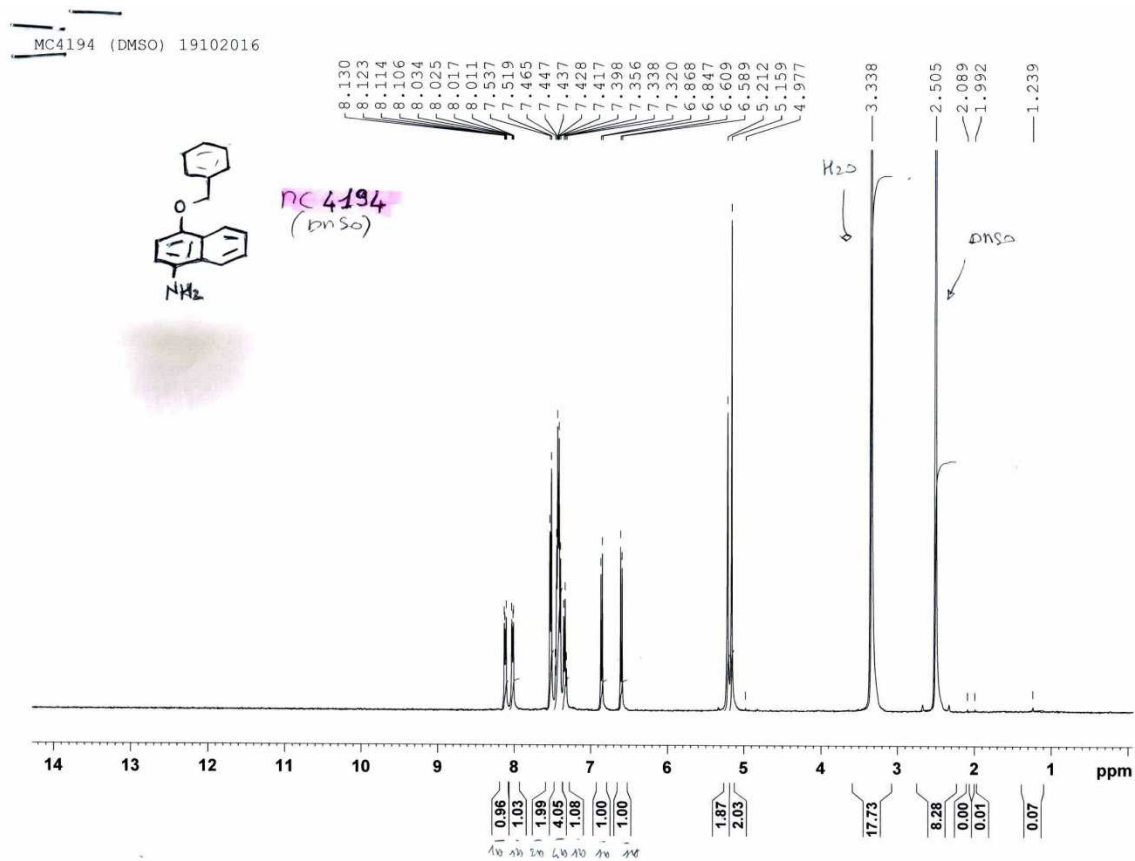
MC4197 (DMSO) 19102016



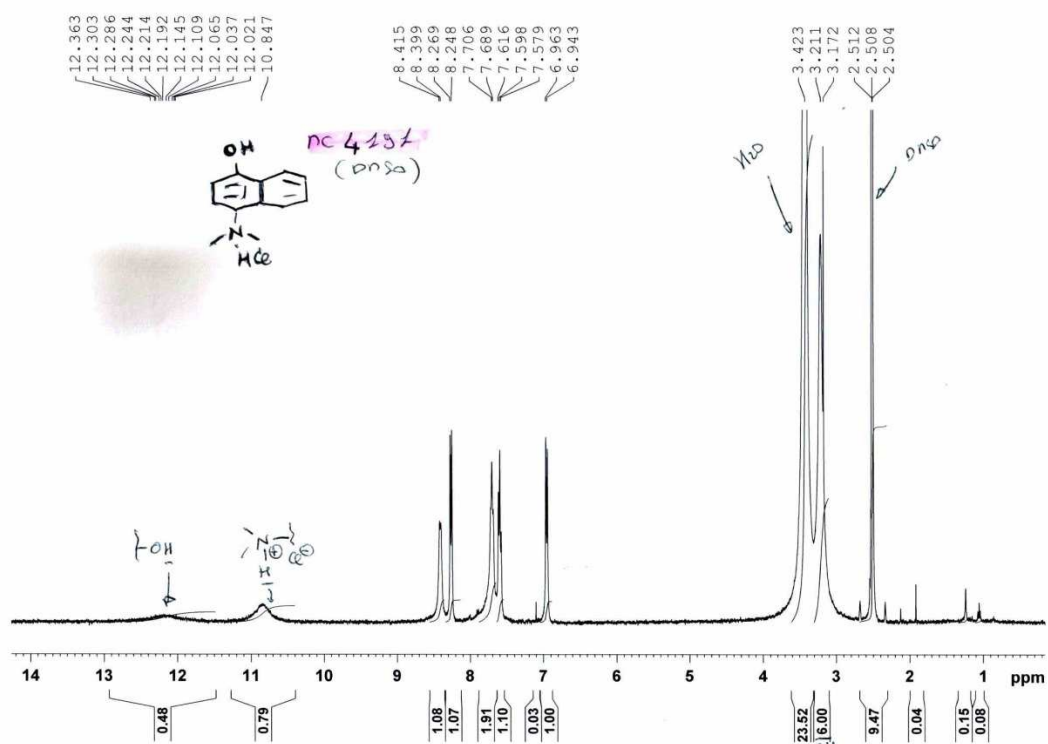
MC4197 (DMSO) 26/09/2016



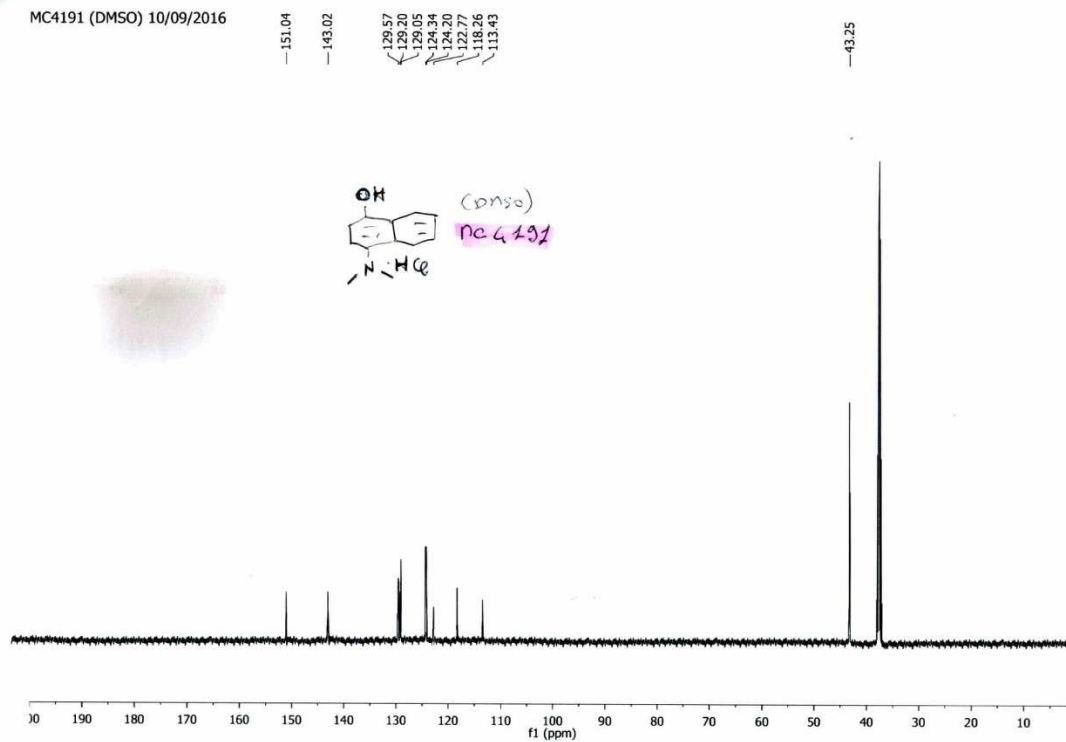


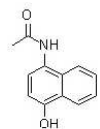


MC4191 (DMSO) 10/09/2016

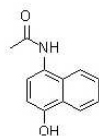
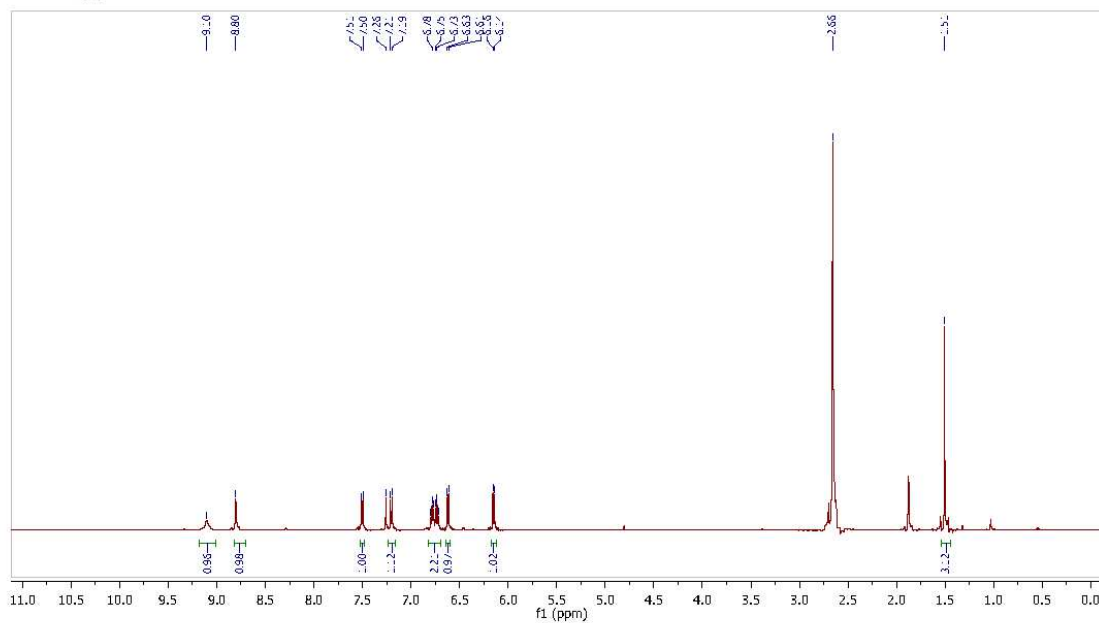


MC4191 (DMSO) 10/09/2016

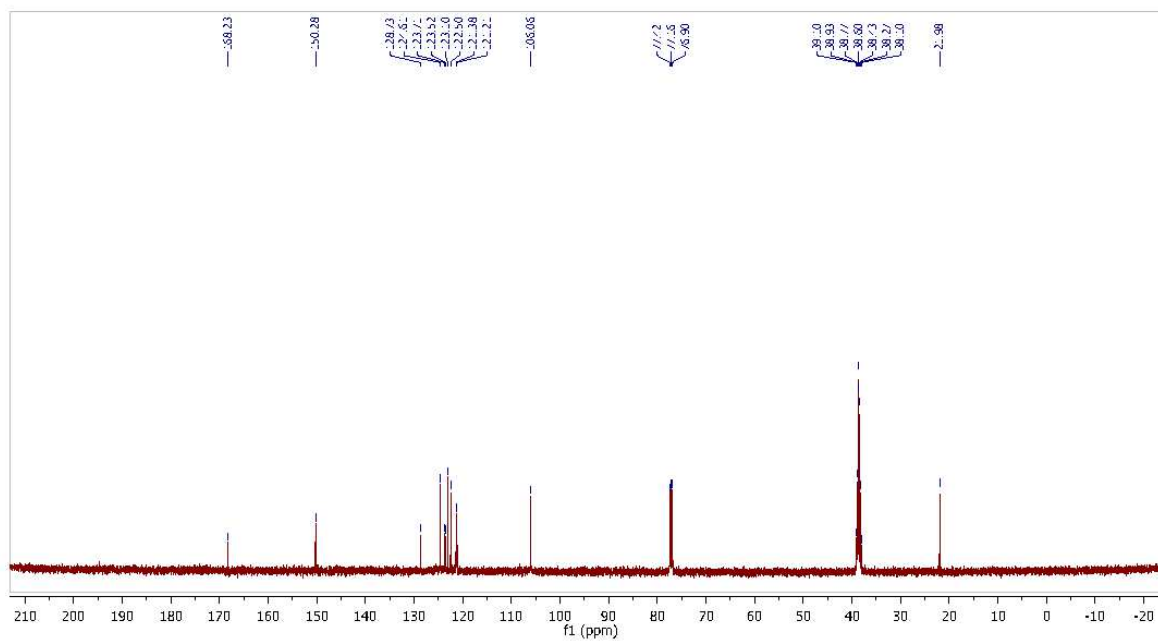


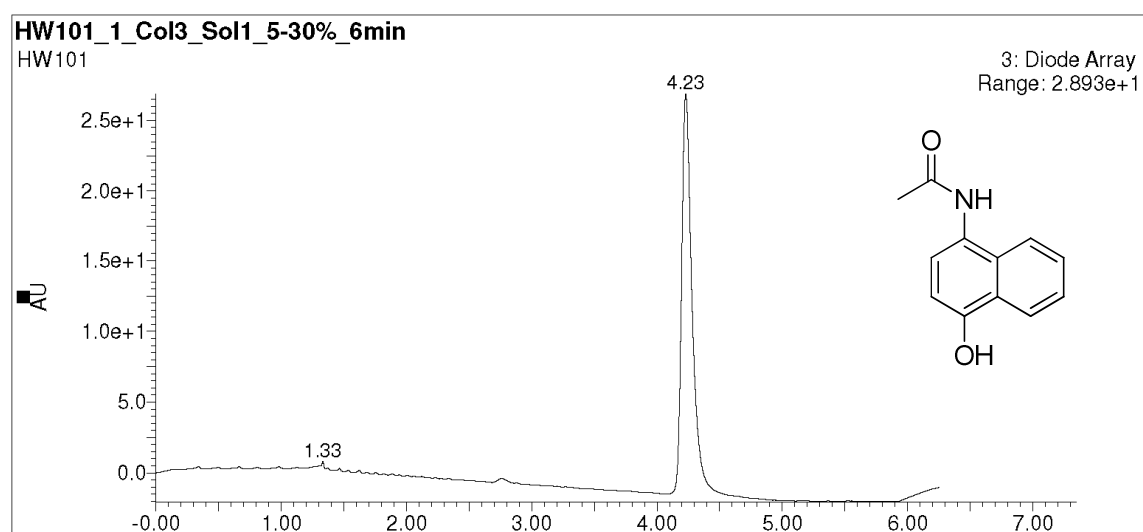


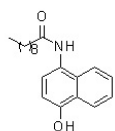
N-(4-hydroxynaphthalen-1-yl)acetamide



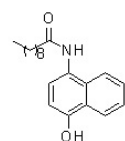
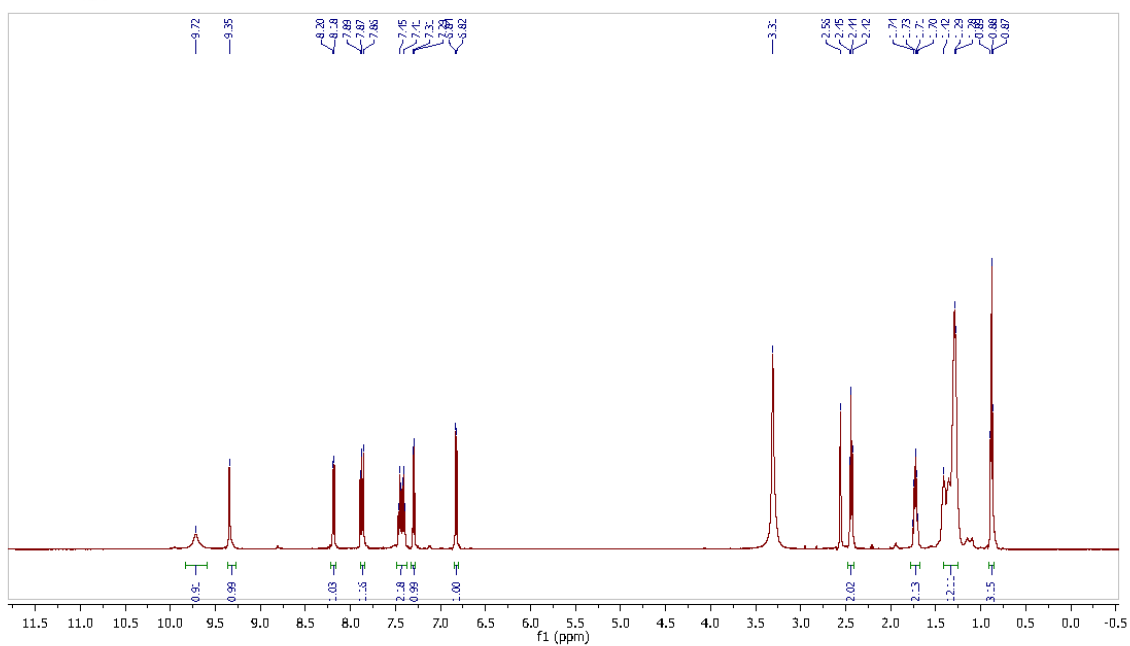
N-(4-hydroxynaphthalen-1-yl)acetamide



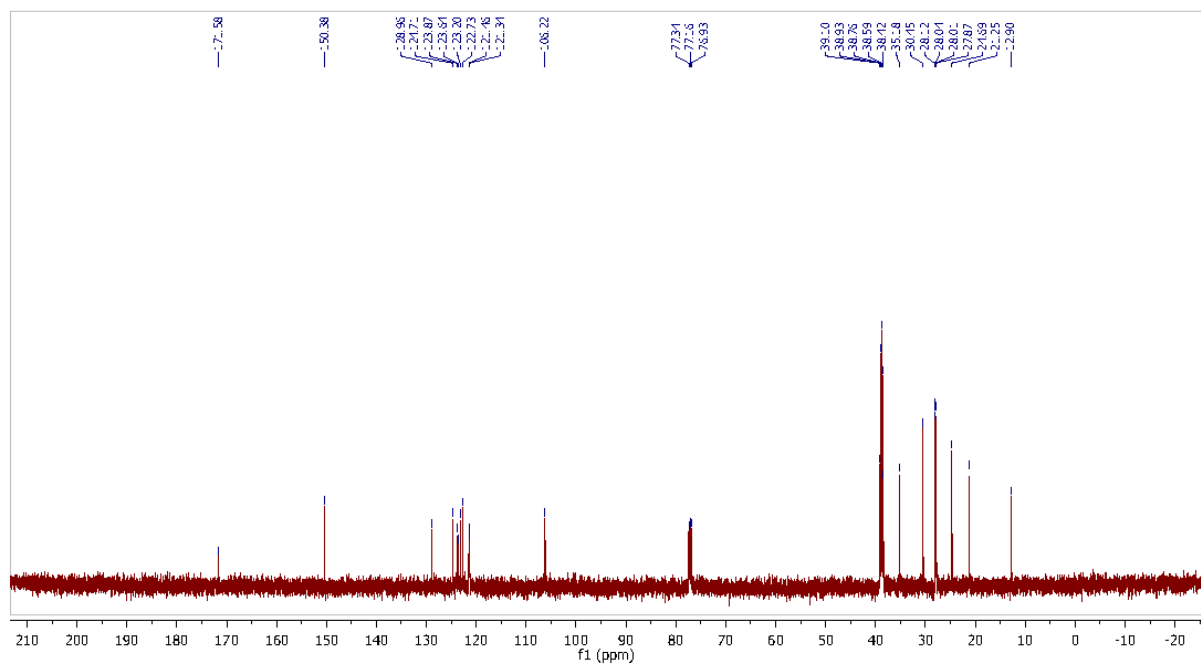


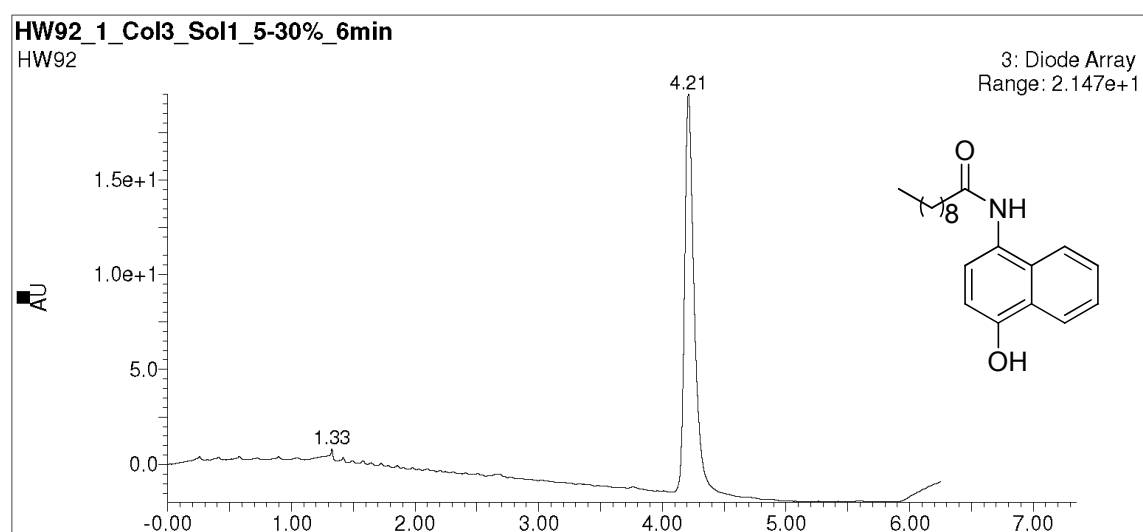


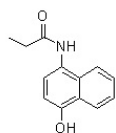
N-(4-hydroxynaphthalen-1-yl)decanamide



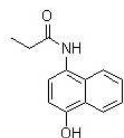
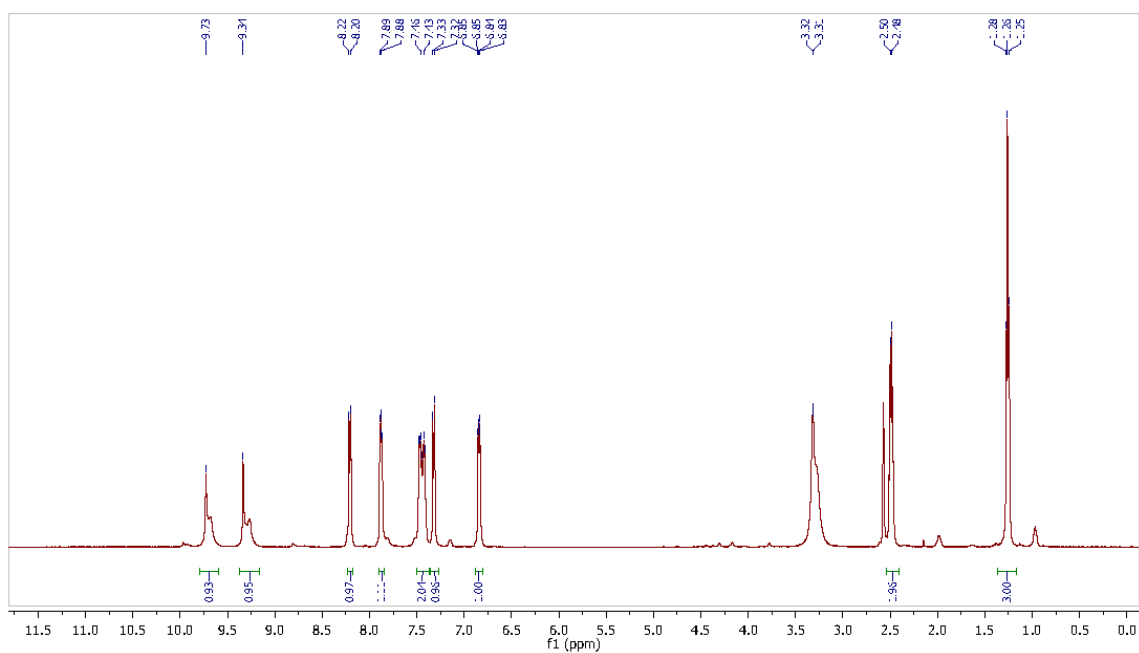
N-(4-hydroxynaphthalen-1-yl)decanamide



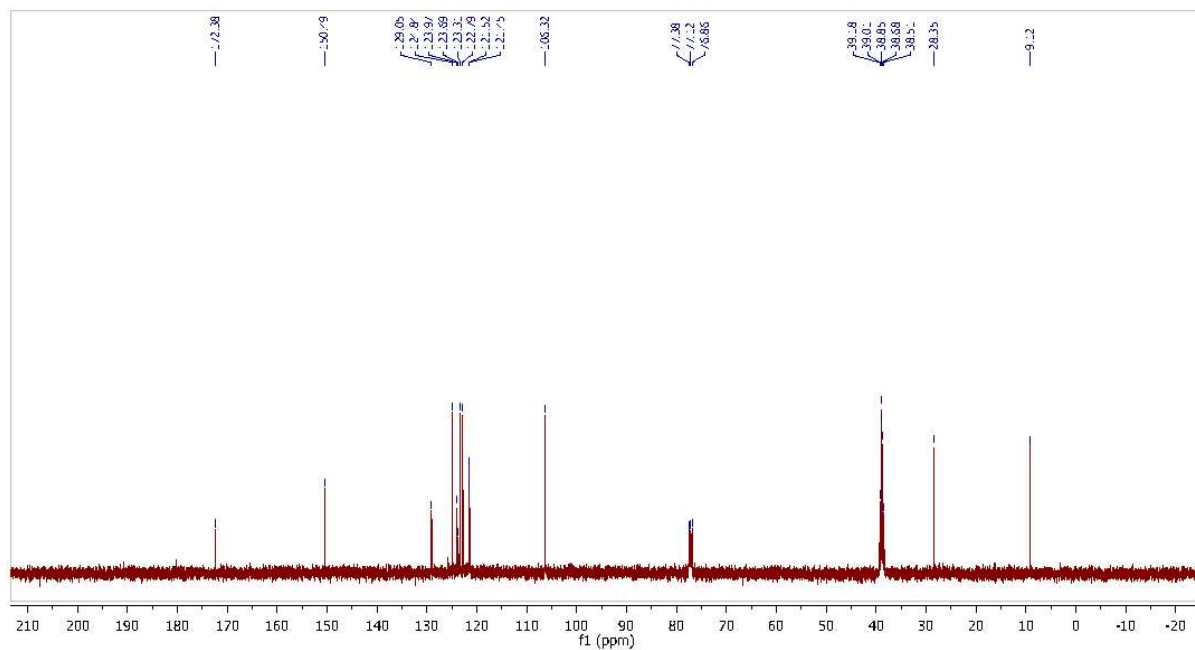


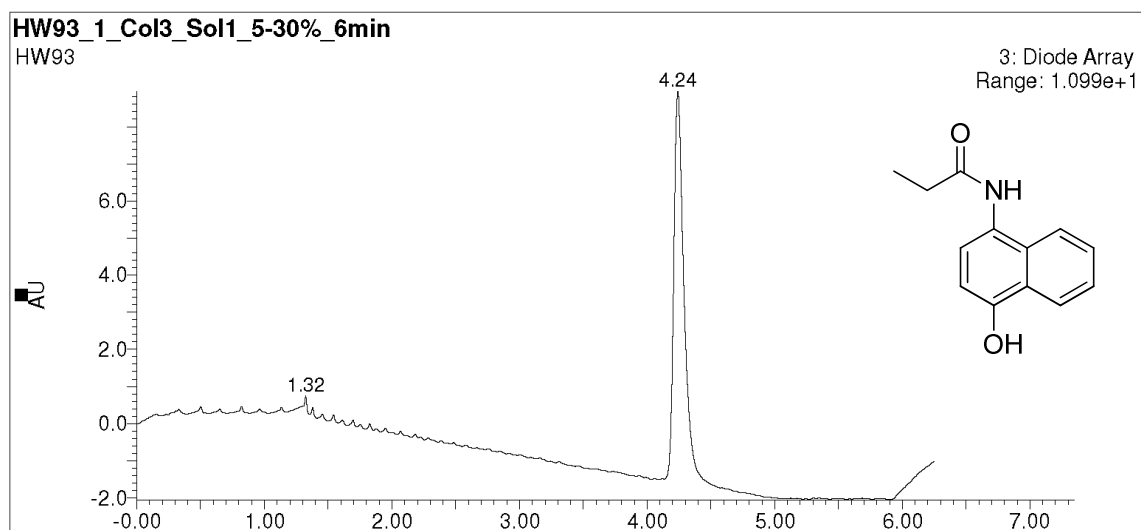


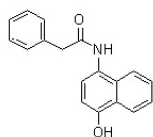
N-(4-hydroxynaphthalen-1-yl)propionamide



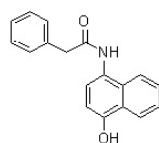
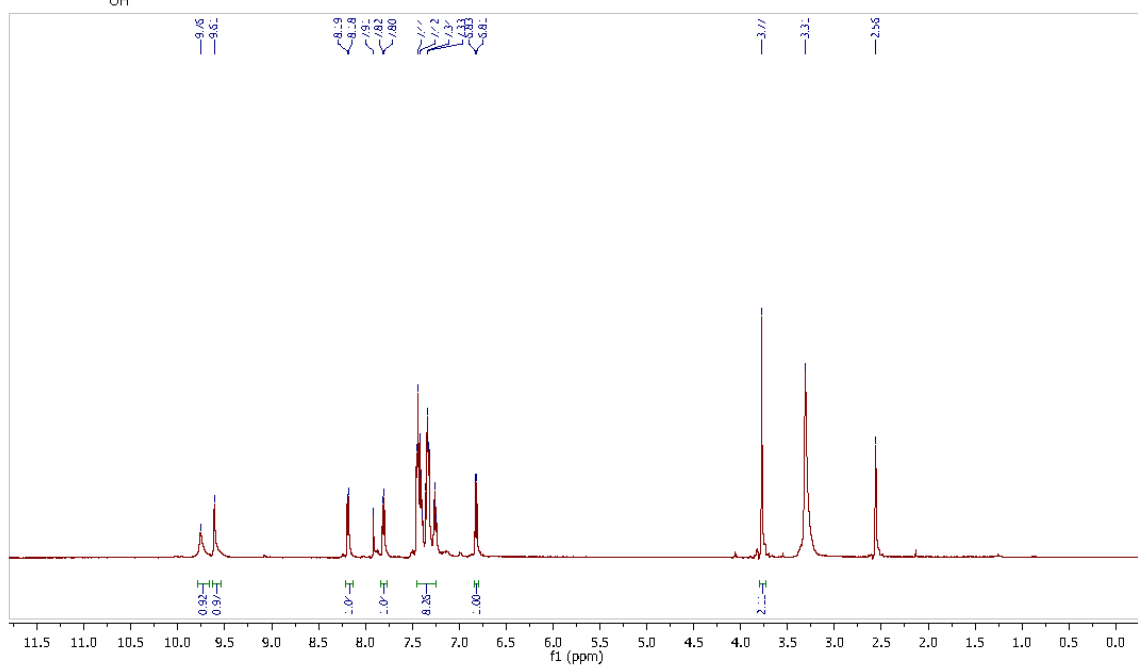
N-(4-hydroxynaphthalen-1-yl)propionamide



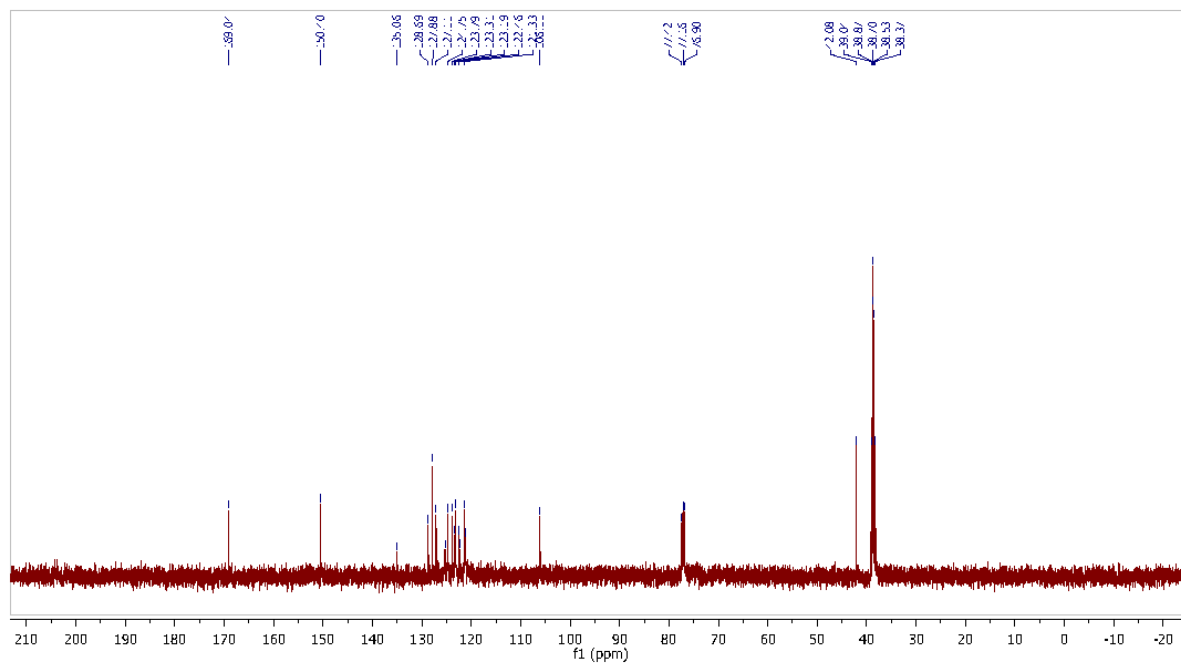


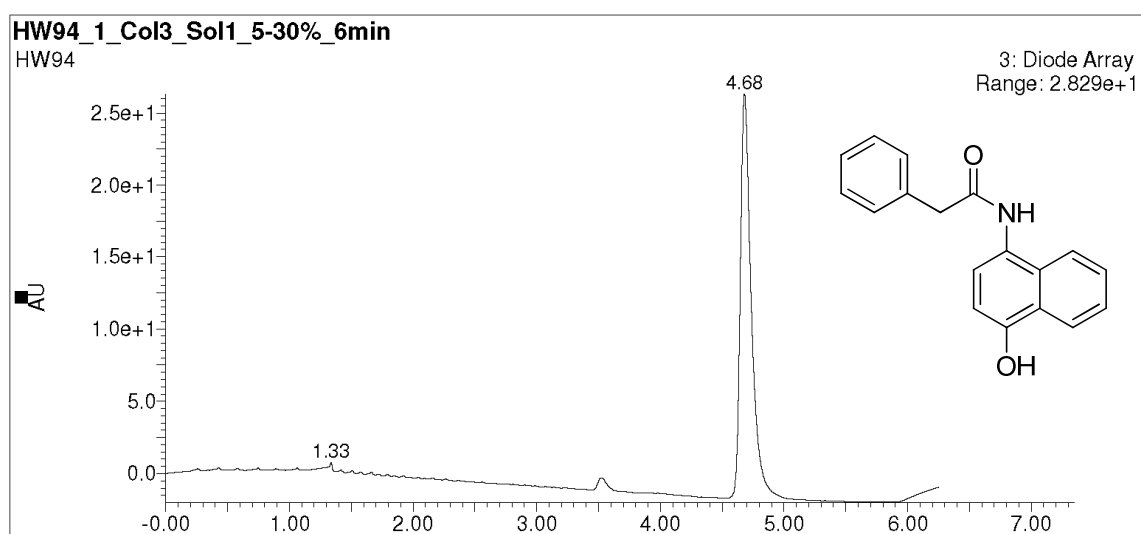


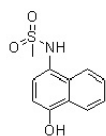
N-(4-hydroxynaphthalen-1-yl)-2-phenylacetamide



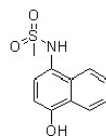
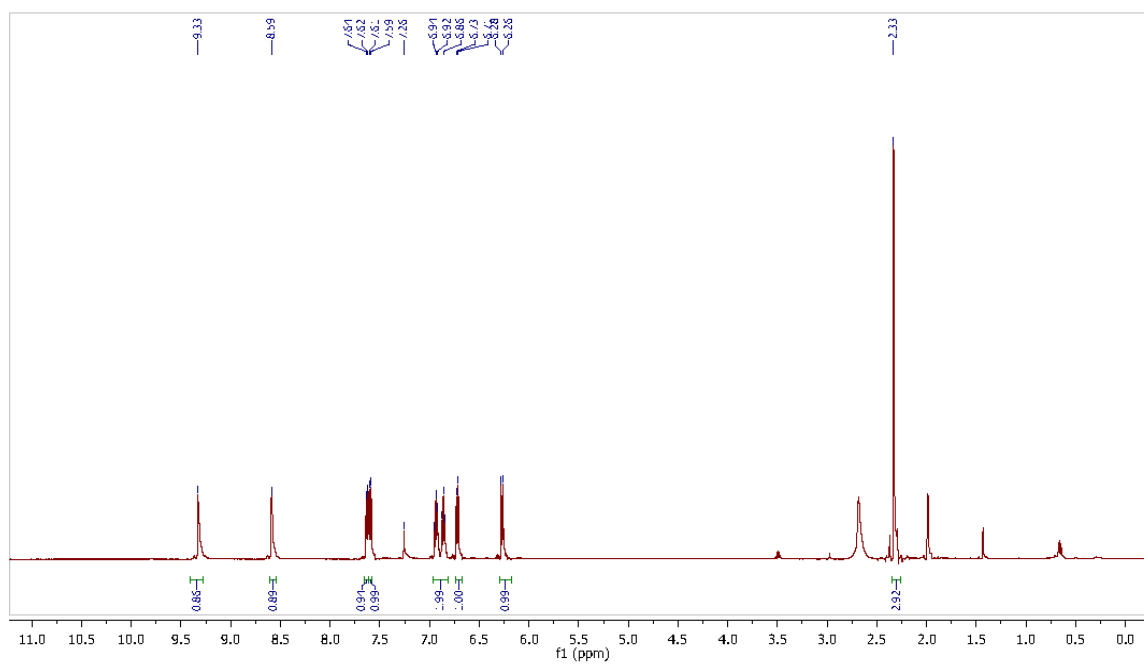
N-(4-hydroxynaphthalen-1-yl)-2-phenylacetamide



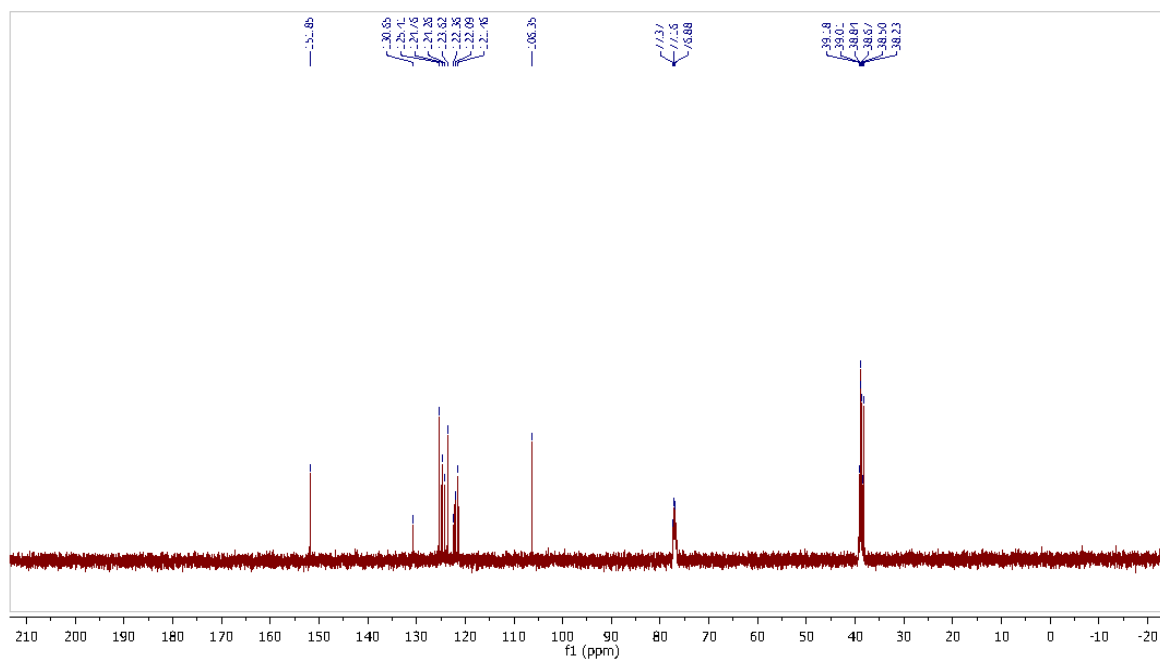


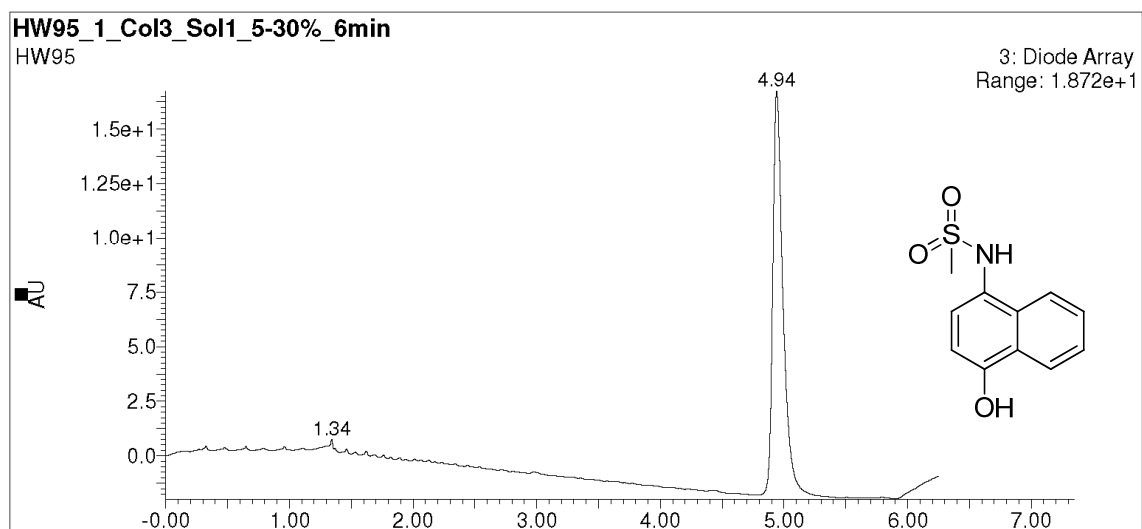


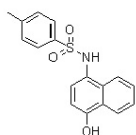
N-(4-hydroxynaphthalen-1-yl)methanesulfonamide



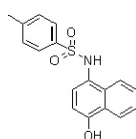
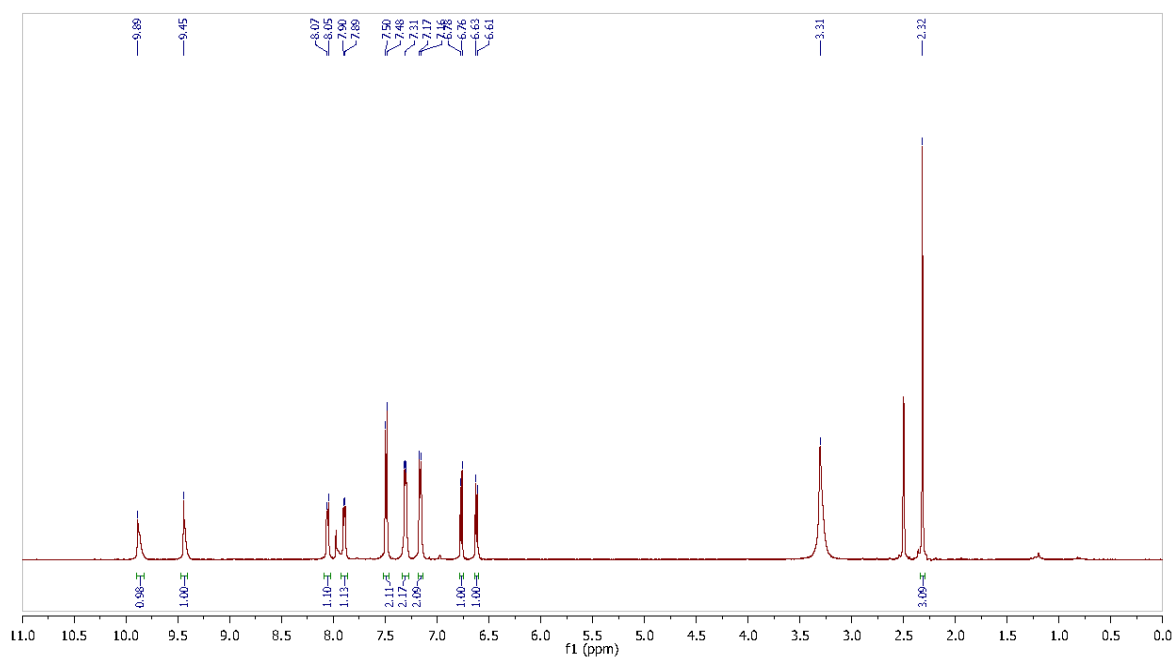
N-(4-hydroxynaphthalen-1-yl)methanesulfonamide



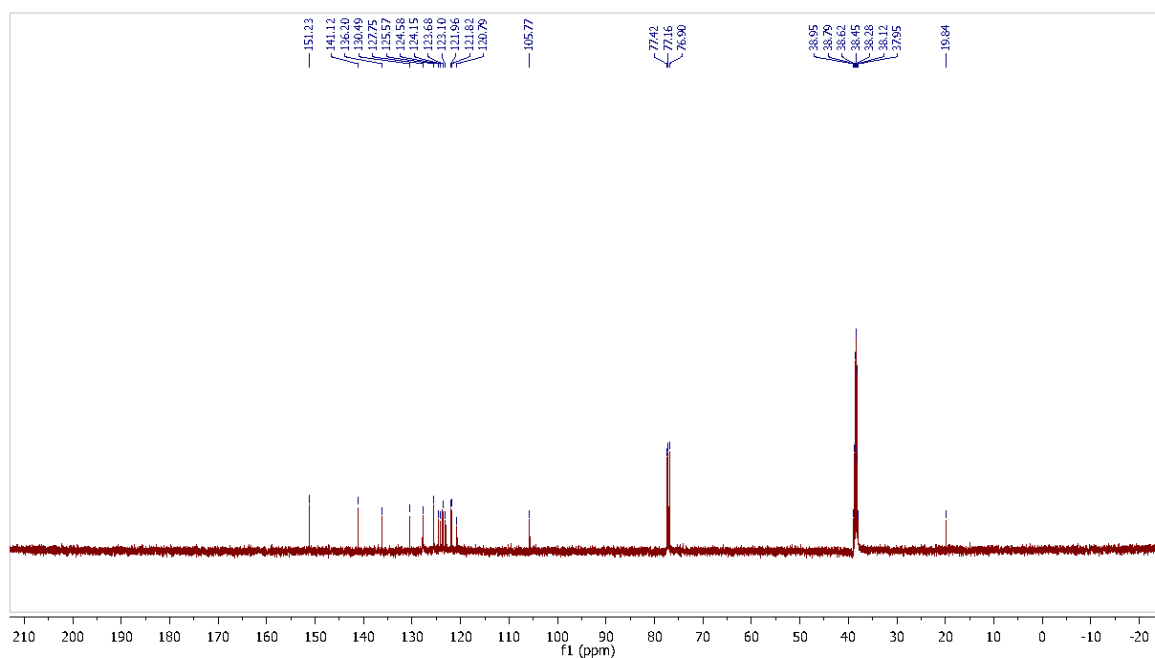


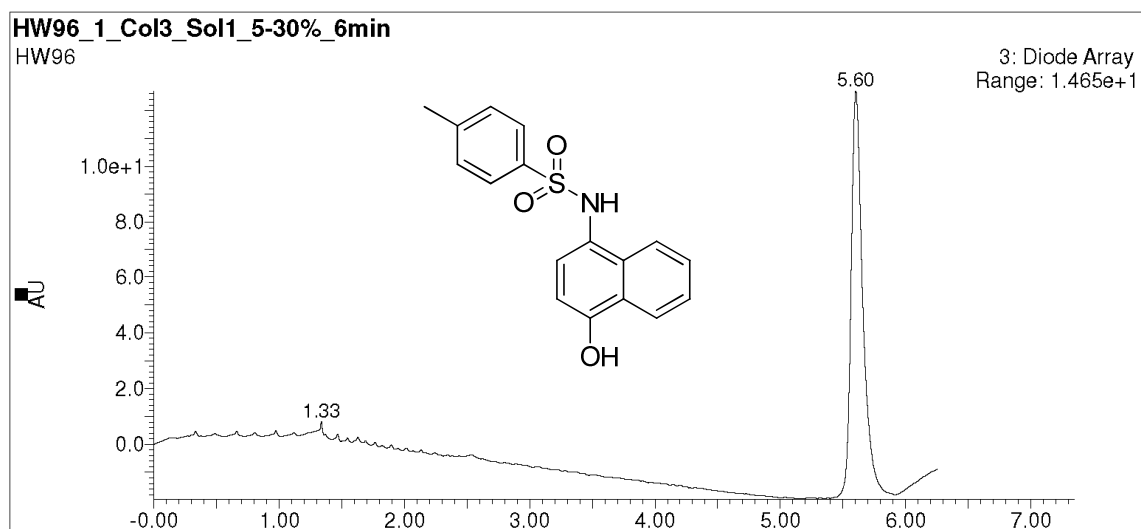


N-(4-hydroxynaphthalen-1-yl)-4-methylbenzenesulfonamide



N-(4-hydroxynaphthalen-1-yl)-4-methylbenzenesulfonamide





**Highlights**

- A novel, potent fragment KAT8 inhibitor was discovered
- Kinetic studies allowed calculation of the inhibitory potency  $K_i$  for KAT8
- Kinetic evaluation of inhibitors is essential for the development of HAT inhibitors